

Physical Sciences

- Emission of Fragment Masses Between 4 Amu and 30 Amu in the Heavy Ion Interaction of (14.0 Me V/u) Pb + Pb
Tabassum Nasir, Ehsan Ullah Khan, Saeed Rahman and Matiullah 59
- Synthesis and Reactivity of Some Peroxo Complexes of Zirconium (IV) Thorium (IV) and Uranium (VI) Ions Containing a Quadridentate, Quadrinegative Ligand and a Pentadentate Dinegative Schiff Base
Md. Tofazzal Hossain Tarafder, Suvash Chandra Pal and Md. Rabiul Karim 63
- Thermal Activation of Bagasse Ash in High Strength Portland Cement Mortar
Noor-ul-Amin 68
- Extraction and Characterisation of *Dioclea reflexa* Hook. F. Seed Oil
Faleye Francis Jide 72
- Antioxidant Properties of *Telfairia occidentalis* as Affected by the Market Storage Method in Nigeria
Foluso Olutope Adetuyi and Gani Adebola Ogundahunsi 76
- Colour Removal from Textile Dyeing Wastewater Using Different Adsorbents
Muhammad Tahir Butt, Naz Imtiaz, Sameer Ahmed, Farooq Arif and Shahid Rehman Khan 81

Biological Sciences

- Studies on Antifungal Activity and Elemental Composition of the Medicinal Plant *Trianthema pentandra* Linn
Abdul Jabbar Pirzada, Wazir Shaikh and Syed Abdul Ghaffar 85
- Culture of *Ceriodaphnia cornuta* Using Chicken Manure as Fertilizer: Conversion of Waste Product into Highly Nutritive Animal Protein
Kareem Altaff and Mehraj Ud Din War 89
- Contribution of Micronutrient Fertilization in Wheat Production and its Economic Repercussions
Ehsan-ul-Haq Chaudhary, Muhammad Akram Chaudhary, Vincent Timmer, Rizwan Khalid and Majid Raheem 92
- Grain Yield Losses in Wheat by Russian Wheat Aphid *Diuraphis noxia* (Mordvilko)
Lal Hussain Akhtar, Altaf Hussain Tariq, Manzoor Hussain, Rana Muhammad Iqbal, Muhammad Arshad and Marghub Amer 98

Short Communication

**Staining Effect of Yellow Dye Extracted from Wood of *Berberis vulgaris* L.
on Angiospermic Stem Tissues**

Faizanullah, Asghari Bano and Yunus Dogan

102

Technology

Effect of Low Cost Iron Oxide with Si Additive on Structural Properties of Ni-Zn Ferrite

Uzma Ghazanfar

104

Review

A Review of Σ Hypernuclear Physics

Masroor Hussain Shah Bukhari

108

Emission of Fragment Masses Between 4 Amu and 30 Amu in the Heavy Ion Interaction of (14.0 MeV/u) Pb + Pb

Tabassum Nasir^{a*}, Ehsan Ullah Khan^b, Saeed Rahman^b and Matiullah^c

^aDepartment of Physics, Gomal University, Dera Ismail Khan, Pakistan

^bDepartment of Physics, CIIT, Islamabad, Pakistan

^cPhysics Division, PINSTECH, P.O. Nilore, Islamabad, Pakistan

(received December 7, 2009; revised January 25, 2010; accepted February 1, 2010)

Abstract. Using two threshold solid state nuclear detectors, mica and CN-85, the reaction of (14.0 MeV/u) Pb + Pb was studied. Reaction cross-section was determined experimentally as well as theoretically. Both elastic and inelastic data were used to calculate the experimental reaction cross-section. Theoretical reaction cross-section for 14.0 MeV/u Pb + Pb is 3809 ± 428 mb. Reaction cross-sections from elastic data were 3830 ± 500 mb and 3875 ± 500 mb for mica and CN-85, respectively, While reaction cross-sections calculated from inelastic data for mica and CN-85 were 4081 ± 500 mb and 4092 ± 500 mb, respectively. The partial reaction cross-sections for mica and CN-85 detectors were also determined. It was observed that partial cross-section of inelastic binary events in mica was higher than that in CN-85, whereas, cross section of 4 and 5-pronged events in mica were lower than those in CN-85. However, the number of three pronged events was identical in the two detectors. Using the difference in mass registration threshold of the two detectors, for fragment masses between 4 amu (registration threshold of CN-85) and 30 u (registration threshold of mica) were searched, which were registered in CN-85 but not in mica.

Keywords: heavy ion interaction, solid state nuclear track detectors, total and partial reaction cross-sections, theoretical reaction cross-section, light particle emission.

Introduction

Understanding the properties of nuclear matter is the most important challenge in nuclear physics. To achieve this goal, first the nuclei have to be prepared in extreme conditions of excitation energy, temperature, pressure, spin and isospin. The tool used to obtain such extreme conditions is heavy ion induced reaction. Emission of light particles in heavy-ion-induced reactions contains important information about the reaction mechanism.

Solid state nuclear track detectors (SSNTD) yield useful results in the study of heavy ion interactions. Due to registration of all the heavy reaction products, moving in the forward hemisphere, the use of SSNTDs become unbiased and more versatile in giving information regarding the heavy ion interactions. Solid state nuclear track detectors have been extensively used to investigate the heavy ion ($A > 4$) interactions (Nasir *et al.*, 2009; 2008; Khan *et al.*, 2001; 1998; Brandt, 1980). Each SSNTD has its own mass registration threshold and registers only that particle whose mass is greater than this threshold value (Khan *et al.*, 1984). In the present research work, CN-85 and mica track detectors were used to study 14.0 MeV/u $^{208}\text{Pb} + ^{208}\text{Pb}$ reactions. CN-85 (cellulose nitrate) with chemical formula $\text{C}_6\text{H}_8\text{O}_9\text{N}_2$ is a sensitive plastic

while mica with chemical formula $\text{K Al}_3\text{Si}_3\text{O}_{10} (\text{OH})_2$ is a mineral crystal. Both are etchable solid state nuclear track detectors.

The data presented in this paper consists of 2-, 3-, 4-, and 5-pronged events studies with two detectors, mica and CN-85, having different mass registration thresholds. They registered the fragment masses greater than their mass registration thresholds. Using the inelastic binary and multi-pronged events, the partial and total experimental reaction cross-sections were determined. The experimental reaction cross-section was determined from the elastic binary events and theoretical reaction cross-section for the reaction was also calculated. Analysis of the observed partial cross-sections of various multiplicities and the indirect events have been reported as the signal for the emission of mass fragments having masses between 4 amu and 30 amu, registered by CN-85 (having low registration threshold) and not by mica (having high registration threshold = 30 u), along with the heavy fragment masses in the present reaction.

Materials and Methods

A thin layer of Pb was vacuum deposited on each of the three mica and the two CN-85 detector pieces. These target-detector assemblies were exposed, to a beam of (14.0 MeV/u) Pb

*Author for correspondence; E-mail: tabassum642003@yahoo.com

Table 1. Statistics of direct (D) and indirect (ID) multi-pronged events

Detector	Three pronged		Four pronged		Five pronged	
	D	ID	D	ID	D	ID
Mica	320	163 (34%)	74	81 (52%)	1	3 (75%)
CN-85	95	86 (48%)	45	41 (48%)	4	3 (43%)

ions, having the fluence of $\sim 1.5 \times 10^6/\text{cm}^2$ at the UNILAC of GSI, Darmstadt, Germany. After the exposure the target material was removed from the detectors with HNO_3 . Mica detectors were then etched in 48% HF at 23 °C and CN-85 in 10% NaOH at 60 °C. The etching was made in successive time steps at the intervals of a few minutes. After 80 minutes of etching, majority of the latent ‘tracks’ in mica were etched to their full lengths. In CN-85, however, the etching lasted for 120 minutes.

Events of different multiplicities, direct (D) and indirect (ID), registered in a detector are given in Table-1.

From the total normal binary events ‘1091’ observed in mica and ‘251’ observed in CN-85, a set of elastic binary events was bifurcated using angular and energy correlation for Rutherford elastic scattering (Baluch *et al.*, 1996). The bifurcated elastic binary events were 973 and 221 in case of mica and CN-85, respectively. The number of inelastic binary events was obtained by subtracting the elastic binary events from the total observed binary events. The number of inelastic binary and total multi-pronged events is given in Table-2. Also the number of target nuclei, average fluence, average target thickness and total scanned area is given in Table-3.

Table 2. Events of various multiplicities (2-pronged inelastic (IE) events and 3-, 4- and 5-pronged total events)

Detector	Number of events of different multiplicities			
	2-pronged	3-pronged	4-pronged	5-pronged
Mica	118	483	155	4
CN-85	30	181	86	7

Table 3. Number of target nuclei (N), average fluence (\bar{O}), average target thickness (t) and total scanned area (a) Detector

Detector	(N) $\times 10^{19}$	(\bar{O}) $\times 10^6$ (cm^{-2})	(t) (mg/cm^2)	(a) (cm^2)
Mica	10.9	1.70	1.00	37.68
CN-85	8.3	0.90	1.30	25.12

Results and Discussion

Reaction cross-section. Reaction cross-section was determined experimentally as well as theoretically. The experimental reaction cross-section was determined both from elastic and inelastic data.

The values of reaction cross-sections σ_R^{exp} (el.) from elastic data were 3830 ± 500 mb and 3875 ± 500 mb in case of mica and CN-85, respectively.

The partial reaction cross-sections for mica and CN-85 detectors were also determined. The determined values of partial and total inelastic reaction cross-sections σ_R^{exp} (inel.) are given in Table-4. Total experimental reaction cross-section is also equal to the sum of partial reaction cross-sections.

Table 4. Detector wise partial and total experimental reaction cross-sections using inelastic events

Detector	Reaction cross-section (mb)				
	(σ_2)	(σ_3)	(σ_4)	(σ_5)	σ_R^{exp} (inel.)
Mica	634 ± 50	2594 ± 465	832 ± 200	20 ± 10	4081 ± 500
CN-85	404 ± 96	2436 ± 427	1158 ± 240	94 ± 35	4092 ± 500

Theoretical reaction cross-section for 14.0 MeV/u Pb +Pb was 3809 ± 428 mb. The final experimental reaction cross-sections obtained by taking weighted average of elastic and inelastic reaction cross-sections, for both mica and CN-85 detectors, came out to be 3970 ± 500 mb and is graphically represented by straight line in Fig. 1.

Emission of fragment masses between 4 amu and 30 amu.

The highest partial reaction cross section is for three pronged events which is almost equal in both the detectors (Table-4). It is also illustrated in Fig. 2, which shows the partial reactions cross-sections for different multiplicities in both types of the detectors.

It can also be seen (Table-4) that the partial cross section of inelastic binary events in mica is higher than that in CN-85, whereas cross-sections of 4 and 5-pronged events in mica are lower than those in CN-85.

This trend is pronounced in Fig. 3, where the ratio of cross-sections has been plotted for the ratio of various multiplicities for both type of the detectors. The cross sections of the multiplicity ratio of 2/3 and 4/5 are same, within the experimental error, in both the detectors. However, the ratio of the cross section of the ratio of 3/4 in mica is significantly higher than in case of CN-85.

Since mica is over estimating the two pronged cross-sections, and since the number of three pronged events is identical in the two detectors, it can be concluded, therefore, that in the 2-pronged events there are some events of higher multiplicities (4- or 5-pronged) in which two or even more tracks could not be registered in mica and hence could not be assigned the correct multiplicities. These types of events were, however, registered in CN-85 with correct multiplici-

ties (4- and 5- pronged events) due to its lower registration threshold value. The deficit in the cross-section of 4- and 5-pronged events in mica indicates that there could be as many as 25% of the total events which may be accompanied with the emission fragment masses between 4 and 30 u. This conclusion is also supported by Khan *et al.* (2001) and by the fact that the ratio of the cross-sections of indirect to that of the direct events slightly increases with the increasing multiplicity of events, shown by the straight line in Fig. 4.

Since the higher multiplicity in such a reaction is associated with the higher energy dissipation (Vater *et al.*, 1986), more particles with masses between 4 and 30 u were emitted and hence more indirect events were observed in the case of higher multiplicities. The argument is further supported by the plot of differential cross-sections of even direct events to total events in each multiplicity for both the detectors, shown in Fig. 5.

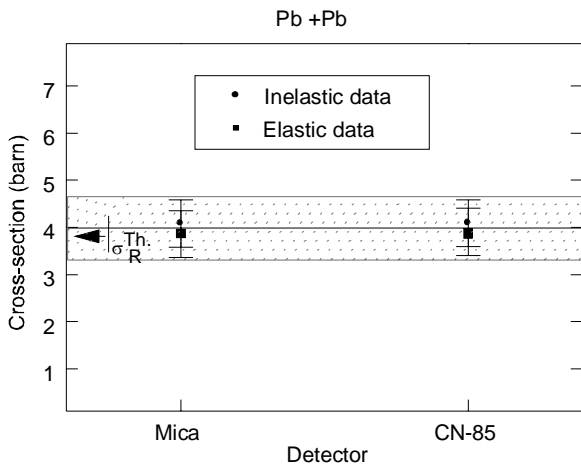


Fig. 1. Experimental reaction cross-sections along with their experimental errors. Theoretical cross-sections is also shown.

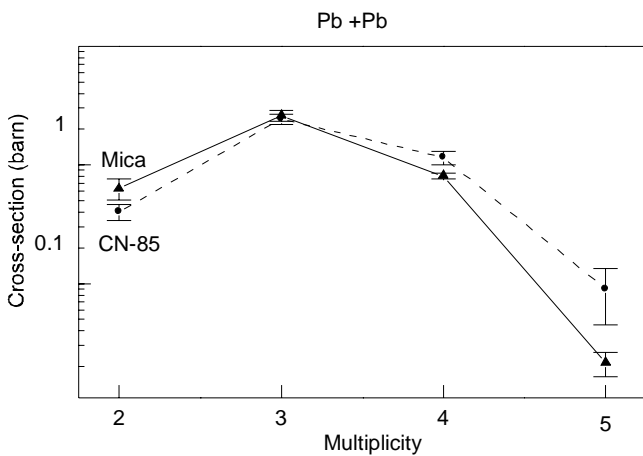


Fig. 2. Partial cross-sections of various multiplicities observed in both types of the detectors.

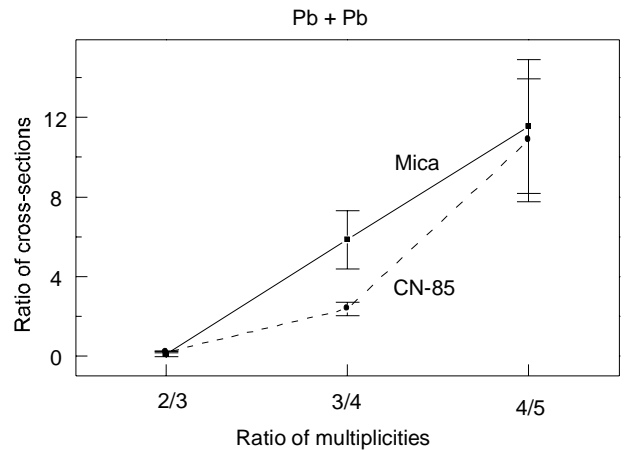


Fig. 3. Ratio of cross-sections with respect to the ratio of multiplicities for both types of detectors.

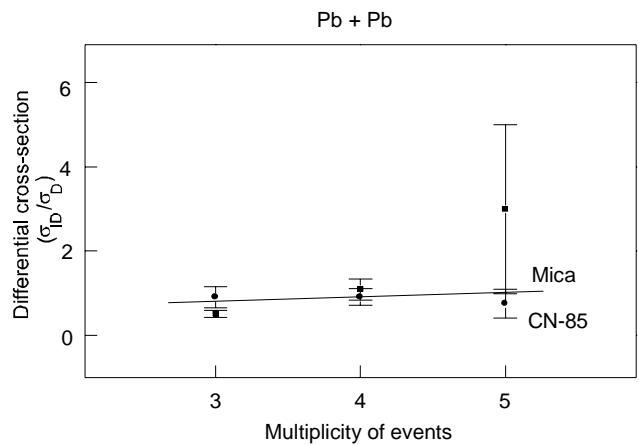


Fig. 4. Differential cross-sections of indirect to direct events for each multiplicity shown for both the reaction and both types of detectors. Error bars are the statistical errors.

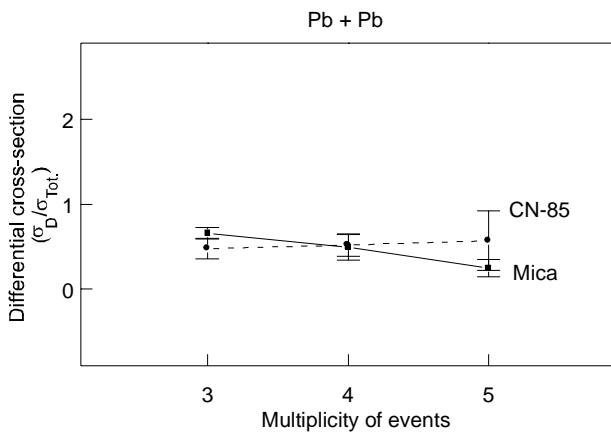


Fig. 5. Differential cross-sections of direct events to total events for each multiplicity shown for both the reactions and for both the types of detectors. Error bars are the statistical errors.

It is clearly demonstrated here that with the increasing multiplicity, the number of direct events in mica decreases while in CN-85, it is the reverse. Hence, as the multiplicity increases, more particles having masses between 4 and 30 u are emitted which mica denies to register due to its higher registration threshold. Such particles are, however, readily registered in CN-85. The emission of such particles affects the kinematics of such events which cannot, therefore, be analyzed on the basis of sequential fission process (Vater *et al.*, 1986).

Conclusion

The experimental reaction cross-sections calculated from the weighted average and derived from elastic and inelastic data sets agree reasonably well with the one calculated theoretically. The study of partial cross-sections based on different multiplicities of the reaction (14.0 MeV/u) Pb + Pb shows that the three-particle exit channel is significantly dominant as compared to other multiplicities registered in both mica and CN-85 track detectors. Moreover a significant number of light fragments having masses between 4 amu and 30 amu are emitted along with heavy fragments. An estimated upper limit for such events is 25%.

References

- Baluch, J.J., Khan, E.U., Zafar, M.S., Qureshi, I.E., Khan, H.A. 1996. Reproduction of projectile and target masses from binary data in the heavy ion interaction of 17.0 MeV/N ^{132}Xe with ^{238}U : *Nuclear Instruments and Methods in Physics Research, Section B*, **111**: 91-94.
- Brandt, R. 1980. Application of SSNTD to nuclear physics: Multiprong events in heavy ion reactions due to multiple sequential fission. *Nuclear Instruments and Methods*, **173**: 111-119.
- Khan, E.U., Shahzad, M.I., Khattak, F.N., Blauch, J.J., Qureshi, I.E., Khan, H.A. 1998. Reaction cross-section of (14.0 MeV/u) $^{208}\text{Pb} + ^{197}\text{Au}$. *The Nucleus*, **35**: 139-144.
- Khan, E.U., Qureshi, I.E., Shahzad, M.I., Khattak, F.N., Khan, H.A. 2001. Emission of intermediate mass fragments in the heavy ion reaction of (14.0 MeV/u) $\text{Pb} + \text{Au}$. *Nuclear Physics A*, **690**: 723-730.
- Khan, E.U., Vater, P., Brandt, R., Khan, H.A., Jamil, K., Khan, N.A., Sial, M.A. 1984. Emission of light and energetic medium masses in multiparticle exit channel in the reaction $^{218}\text{U} + ^a\text{U}$ and $^{23}\text{U} + \text{Au}$ at 16.7 MeV energy. *Communication Note*, CEA-N-2406, 40-44.
- Nasir, T., Khan, E.U., Baluch, J.J., Qureshi, I.E., Sajid, M., Shahzad, M.I., Khan, H. A. 2008. Measurement of distance parameter using semi-classical model in various heavy ion interactions. *Radiation Measurements*, **43**: S279-S282.
- Nasir, T., Khan, E.U., Baluch, J.J., Shafi-ur-Rehman, Matiullah, Rafiq, M. 2009. Sequential and double sequential fission observed in heavy ion interaction of (11.67 MeV/u) ^{197}Au projectile with ^{197}Au target. *Brazilian Journal of Physics*, **39**: 539-542.
- Vater, P., Khan, E.U., Beckmann, R., Gottschalk, P.A., Brandt, R. 1986. Sequential fission studies in the interaction of 9.03 MeV/N ^{238}U and ^{nat}U using mica track detectors. *International Journal of Radiation Applications and Instrumentation. Part D. Nuclear Tracks and Radiation Measurements*, **11**: 5-16.

Synthesis and Reactivity of Some Peroxo Complexes of Zirconium(IV) Thorium(IV) and Uranium(VI) Ions Containing a Quadridentate, Quadrinegative Ligand and a Pentadentate Dinegative Schiff Base

Md. Tofazzal Hossain Tarafder*, Svash Chandra Pal and Md. Rabiul Karim

Department of Chemistry, Rajshahi University, Rajshahi - 6205, Bangladesh

(received May 5, 2009; revised January 25, 2010; accepted January 30, 2010)

Abstract. Some new peroxo complexes of zirconium, thorium and uranium containing a quadridentate, quadrinegative organic ligand and a pentadentate dinegative Schiff base ligand have been synthesized and characterized by elemental analyses, magnetic measurements and various spectral studies. Oxygen transfer reactions of some complexes toward different substrates have been investigated. The Schiff base, LH₂, was derived from the condensation of 2,6-diaminopyridine with salicylaldehyde. The present ligands undergo deprotonation during complexation coordinating with (OOOO)⁴⁻ and ⁻ONNNO donor sequences, respectively. The complexes have the compositions, [M(O₂) (OOOO)]. 2H₃O⁺ [M = Zr(IV) and Th(IV), OOOO = DCTA], [UO(O₂) (OOOO)].2H₃O⁺; [M(O₂) (ONNNO)] [M = Zr(IV) and Th(IV), ⁻ONNNO = L] and [U(O) (O₂) (ONNNO)].H₂O. The chelate effect of the quadridentate and pentadentate ligands stabilizes the metal peroxide moieties precluding oxygen transfers to organic and inorganic substrates. The mode of coordination is also influenced by the σ-donor electronic nature of the multidentate ligands. The IR spectral data also indicate that the ν₁(O-O) stretching modes decrease with and increase in the atomic number of the metals in a group.

Keywords: peroxo complexes, quadridentate and pentadentate ligands, heavy metal ions

Introduction

The chemistry of peroxo complexes has received considerable attention in recent years. Metal peroxides incorporated with other co-ligands exhibit different reactivities. The metal peroxo complexes are potential sources of active oxygen atoms and can be employed as efficient stoichiometric as well as catalytic reagents for the oxidation of organic and inorganic substrates. Peroxo complexes containing monodentate and bidentate auxiliary ligands have been found to be the sources of active oxygen atoms for oxidation reactions. Complexes containing tridentate and quadridentate co-ligands were inert towards such oxidative processes (Sharma *et al.*, 2009; Bonchio *et al.*, 2001; Justino *et al.*, 2000; Tarafder and Khan, 1991a; 1991b; 1987; Tarafder and Islam, 1989; Tarafder, 1987; Tarafder and Ahmed, 1986; Tarafder and Miah, 1986; Westland and Tarafder, 1982; 1981; Westland *et al.*, 1980; Mimoun, 1980; Jacobson *et al.*, 1978). The crystal structures of many of these complexes have also been reported (Ole *et al.*, 2008; Kondo *et al.*, 2008; Hou *et al.*, 2006; Nica *et al.*, 2005; Kaizer *et al.*, 2004; Hinnerb *et al.*, 2003; Chishiro *et al.*, 2003; Deubel *et al.*, 2001; Lewis and Wilson, 2001; Meyer and Pritzkow, 2000). However, there seems to be no reports on peroxo complexes containing some multidentate ligands with OOOO and ONNNO donor sequences.

In the present studies, synthesis of some novel peroxo complexes of Zr(IV), Th(IV) and U(VI) containing a quadridentate, quadrinegative and a pentadentate, dinegative ligands and their potential as oxygen transfer reagents have been reported. An attempt is also made to correlate the effect of the size of the metal ions on the ν₁(O-O) stretching modes from the IR spectra of the complexes. The structures of the ligands are shown in Fig. 1 and 2.

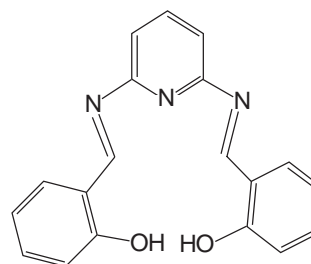


Fig. 1. LH₂: Bis-N,N'-(2-hydroxyphenylmethylene)2,6-diaminopyridine.

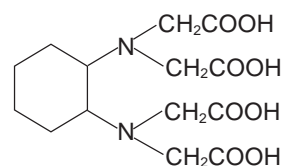


Fig. 2. 1,2-Diaminocyclohexane N,N'-tetraacetic acid.

*Author for correspondence; E-mail: ttofazzal@yahoo.com

Materials and Methods

Physical measurements. The infrared spectra of the complexes were obtained as KBr discs on a Pye Unicam SP3-300 infrared spectrophotometer in the range 4000-200 cm^{-1} . Electronic spectra were obtained on a Shimadzu UV-visible spectrophotometer in nujol mulls spreaded on a filter paper. Carbon, hydrogen and nitrogen analyses were carried out at the Instrumentation Centre, Central Drug Research Institute, Lucknow, India. Metals were determined gravimetrically by standard procedures. Molar masses were determined by the Rast method using camphor as medium.

Reagents and chemicals. All chemicals were of reagent grade and used as supplied by Merck or BDH Ltd. Ethanol was purified by refluxing with iodine and magnesium turnings and finally distilling and storing over molecular sieves.

Preparation of the Schiff base ligand of 2,6-diaminopyridine with salicylaldehyde, $\text{C}_{10}\text{H}_{13}\text{M}_3\text{O}_2\text{H}_2$ (LH_2). 2,6-Diaminopyridine (50 mmol, 5.4 g) was dissolved in boiling ethanol (150 mL) and filtered to remove the undissolved portion. To the clear, brown filtrate a solution of salicylaldehyde (100 mmol, 12.2 g) in ethanol (20 mL) was added and the mixture was kept under reflux for 8 h when the colour of the solution became orange-yellowish with a distinct turbidity. The mixture was then left overnight at room temperature when a brilliant orange-coloured solid appeared. It was then filtered and washed thoroughly with cold ethanol and dried *in vacuo* over fused CaCl_2 . Yield 7.5 g, and mp. 230 °C (d). Anal. calc., C, 72.38%; H, 4.13%; and N, 13.3%. Found: C, 72.52%; H, 4.01%; and N, 13.42%. Mass spectra of the Schiff base ligand showed diagnostic peaks at m/z 43, 69, 81 and 122.

Preparation of complexes. $[\text{Zr}(\text{O}_2)(\text{DCTA})]2\text{H}_3\text{O}^+$ (1**).** $\text{Zr}(\text{NO}_3)_4 \cdot 6\text{H}_2\text{O}$ (2 mmol, 0.89 g) dissolved in hot methanol (40 mL) was added to a solution of the DCTA (2 mmol, 0.73 g) in the same solvent (200 mL). To this mixture was added 30% H_2O_2 (50 mL). The volume of the mixture was reduced to *ca.* 100 mL when a white product appeared. It was then separated, washed successively with methanol and ether and finally dried *in vacuo* over fused CaCl_2 . Yield, 0.6 g.

$[\text{Th}(\text{O}_2)(\text{DCTA})]2\text{H}_3\text{O}^+$ (2**).** $\text{Th}(\text{NO}_3)_4 \cdot 5\text{H}_2\text{O}$ (2 mmol, 1.14 g) dissolved in hot methanol (40 mL) was cooled in an ice bath to which a solution of the DCTA (2 mmol, 0.73 g) in hot methanol (160 mL) was added followed by the addition of H_2O_2 (30%, 30 mL). The mixture was then heated at ~ 60 °C for 0.5 h, when a white product appeared. It was then left overnight at room temperature and the product was separated, washed successively with methanol and finally dried *in vacuo* over fused CaCl_2 . Yield 0.4 g.

$[\text{U}(\text{O})(\text{O}_2)(\text{DCTA})]2\text{H}_3\text{O}^+$ (3**).** $\text{UO}_2(\text{NO}_3)_2 \cdot 6\text{H}_2\text{O}$ (2 mmol, 1.04 g) dissolved in water (25 mL) was cooled in an ice bath and the solution of the DCTA (2 mmol, 0.73 g) in hot methanol (160 mL) was added to it followed by the immediate addition of 30% H_2O_2 (30 mL). The mixture was then stirred for 10 min when a yellow solid product appeared. The mixture was then kept in refrigerator for a few hours to allow the precipitate to settle. The product was then separated, washed successively with water and ether and then stored as above. Yield, 0.85 g.

$[\text{Zr}(\text{O}_2)\text{L}]$ (4**).** $\text{Zr}(\text{NO}_3)_4 \cdot 6\text{H}_2\text{O}$ (1 mmol, 0.45 g) was dissolved in methanol (30 mL) and a solution of the Schiff base (1 mmol, 0.3 g) in acetone (100 mL) was added to it followed by the addition of 30% H_2O_2 (40 mL). The volume of the mixture was then reduced to *ca.* 80 mL and kept at room temperature overnight, when a colourless crystalline product appeared. It was filtered, washed successively with water and acetone and finally dried *in vacuo* over fused CaCl_2 . Yield, 0.61 g.

$[\text{Th}(\text{O}_2)\text{L}]$ (5**).** To a solution of $\text{Th}(\text{NO}_3)_4 \cdot 5\text{H}_2\text{O}$ (1 mmol, 0.6 g) in water (20 mL), a solution of the Schiff base (1 mmol, 0.3 g) in acetone (40 mL) was added followed by quick addition of 30% H_2O_2 (30 mL) at 0 °C. After a few minutes the brownish product was separated by filtration, washed with cold acetone and finally stored *in vacuo* over fused CaCl_2 . Yield, 0.45 g.

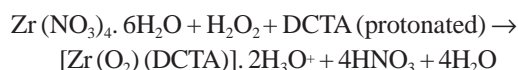
$[\text{UO}(\text{O}_2)\text{L}]\text{H}_2\text{O}$ (6**).** To a solution of $\text{UO}_2(\text{NO}_3)_2 \cdot 6\text{H}_2\text{O}$ (1 mmol, 0.5 g) in water (20 mL), a solution of the Schiff base (1 mmol, 0.3 g) in acetone (40 mL) was added followed by the addition of 30% H_2O_2 (50 mL) at 0 °C. A yellow product was produced which was separated, washed thoroughly with acetone and finally with ether and then stored *in vacuo* over fused CaCl_2 . Yield, 0.3 g.

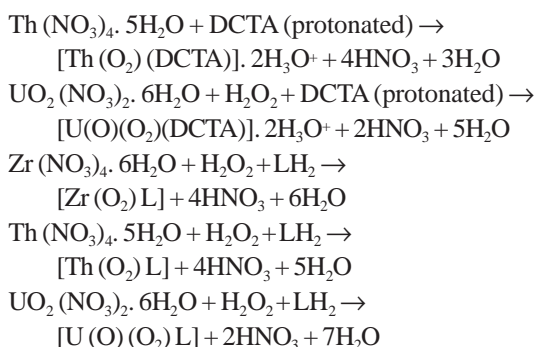
Attempted reactions of compounds (1**) and (**3**) with allyl alcohol, (**4**) with triphenylphosphine and (**5**) with triphenylarsine.** Refluxing **1** and **3** separately with allyl alcohol in a 1:1 molar ratio in 50 mL THF (tetrahydrofuran) medium for 48 h at 90 °C failed to produce any reaction. Compounds **1** and **3** were recovered unchanged.

Refluxing **4** or **5** with stoichiometric quantities of triphenylphosphine or triphenylarsine, in 50 mL THF, for 48 h at 90 °C failed to produce any reaction. Compounds **4** and **5** were recovered unchanged.

Results and Discussion

The syntheses of the present peroxo complexes are presented in the following scheme:





The analytical data of the complexes are presented in Table 1. The molar conductance measurements could not be made because the complexes were insoluble in almost all common organic solvents. The analytical and spectral data (Table 2) are consistent with six-fold coordination of Zr(IV) and Th(VI) in **1** and **2**, respectively, seven-fold coordination of U(VI), Zr(IV) and Th(IV) in complexes **3**, **4** and **5**, respectively, and eight-fold coordination of U(VI) in **6**.

Infrared spectral studies. The important IR spectral bands of the complexes are presented in Table 2. The ligand 1,2-diamino-

cyclohexane NNN©N© tetraacetic acid (the DCTA) is potentially quadridentate, quadrinegative coordinating *via* four carboxylato anions (OOO⁻) generated during complexation. The $\nu(\text{OH})$ band observed of the Hy DCTA at 3557 cm^{-1} disappeared in the complexes indicating deprotonation at the -OH group thus providing carboxylate binding in **1**, **2** and **3**. This is further evident from the appearance of strong $\nu(\text{C}=\text{O})$ (1635 - 1650 cm^{-1}) and $\nu(\text{C}-\text{O})$ (1380 - 1390 cm^{-1}) modes in the spectra of these complexes. Besides, the far-IR spectra of the complexes display bands (Tarafder, 1987; Tarafder and Khan, 1987; Westland and Tarafder, 1982; 1981) at 320-375 cm^{-1} assignable to $\nu(\text{M}-\text{O}^\ominus)$ modes. Complexes **4** - **6** show characteristic strong $\nu(\text{C}=\text{N})$ modes at 1540-1560 cm^{-1} , suggesting that the ring and imino nitrogen of the Schiff base had been coordinated to the metals (Mimoun *et al.*, 1982). This is also apparent from the $\nu(\text{M}-\text{N})$ modes at ~ 300 cm^{-1} in the far-IR spectra of these complexes (Tarafder and Khan, 1991a; 1991b). The complexes **3** and **6** showed very strong diagnostic $\nu(\text{U}=\text{O})$ bands (Tarafder and Islam, 1989; Tarafder *et al.*, 1989; Westland and Tarafder, 1981) at ~ 900 cm^{-1} . The metal peroxo moiety

Table 1. Analytical data and some physical properties of the Hy DCTA and LH₂ peroxo complexes

Compound ^{a, b}	Molecular mass; found (calculated)	Melting point (°C)	Found (calculated), x			
			C	H	N	Metal
1. [Zr(O ₂)(DCTA)].2H ₃ O ⁺ (C ₁₄ H ₂₄ O ₁₂ N ₂ Zr)	490.20 (503.22)	>160	33.09 (33.38)	4.31 (4.77)	5.39 (5.56)	17.82 (18.13)
2. [Th(O ₂)(DCTA)].2H ₃ O ⁺ (C ₁₄ H ₂₄ O ₁₂ N ₂ Th)	632.50 (644.03)	110-115(d)	26.18 (26.09)	3.27 (3.73)	4.18 (4.35)	35.75 (36.03)
3. [U(O)(O ₂)(DCTA)].2H ₃ O ⁺ (C ₁₄ H ₂₄ O ₁₃ N ₂ U)	660.40 (666.03)	150-160(d)	25.45 (25.22)	3.29 (3.60)	4.20 (4.20)	35.50 (35.74)
4. [Zr(O ₂)L] (C ₁₉ H ₁₃ O ₄ N ₃ Zr)	430.30 (438.22)	80	51.85 (52.03)	2.82 (2.97)	9.51 (9.58)	20.59 (20.82)
5. [Th(O ₂)L] (C ₁₉ H ₁₃ O ₄ N ₃ Th)	570.30 (579.03)	>280	39.10 (39.38)	2.28 (2.25)	7.10 (7.25)	39.72 (40.07)
6. [UO(O ₂)L].H ₂ O (C ₁₉ H ₁₅ O ₆ N ₃ U)	608.04 (619.03)	240-250(d)	36.62 (36.83)	2.51 (2.42)	6.82 (6.78)	38.20 (38.45)

^a = DCTA = deprotonated 1,2-diaminocyclohexane NNN'N'-tetraacetic acid, (C₁₄H₁₈O₈N₂)⁴⁻; ^b = L = deprotonated Schiff base, (C₁₉H₁₃O₂N₃)²⁻; d = decomposition.

Table 2. Characteristic infrared spectral bands of the complexes (band maxima in cm^{-1})

Compd.	$\nu(\text{C}-\text{O})$	$\nu(\text{C}=\text{O})$	$\nu(\text{C}=\text{N})$	$\nu_1(\text{O}-\text{O})$	$\nu_3(\text{MO}_2)$	$\nu_2(\text{MO}_2)$	$\nu(\text{U}=\text{O})$	$\nu(\text{M}-\text{O}')$	$\nu(\text{M}-\text{N})$
1.				925 m	540 m	500 m			
2.	1390 vs	1650 s		890 m	540 w	500 m			295 m
3.	1380 m	1635 s		840 vs	600 m	500 w	900 vs		295 w
4.			1560 vs	890 vs	618 vs	550 vs		375 vs	300 w
5.			1560 vs	830 m	620 m	540 w		320 w	295 s
6.			1540 s	810 m	600 m	520 w	910 vs	350 vs	295 w

(local C_{2v} symmetry) gives three infrared and Raman-active vibrational modes *viz.*, (i) O-O stretching (ν_1), (ii) the symmetric M-O stretching (ν_2) and (iii) the asymmetric M-O stretching (ν_3). The characteristic ν_1 (O-O) stretching bands of compounds **1-6** appeared at 810-925 cm^{-1} (Table 2). The ν_1 modes are shifted to lower wave numbers upon passing from zirconium compounds **1** and **4** (925 and 890 cm^{-1}) to the corresponding thorium analogues, **2** and **5** (890 and 830 cm^{-1}), indicating that for the $M(\text{O}_2)$ grouping, the ν_1 (O-O) stretching band decreases with an increase in the atomic number of the metals in a group. The present complexes exhibit ν_2 and ν_3 modes at 500-550 cm^{-1} and 540-620 cm^{-1} , respectively. It is important, however, that the ν_1 modes of the present zirconium, thorium and uranium complexes appear at lower frequencies than the peroxo complexes of these metals containing mono-, bi- and tridentate ancillary ligands (Tarafder and Islam, 1989; Westland and Tarafder, 1981;). This is presumably due to the greater charge neutralization of the metal centres by the quadridentate, quadrinegative and pentadentate dinegative s-donor ligands causing a weaker coulombic interaction in the $M^{n+}-\text{O}_2^-$ moieties ($n = 4$ or 6). The protonic nature of the complexes **1-3** is evident from the positive response of these complexes to litmus solution. These complexes showed conductivity values of the order $\sim 10^{-4}$ ohm/cm in their saturated aqueous solutions. The alkalimetric titration to determine the number of acidic protons outside the coordination sphere could not be carried out, because the complexes were very poorly soluble in water. Bands at ~ 3400 cm^{-1} in **1**, **2** and **3** arise from hydronium ions outside the coordination sphere.

Magnetic measurements and electronic spectra. Magnetic measurements were carried out in Nujol mulls spreaded on a filter paper and all the complexes were found to be diamagnetic in nature. The electronic spectra revealed that the complexes showed various bands in the range 245 - 385 nm, presumably arising from metal to ligand charge transfers.

Reactivity. The present peroxo complexes were found to be inert towards olefins and other substrates. Complexes **1** and **3** failed to oxidize allyl alcohol even when refluxing was continued at ~ 90 °C for 48 h. Complexes **4** and **5** also did not react with triphenylphosphine or triphenylarsine. These negative results outline the greater stability of the metal peroxo moiety in the presence of the quadridentate, quadrinegative and the pentadentate, dinegative chelating ligands which hinder oxygen transfers. A similar behaviour was observed for various peroxo complexes containing multidentate ligands (Tarafder and Khan, 1991a; 1991b; Tarafder and Islam, 1989; Tarafder, 1987). According to Mimoun *et al.* (1982) and Mimoun (1980), although the insertion of substrates into the

metal peroxo triangle forming a metallocycle is an agreed process, the presence of multidentate ligands stabilize the triangle to such an extent that nucleophiles (Ph_3P or Ph_3As) apparently fail to open up the triangle, thus precluding oxygen transfers.

References

- Bonchio, M., Bortolini, O., Conte, V., Moro, S. 2001. Characterization and reactivity of triperoxo vanadium complexes in protic solvents. *European Journal of Inorganic Chemistry*, 2913-2919.
- Chishiro, T., Shimazaki, Y., Tani, F., Tachi, Y., Naruta, Y., Karasawa, S., Hayami, S., Maeda, Y. 2003. Isolation and crystal structure of a peroxo-bridged heme-copper complex. *Angewandte Chemie International Edition*, **115**: 2894-2897.
- Deubel, D.V., Sundermeyer, J., Frenking, G. 2001. Olefin epoxidation with transition metal η 2-peroxo complexes: The control of reactivity. *European Journal of Inorganic Chemistry*, 1819-1827.
- Hinnerb, M. J., Grosche, M., Herdtweck, E., Thiel, W. R. 2003. A merrifield resin functionalized with molybdenum peroxo complexes: Synthesis and catalytic properties. *Zeitschrift für Anorganische und Allgemeine Chemie*, **629**: 2251-2257.
- Hou, S.Y., Zhou, Z.H., Lin, T.R., Wan, H.L. 2006. Peroxotungstates and their citrate and tartrate derivatives. *European Journal of Inorganic Chemistry*, 1670-1677.
- Jacobson, S.E., Tang, R., Mares, F. 1978. Group 6 transition metal peroxo complexes stabilized by polydentate pyridinecarboxylate ligands. *Inorganic Chemistry*, **7**: 3055-3063.
- Justino, L.L.G, Ramos, M.L., Caldeira, M.M., Gil, V.M.S. 2000. Peroxovanadium(V) complexes of L-lactic acid as studied by NMR spectroscopy. *European Journal of Inorganic Chemistry*, 1617-1621.
- Kaizer, J., Pap, J., Speier, G., Pa' rka' nyi, L. 2004. The Reaction of μ - η 2: η 2-peroxo- and bis(μ -oxo)dicopper complexes with flavonol. *European Journal of Inorganic Chemistry*, 2253-2259.
- Kondo, S., Karuhashi, K., Seki, K., Matsubara, K., Miyaji, K., Kubo, T., Matsumoto, K., Katsuki, T. 2008. A μ -Oxo - μ - η 2: η 2-Peroxo titanium complex as a reservoir of active species in asymmetric epoxidation using hydrogen peroxide. *Angewandte Chemie International Edition*, **47**: 10195-10198.
- Lewis, G.R., Wilson, C. 2001. Mue-Peroxo-bis[trans-chloro (1,4,8,11-tetraazacyclotetradecane)cobalt(III)] bis (tetraphenylborate) diacetone solvate. *Acta Crystallographica C*, **57**: 1159 -1161.

- Meyer, F., Pritzkow, H. 2000. μ_4 -Peroxo versus bis(μ_2 -hydroxo) cores in structurally analogous tetracopper(II) complexes. *Angewandte Chemie International Edition*, **39**: 2112-2115.
- Mimoun, H., Postel, M., Casabianca, F., Fischer, J., Mitschler, A. 1982. Novel unusually stable peroxotitanium(IV) compounds. Molecular and crystal structure of peroxobis(picolinato) (hexamethylphosphoric triamide) titanium(IV). *Inorganic Chemistry*, **21**: 1303-1306.
- Mimoun, H. 1980. The role of peroxymetallation in selective oxidative processes. *Journal of Molecular Catalysis*, **7**: 1-29.
- Nica, S., Pohlmann, A., Plass, W. 2005. Vanadium (V) oxoperoxo complexes with side chain substituted *N*-salicylidenehydrazides: modeling supramolecular interactions in vanadium haloperoxidases. *European Journal of Inorganic Chemistry*, 2032-2036.
- Ole, S., Anja H., Christian, N., Christian W., Max, C.H., Siegfried, S., Felix, T. 2008. Aromatic hydroxylation in a copper bis(imine) complex mediated by a μ - η^2 : η^2 peroxo dicopper core: A mechanistic scenario. *Chemistry-A European Journal*, **14**: 9714-9729.
- Sharma, M., Saleem, M., Pathania, M.S., Sheikh, H.N., Kalsotra, B.L. 2009. Peroxo complexes of molybdenum (VI) containing mannich base ligands. *Chinese Journal of Chemistry*, **27**: 311-316.
- Tarafder, M.T.H., Khan, A.R. 1991a. Peroxo complexes of zirconium(IV), thorium(IV), molybdenum(VI), tungsten(VI) and uranium(VI) containing a quadridentate SNNS Schiff base. *Polyhedron*, **10**: 973-976.
- Tarafder, M.T.H., Khan, A.R. 1991b. Peroxo complexes of zirconium(IV), thorium(IV), molybdenum(VI), tungsten(VI) and uranium(VI) containing two quadridentate ONNO Schiff bases. *Polyhedron*, **10**: 819-822.
- Tarafder, M.T.H., Islam, A.A.M.A. 1989. Peroxo complexes of Zr(IV), Th(IV), W(VI) and U(VI) ions stabilized by multidentate organic ligands. *Polyhedron*, **8**: 109-112.
- Tarafder, M.T.H., Howlader, M.B.H., Nath, B., Islam, A.A.M.A. 1989. Peroxo complexes of Zr(IV), Th(IV), Mo(VI) and U(VI) ions containing some bidentate organic ligands. *Polyhedron*, **8**: 977-981.
- Tarafder, M.T.H. 1987. Adduct type peroxo complexes of thorium. *Indian Journal of Chemistry*, **26A**: 874-876.
- Tarafder, M.T.H., Khan, A.R. 1987. Some organoperoxo complexes of molybdenum and tungsten. *Polyhedron*, **6**: 275-279.
- Tarafder, M.T.H., Ahmed, A. 1986. Some organoperoxo complexes of Zr(IV), Th(IV), Mo(VI), W(VI) and U(VI). *Indian Journal of Chemistry*, **25A**: 729-732.
- Tarafder, M.T.H., Miah, M.A.L. 1986. Novel peroxo complexes of zirconium containing organic ligands. *Inorganic Chemistry*, **25**: 2265-2268.
- Westland, A.D., Tarafder, M.T.H. 1982. Novel peroxo complexes of thorium containing organic ligands. *Inorganic Chemistry*, **21**: 3228-3232.
- Westland, A.D., Tarafder, M.T.H. 1981. Novel peroxo complexes of uranium containing organic ligands. *Inorganic Chemistry*, **20**: 3992-3995.
- Westland, A.D., Haque, F., Bouchard, J.M. 1980. Peroxo complexes of molybdenum and tungsten stabilized by oxides of amines, phosphines, and arsines. Stability studies. *Inorganic Chemistry*, **19**: 2255-2259.

Thermal Activation of Bagasse Ash in High Strength Portland Cement Mortar

Noor-ul-Amin

Department of Chemistry, Abdul Wali Khan University, Mardan, Pakistan

(received September 18, 2009; revised January 27, 2010; accepted January 28, 2010)

Abstract. The pozzolonic reactivity of bagasse ash was enhanced using thermal activation technique by curing mortar specimens containing bagasse ash, at 20, 40 and 60 °C and the samples were tested for compressive strength at the age of 3, 7 and 28 days. Results indicated that bagasse ash is very sensitive to temperature rise and thus the application of thermal activation is very useful when early age strength development is desired. Bagasse replacement by 30% at 40 °C and 60 °C increased the mortar strength at 7 days by 10 and 18% more than the control, respectively.

Keywords: bagasse ash, thermal activation, portland cement mortar

Introduction

Different types of pozzolanic material are widely used for cement replacement in high strength Portland cement mortars and concrete for improving mechanical properties and durability and bringing environmental and economic benefits. The reasons for partially replacing cement in mortar and concrete with pozzolanic materials are diverse, which include strength enhancement and improvement in durability (Coleman and Page, 1997; Wild *et al.*, 1996; Caldarone *et al.*, 1994). There are also clear environmental advantages in reducing the quantity of cement used in construction materials. Indeed, cement production is highly energy intensive process involving significant environmental damage with respect to CO₂ production and raw material acquisition (Schindler, 2004).

Various studies have investigated ways to enhance the reactivity of the pozzolanic material. The principal aim of these attempts was to enhance the reactivity of the pozzolan, so as to improve the mechanical and durability properties of the final product. Prolonged grinding curing at elevated temperatures, alkali-activation and chemical activation are some of the methods that have been used to achieve this target (Xie and Xi, 2001; Shi and Day, 2000; 1995; 1993; Palomo *et al.*, 1999; Bouzoubaa *et al.*, 1997). The efficiency, however of some of these methods is debatable being too energy demanding, while others fail simple cost-benefit analysis. For example Helmuth (1994) suggested the grinding of Portland cement to very high specific area for use with slag to overcome the problem of low early strength. Schroder (1968) showed that with slag contents up to about 50-60%, the early strength is mainly determined by the fineness of

E-mail: noorulamin_xyz@yahoo.com

the clinker fraction and then by that of the slag fraction. With cements of higher slag content, the fineness of slag was found to be of major importance at all ages. Wainwright and Tolloczko (1986), using temperature matched curing, indicated that concretes containing 50 and 70% slag replacement were far more sensitive to increases in temperature, with respect to their strength development, than equivalent Portland cement concretes. Further, Brooks and Al-Kaisi (1990) were able to use the adiabatic temperature rise of mass concrete to estimate the strength of OPC and OPC/slag concretes. They observed that 28-day strength of OPC/slag clearly exceeded those of OPC concrete only. This difference in behaviour has been attributed to the reduction of the overall quantity of C₃S in blended cement, which results in some C₃S hydrates being replaced by slower forming slag hydrates.

The objective of the present work is to evaluate the bagasse ash as supplementary cementitious material and its activation by thermal method to enhance the reactivity of bagasse ash and to improve the mechanical properties and durability of the final mortar.

Materials and Methods

Chemical composition of high strength Portland cement and bagasse ash used are given in Table 1 and physical parameters of bagasse ash, in Table 2. High strength Portland cement was ground to a fineness of 310 m²/kg. The sand used in the mortar had a specific gravity of 2.5 and a fineness modulus of 2.65. Bagasse ash was obtained from the Premier Sugar Mill Mardan (PSM), Khazana Sugar Mill Peshawar (KSM) and Frontier Sugar Mill (FSM), Thakthbai, Mardan. The samples were collected randomly from the heaps present in the yard of

Table 1. Chemical composition of cement and bagasse ash

Material	SiO ₂	Al ₂ O ₃	Fe ₂ O ₃	CaO	MgO	Na ₂ O	K ₂ O	SO ₃
Cement	21.55	5.69	3.39	64.25	0.85	0.33	0.59	2.47
Bagasse ash	87.40	3.60	4.90	2.56	0.69	0.15	0.47	0.11

Table 2. Physical parameters of bagasse ash

Moisture (%)	Ash (%)	LOI (%)	Calorific value (kcal/kg)	Fineness passing 50 µm sieve
2.93	86.69	8.45	50	50

the sugar mills and carried to the laboratory in polyethylene bags. Bagasse ash was black in color due to the high amount of carbon content. The mill fired bagasse ash was further burnt under controlled temperature at 90 °C for one hour, which brought down the carbon content up to 4.5 %.

Determination of setting time. Setting time of the mortars was determined in accordance with British Standard EN196-3 (2005a) using the Vicat apparatus.

Determination of compressive strength. Compressive strength of all the mortars was tested according to British Standard EN196-1 (2005b). Cement-sand-water mass ratio was 1-3-0.5. The mixtures were tested for compressive strength at 3, 7, and 28 days. Three cubes were tested for each data point and the average were reported with standard deviation less than 8%. The samples were remolded, 24 h after casting, and then cured in a controlled environment at 98% relative humidity at the temperature of 20, 40 and 60 °C until tested.

Results and Discussion

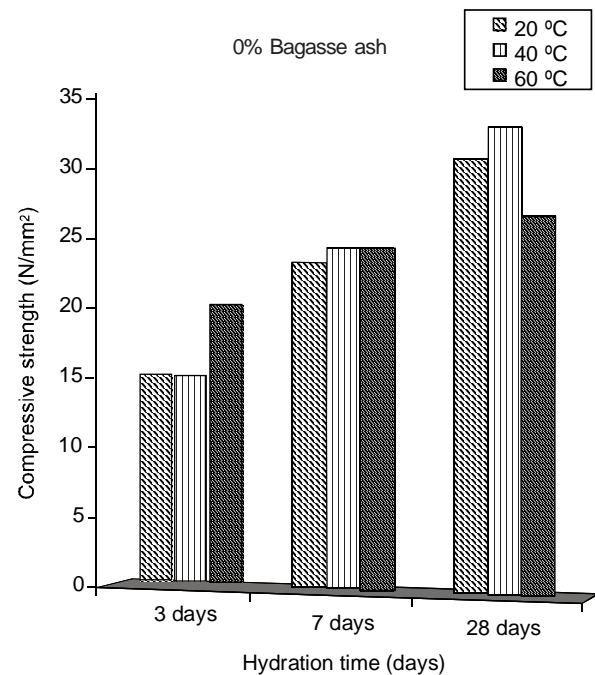
Setting time. Table 3 presents the result of the setting time. It is evident that the effect of increasing bagasse ash replacement level was to delay the initial setting time of mortar probably resulting from the dilution effect and the latent properties (Eren, 2002). The effect of 30% ash replacement resulted in retardation in the initial and final setting time

Table 3. Setting time of the mortars containing bagasse ash

Bagasse ash (wt%)	Initial setting time (min)	Final setting time (min)
0	145	188
30	210	279
50	221	290

by about 1 h and 1.5 h, respectively. However, increasing bagasse ash content from 30% to 50% did not produce any significant difference in the setting time.

Compressive strength with activated ash. Compressive strength development for the cement mortars containing different percentages of bagasse ash, cured at different temperatures is shown in Fig. 1-3. A general feature observed in all the samples is that the initial strength increased with an increase in temperature, but this tendency is reversed with aging. This behaviour is similar to that observed by several other investigators (Eren, 2002). It suggests that curing at higher temperature results in non-uniform distribution of the hydration products within the microstructure, while at low temperature, hydration products have sufficient time to diffuse and precipitate relatively more uniformly throughout the cement matrix. The results of increasing curing temperature from 20 °C to 40 °C can be compared with those of Barnett *et al.* (2006), who studied in UK that mortars containing 35% slag replacement, gained 115% of strength after 3 days. However, mortars with 30% bagasse ash content achieved 90% of strength gain after the same period. This result indicated that bagasse ash was less sensitive to elevated temperatures than slag. This could be explained by their different activation energies. Fig. 2 and 3 show that at 28 days the reduction in strength, as a result of increasing

**Fig. 1.** Effect of curing temperature on the mortar strength without bagasse ash.

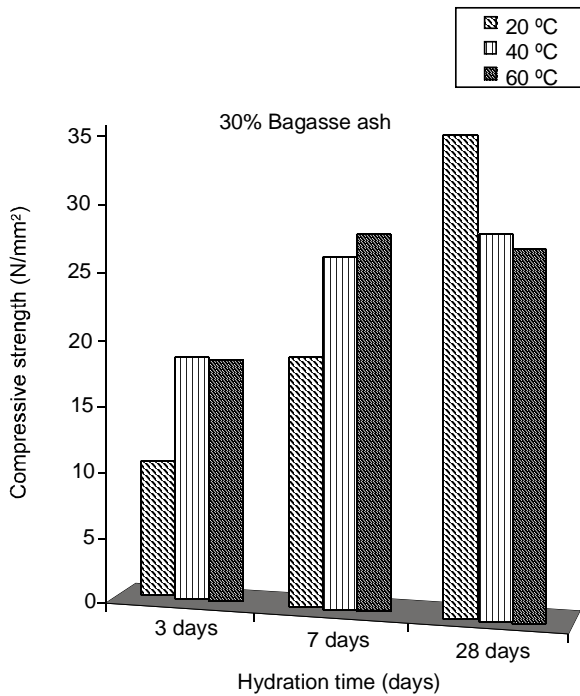


Fig. 2. Effect of curing temperature on the ash mortar strength containing 30% bagasse ash.

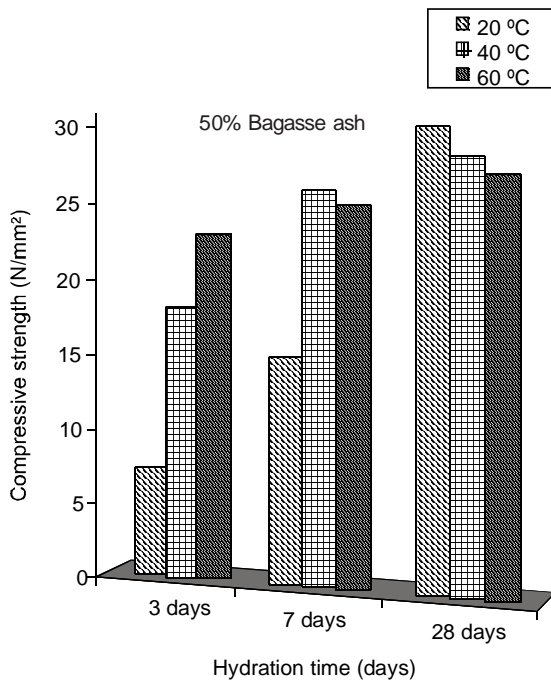


Fig. 3. Effect of curing temperature on the ash mortar strength containing 50% bagasse ash.

temperature in the mortars incorporating 30 and 50% of ash, was more pronounced than the corresponding mortars cured at 20 °C. The difference in strength development between the mortars was clearly apparent as shown in the figures. Cement mortars cured at 40 and 60 °C started to show a reduction in strength development after about one week compared with mortar cured at 20 °C. However, in bagasse ash cement mortars with 30 and 50% replacement level, strength development started to slow down after about 2 and 3 weeks, respectively. This suggests that increase in ash replacement will delay the reduction of strength development. Some authors referred to this phenomenon as the cross-over effect. Eren (2002) reported similar finding using fly ash to combat the loss of strength that would have resulted from the use of cement concrete without any replacement. The gain in strength development at early age increased with the increase in ash content and the loss of strength decreased also with the increase in ash content at later age. This shows the beneficial effect of incorporating bagasse ash in concrete when applying thermal activation. Thus, ash cement is more sensitive to changes in temperature than high strength Portland concrete. These findings are in agreement with the results observed by Wainwright and Tolloczko (1986). The strength of mortar containing 30% ash cured at 40 °C reached that of the mortar cured at 60 °C after 3 days of curing and exceeded it after 28 days. With 50% replacement level, the mortar cured at 40 °C achieved the strength of 60 °C cured mortar after 7 days and exceeded it after 28 days. The effect of curing at 40 °C and 60 °C was to increase the early age strength of bagasse ash mortar (both for 30% and 50% replacement) over that of the ash mortar, cured at 20 °C. This initial gain in strength for ash mortar, as a result of temperature, slows down after about 10 days but picks up again for the mortar, cured at 40 °C, reaching that of the counterpart cured at 20 °C. This suggests that 40 °C is the optimum temperature for strength development in both 30 and 50% ash cement mortars. In the same way, Escalante-Garcia and Sharp (2001) found the optimum temperature, in slag-cement paste with 60% of slag, to be around 30 °C. The highest strength value was reported for the mortar containing 30% bagasse ash cured at 40 °C, indicating that this replacement level is the most favourable for this blended cement.

Conclusion

Thermal treatment of bagasse ash is a very good activation technique to increase the strength development of mortar. The gain in strength at 7 days for mortar with 30% bagasse ash replacement cured at 40 °C and 60 °C was 10 and 18% higher than those for the control, respectively. The test results demonstrate that the application of thermal activation

is very useful when early age strength development is desired. Increasing curing temperature for ash cement mortar increases the strength at early age and reduces it at later age. The curing temperature of 40 °C seems to be optimum for strength development of the ash cement.

References

- Barnet, S.J., Soutsos, M.N., Millard, S.G., Bungey, J.H. 2006. Strength development of mortars containing ground granulated blast-furnace slag: Effect of curing temperature and determination of apparent activation energies. *Cement and Concrete Research*, **36**: 434-440.
- Bouzoubaa, N., Zhang, M.H., Bilodeau, A., Malhotra, V.M. 1997. The effect of grinding on the physical properties of fly ashes and a high strength Portland cement clinker. *Cement and Concrete Research*, **27**: 1861-1874.
- British Standard EN 196-3, 2005a. Methods of testing cement. Part 3. *Determination of Setting Times and Soundness*, British Adopted European Standards, pp. 18, British Standards Institution, UK.
- British Standard EN 196-1, 2005b. Methods of testing cement. Part 1. *Determination of Strength*. British Adopted European Standards, British Standards Institution, UK.
- Brooks, J.J., Al-Kaisi, A.F. 1990. Early strength development of Portland and slag cement concretes cured at elevated temperatures. *ACI Materials Journal*, **87**: 503-507.
- Caldarone, M.A., Gruber, K.A., Burg, R.G. 1994. High reactivity metakaolin: a new generation mineral admixture. *Concrete International*, **16**: 37-40.
- Coleman, N.S., Page, C.L. 1997. Aspect of the pore solution chemistry of hydrated cement pastes containing metakaolin. *Cement and Concrete Research*, **27**: 147-154.
- Eren, O. 2002. Strength development of concrete with ordinary Portland cement, slag or fly ash cured at different temperatures. *Materials and Structures/Materiaux et Construct*, **35**: 536-540.
- Escalante-Garcia, J.I., Sharp, J.H. 2001. The microstructure and mechanical properties of blended cements hydrated at various temperatures. *Cement and Concrete Research*, **31**: 695-702.
- Helmuth, R.A. et al., 1994. *Performance of Blended Cements made with Controlled Particle Size Distribution*. ASTM SP897, G. Frohnsdorff (ed.), Philadelphia, USA.
- Palomo, A., Grutzeck, M.W., Blanco, M.T. 1999. Alkali-activated fly ashes; a cement for the future. *Cement and Concrete Research*, **29**: 323-332.
- Schindler, A.K. 2004. Effect of temperature on hydration of cementitious materials. *ACI Materials Journal*, **101**: 72-81.
- Schroder, F. 1968. Blast furnace slag and slag cements. In: *Proceeding of Fifth International Symposium on the Chemistry of Cements*, vol. 4, pp.149-199, Tokyo, Japan.
- Shi, C., Day, R.L. 2000. Pozzolanic reaction in the presence of chemical activators. Part I: Reaction kinetics. *Cement and Concrete Research*, **30**: 51-58.
- Shi, C., Day, R.L. 1995. Acceleration of the reactivity of fly ash by chemical activation. *Cement and Concrete Research*, **25**: 15-21.
- Shi, C., Day, R.L. 1993. Acceleration of strength gain of lime-pozzolan cements by thermal activation. *Cement and Concrete Research*, **23**: 824-832.
- Wainwright, P.J., Tolloczko, J.J.A. 1986. Early and later age properties of temperature cycled slag-OPC concretes. In: *Proceedings of The Second International Conference on Fly Ash Silica and Fume, Slag and Natural Pozzolanas in Concrete*, CANMET/ACI SP-91, vol. 2, pp. 1293-1321.
- Wild, S., Khatib, J.M., Jones, A. 1996. Relative strength, pozzolanic activity and cement hydration in super-plasticised metakaolin concrete. *Cement and Concrete Research*, **26**: 1537-1544.
- Xie, Z., Xi, Y. 2001. Hardening mechanisms of an alkaline-activated class F fly ash. *Cement and Concrete Research*, **31**: 1245-1249.

Extraction and Characterisation of *Dioclea reflexa* Hook. F. Seed Oil

Faleye Francis Jide

Chemistry Department, University of Ado-Ekiti, PMB 5363, Ado-Ekiti, Nigeria

(received July 14, 2009; revised February 4, 2010; accepted February 13, 2010)

Abstract. Physicochemical analysis of the oil of *Dioclea reflexa* Hook f. seeds revealed the acid value, saponification value, iodine value, ester value and iodine number of the seeds to be 8.69 mg KOH/g, 251 mg KOH/g, 72.8 mg I/g, 242 and 27.9, respectively. The fatty acid composition determined by gas chromatography (GC) showed individual unsaturated fatty acid to be oleic acid (18:1), 0.8%, while the saturated fatty acids were palmitic acid (16:0), 10.2% and stearic acid (18:0), 21.9%. The infrared spectroscopy (IR) of the oil was also undertaken. The high saponification and iodine values of *D. reflexa* oil suggest its possible utilization in alkyd resin, shoe polish, liquid soap and shampoo production.

Keywords: *Dioclea reflexa*, physicochemical analysis, Fabaceae, fatty acid, seed oil

Introduction

Dioclea reflexa Hook. f. belongs to the family, Fabaceae. It is a hairy woody climbing shrub. It is widely spread in tropical and subtropical areas and is often considered a food crop. The seeds are arranged in pods, which are very hard and brownish in colour. *D. reflexa*, the marble vine, is highly regarded in some parts of Africa. The spherical seeds are used in games; root decoctions used to alleviate coronary pain; seed and root extracts are said to have insecticidal properties (Allen and Allen, 1981). The seeds are used to kill head lice by milling the cotyledons and mixing it with hair cream while the roasted cotyledons, are used for curing piles (Gill, 1992). The anti-microbial activity and phytochemical analysis of crude ethanolic leaf extract of *D. reflexa* has been reported. The leaf extract was reported to show broad spectrum antibacterial activity against *Staphylococcus aureus*, *Proteus mirabilis*, *Klebsiella pneumoniae*, *Salmonella typhi*, *Streptococcus pneumoniae*, *Escherichia coli*, *Candida albicans*, *Aspergillus flavus* and *Fusarium solani* (Ogundare and Olorunfemi, 2007). The phytochemical analysis of the leaf extract showed the presence of alkaloids, tannins, phenols and glycosides (Ogundare and Olorunfemi, 2007).

In Nigeria, the seeds of *Mucuna pruriens*, another species, are used in popular medicine for prevention against the effects of snake (*Echis carinatus*, *Naja naja*) bite (Guerranti *et al.*, 1999). Proteins inducing an immune response against the venom of *Echis carinatus* have been isolated from the cold water extract of the seeds of *Mucuna pruriens* (Guerranti *et al.*, 2002). The present study was carried out to investigate the physicochemical properties and fatty acid compositions of the seed oil of *D. reflexa* Hook f.

E-mail: fjfaleye2002@yahoo.com

Materials and Methods

Plant material. *Dioclea reflexa* Hook. f. (Fabaceae) seeds were obtained from Iropora Ekiti in Ekiti State, Nigeria. They were authenticated by Mr. F. O. Omotayo of the Herbarium Section, Department of Botany, University of Ado-Ekiti, Ado-Ekiti, Ekiti State, Nigeria. The brown hard shells of the seeds were broken to remove the cotyledons.

Extraction. The cotyledons were further broken into small pieces to enhance quick extraction. The coarse powder of the seeds of *D. reflexa* was extracted with *n*-hexane for 72 h at room temperature. Extraction was further repeated with *n*-hexane. The combined extract was concentrated *in vacuo* at 40 °C to obtain the seed oil which was analyzed for iodine value, saponification value, acid value, ester value and iodine number by the methods described by British Pharmacopoeia (1988).

Acid value determination. The oil (10 g) was weighed in 250 mL conical flask. A mixture of 25 mL of 95% alcohol, 25 mL of ether and 1 mL of phenolphthalein solution was added to the conical flask containing the oil. The oil was allowed to dissolve in the solvent mixture and titrated against 0.1 M aqueous potassium hydroxide. It was shaken constantly until blue colour was observed. The process was repeated twice in exactly the same manner.

$$\text{Acid value} = (a \times 5.61)/W$$

where:

W = mass (g) of oil weighed

a = volume of 0.1 M KOH required

Saponification value. The oil (2 g) was weighed in 250 mL quick fit flask. 25 mL of 1 M alcoholic potassium hydroxide was added using burette. A reflux condenser was attached to

the quick fit flask and the mixture was refluxed for one hour on a water bath, while swirling the contents frequently. The water bath was removed under the flask and 5 mL of phenolphthalein solution was poured down the condenser. The flask was allowed to cool for 5 min under the tap water and the content was titrated with 0.5 M HCl. A blank determination was carried out with the same quantities of reagents without the oil under the same experimental conditions. The procedure was repeated in the same manner.

$$\text{Saponification value} = (b-a) 28.05/W$$

where:

W = mass (g) of oil weighed

a = volume of 0.5 M HCl required

b = volume of 0.5 M HCl required for blank

Iodine value. The oil (0.25 g) was weighed and dissolved in a conical flask containing 15 mL of tetrachloromethane. 25 mL of Wij's solution was added to the mixture. Wij's solution was prepared by dissolving 1.9 g of iodine monochloride in a litre brown bottle containing one litre of a mixture of 70 mL acetic acid and 30 mL carbon tetrachloride. The flask containing the oil and the Wij's solution was closed and swirled to mix the content. The solution was allowed to stand in the dark at about 20 °C for one hour. 20 mL of 10% aqueous potassium iodide solution and 150 mL water were added. The solution was titrated with 0.5 M sodium thiosulphate solution; small amount of starch was added as indicator. A blank determination was carried out, with the same quantities of reagents under the same conditions. The procedure was repeated in exactly the same manner.

$$\text{Iodine value} = 1.269(V_2 - V_1)/W$$

where:

W = mass (g) of oil weighed

V₁ = volume of sodium thiosulphate solution required

V₂ = volume of sodium thiosulphate solution required for blank

Ester value. Ester value was determined by subtracting acid value (AV) from saponification value (SV).

$$\text{Ester value} = (SV) - (AV)$$

Iodine ratio. The iodine ratio was determined by the ratio of the ester value (EV) to the acid value (AV).

$$\text{Iodine ratio} = (EV)/(AV)$$

Methylation of the oil for GC analysis. The oil (0.5 g) was weighed and added to 3 mL of diethylether. The oil was allowed to dissolve by shaking the mixture thoroughly. 0.2 mL of sodium methoxide was added to the mixture and the

solution was centrifuged to precipitate the solid, which was then filtered and the filtrate was kept for GC analysis (Ceirwyn, 1995).

Gas chromatography of *D. reflexa* seed oil. The fatty acid composition of the methyl ester of *D. reflexa* oil was determined by AI Cambridge GC 94 at Centre Science Laboratory, Obafemi Awolowo University, Ile-Ife, Nigeria. The column length was 105 m, internal diameter was 0.53 mm and the film was 3 µm thick operating conditions of the gas chromatograph comprises of oven temperature programme which was started at 150 °C, held for 6 min and then raised at 10 °C/min to the final temperature of 250 °C. The injector temperature was 150 °C and detector FID at 300 °C. The carrier gas was helium with a flow rate of 8 mL/min with an injected volume of 1 µm.

Infrared spectroscopy analysis. The IR spectroscopy of *D. reflexa* seed oil was done using nujol mull. About 3 mg of the oil was triturated with nujol mull to give a creamy paste which was put between two sodium chloride plates for the determination (Bungard, 1983).

Results and Discussion

Table 1 presents the physicochemical properties of the seed oil of *D. reflexa*. The iodine value of *D. reflexa* oil (72.8 mg iodine/g) places it in the non-drying oil group as drying oils have an iodine value above 100 (Duel, 1951). The iodine value compares favourably with that of *Calophyllum inophyllum* seed oil, 67.2-70.1 mg I/g (Olaofe *et al.*, 2006), *Bombacopsis glabra* seed oil, 71.0 mg I/g (Olaofe *et al.*, 2006) and Khaya seed oil, 68.0 mg I/g (Okiemen, 2002).

Table 1. Physicochemical properties of *Dioclea reflexa* seed oil

Parameter	Value
Acid value (mg KOH/g)	8.69
Saponification value (mg KOH/g)	251
Iodine value (mg iodine/g)	72.8
Ester value	242
Iodine ratio	27.9

The acid value of *D. reflexa* seed oil (8.69 mg KOH/g) is greater than that of the seed oil of *Parkia biglobossa*, 2.5, and that of *Jatropha curcas*, 3.5 (Akintayo, 2004). This suggests that the oil of *D. reflexa* would require refining to make it edible, in view of the fact that acid values of edible oils should not exceed 4.00 mg KOH/g (Akintayo, 1997).

The saponification value of *D. reflexa* oil (251 mg KOH/g) was high compared to the values reported for castor oil (176-187), cod liver oil (180-190) and sesame oil (188-195) (Olaniyi and Ogungbamila, 1991). The saponification value of *D. reflexa* oil when compared with Guna melon oil (213 mg KOH/g) (Oresanya *et al.*, 2000) and Samsoy oil (211 mg KOH/g) has better quality attributes most especially with reference to the stability (Kochhar, 1986). This implies that the *D. reflexa* oil is nutritionally invaluable but highly valuable for industrial purposes especially for the manufacture of pharmaceuticals, soaps, cold creams, pomades and lubricants, emulsions for insect control and fuel for diesel engines.

The ester value and iodine ratio of *D. reflexa* oil were found to be 242 mg KOH/g and 27.9, respectively (Table 1). The iodine ratio is higher than the values reported for palm kernel oil (13-17) and coconut oil (8-10) but compares very well with the iodine ratio reported for milk fat (26-50) (Lewkowitsch, 1921). The value is lower than the value reported for olive oil (79-88) and sesame oil (103-108) (Lewkowitsch, 1921). The iodine ratio of fat or oil tells the degree of unsaturation of the oil or fat. Low value of the iodine ratio of *D. reflexa* oil is supported by the result of the gas chromatography analysis of the oil with a low percentage (0.8) of unsaturated fatty acid, oleic acid (18:1), in the oil as shown in Table 2. The fatty acid composition of *D. reflexa* seed oil from the GC analysis revealed that it contains two saturated fatty acids, namely palmitic (16:0) 10.2 and stearic (18:0) 21.9. The *D. reflexa* oil contains both saturated and unsaturated fatty acids, and some other unidentified fatty acids, in varying proportions.

Table 2. Fatty acid composition of *Dioclea reflexa* seed oil

Fatty acids	Percentage
Stearic	21.9
Palmitic	10.2
Oleic	0.8
Σ Saturated	32.1

The infrared spectroscopy spectrum of the seed oil of *D. reflexa* is presented in Fig. 1. There is a broad band between 3050-3500 cm^{-1} which is associated with the overtones of the glyceride ester carbonyl absorption. The band at approximately 2924 cm^{-1} is indicative of symmetric stretching from the ubiquitous methylene group (Akintayo, *et al.*, 2002). The triglyceride carbonyl stretching vibration is observed in the spectrum at approximately 1727 cm^{-1} . C=C stretching mode of unconjugated olefins usually show

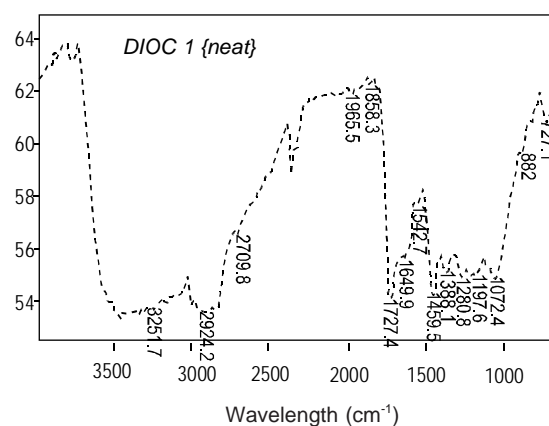


Fig. 1. Spectrum of infrared spectroscopy of *Dioclea reflexa* oil.

moderate to weak absorption bands in the region 1640-1680 cm^{-1} (Silverstein *et al.*, 1979). This band was observed in the oil sample spectrum at approximately 1649 cm^{-1} . The oil sample shows a scissoring band of the bending vibration of methylene group at approximately 1459 cm^{-1} . The band at approximately 1388 cm^{-1} in the spectrum could be assigned to symmetrical bending vibration of methyl groups. Bands occur at approximately 1280 cm^{-1} , 1197 cm^{-1} and 1072 cm^{-1} . Some of these bands could be assigned to the stretching vibrations of the C-O group in esters (Silverstein *et al.*, 1979). The absorption at approximately 727 cm^{-1} results from the overlapping of the methylene rocking vibration and the out of plane bending vibration of *cis*-disubstituted olefin.

References

- Akintayo, E.T. 2004. Characteristics and composition of *Parkia biglobossa* and *Jatropha curcas* oils and cakes. *Bioresources Technology*, **92**: 307-311
- Akintayo, E.T., Olaofe, O., Adefemi, S.O., Akintayo, C.O. 2002. Potential of fourier transform infrared spectroscopy for characterising vegetable oils. *International Journal of Chemistry*, **12**: 151-156.
- Akintayo, E.T. 1997. Chemical composition and physico-chemical properties of fluted pumpkin (*Telfairia occidentalis*) seed and seed oils. *Rivista Italiana Delle Sostanze Grasse*, **74**: 13-15.
- Allen, O.N., Allen, E.K. 1981. *The Leguminosae: A Source Book of Characteristics, Uses and Nodulation*, 812 pp., University of Wisconsin Press, Madison, USA.
- British Pharmacopoeia, 1988. In 4 volumes, Her Majesty's Stationery Office, London, UK.
- Bungard, L. 1983. A new spectrophotometric method for

- selective determination of ampicillin, amoxicillin and cyclacillin in the presence of polymers. *Journal of Pharmaceutical and Biomedical Analysis*, **1**: 29-41.
- Ceirwyn, S.J. 1995. *Analytical Chemistry of Foods*, pp. 140-141, Black Academic and Professional, London, UK.
- Duel, H.J. Jr. 1951. *The Lipids: Their Chemistry and Biochemistry*, vol. **1**, Interscience Publishers Inc., New York, USA.
- Gill, L.S. 1992. *Ethnomedicinal Uses of Plants in Nigeria*, 1st edition, University of Benin, Benin City, Nigeria.
- Guerranti, R., Aguiyi, J.C., Leoncini, R., Pagani, R., Cinci, G., Marinello, E. 1999. Characterization of the factor responsible for the antisnake activity of *Mucuna pruriens* seeds. *Journal of Preventive Medicine and Hygiene*, **1**: 25-28.
- Guerranti, R., Aguiyi, J.C., Neri, S., Leoncini, R. Pagani, R., Marinello, E. 2002. Proteins from *Mucuna pruriens* and enzymes from *Echis carinatus* venom: characterization and cross-reactions. *Journal of Biological Chemistry*, **277**: 17072-17078.
- Kochhar, S.L. 1986. *Tropical Crops, Textbook of Economic Botany*, 176 pp., Macmillan, London, UK.
- Lewkowitsch, J. 1921. *Chemical Technology and Analysis of Oils, Fats and Waxes*, 6th edition, pp. 419-424, Macmillan and Co. Ltd., London, UK.
- Ogundare, A.O., Olorunfemi, O.B. 2007. Antimicrobial efficacy of the leaves of *Dioclea reflexa*, *Mucuna pruriens*, *Ficus asperifolia* and *Tragia spathulata*. *Research Journal of Microbiology*, **2**: 392-396.
- Okiemen, F.E. 2002. Studies in the utilization of vegetable oil. *International Journal of Industrial Crops and Products*, **15**: 71-76.
- Olaniyi, A.A., Ogungbamila, F.O. 1991. *Experimental Pharmaceutical Chemistry*, pp. 57-61, 1st edition, Shaneson C.I. Ltd., Nigeria.
- Olaofe, O., Akintayo, E.T., Adeyeye, E.I., Adubiaro, H.O. 2006. Proximate composition and functional properties of Bulma cotton (*Bombacopsis glabra*) seeds. *Egyptian Journal of Food and Science*, **34**: 81-90.
- Oresanya, M.O., Ebuehi, O.A.T., Aitezetmuller, K., Koleosho, O.A. 2000. Extraction and Characterisation of *Citrullus colocynthis* seed oil. *Nigerian Journal of National Production and Medicine*, **4**: 76-78.
- Silverstein, R.M., Basler, G.C., Morrill, T.C. 1979. *Spectroscopic Identification of Organic Compounds*, pp. 73-79, 3rd edition, John Wiley and Sons, New York, USA.

Antioxidant Properties of *Telfairia occidentalis* as Affected by the Market Storage Method in Nigeria

Foluso Olutope Adetuyi^{a*} and Gani Adebola Ogundahunsi^b

^aFood Science and Technology Department, Rufus Giwa Polytechnic, P.M.B 1019, Owo, Ondo State, Nigeria

^bNutrition and Dietetic Department, Rufus Giwa Polytechnic, P.M.B 1019, Owo, Ondo State, Nigeria

(received November 11, 2009; revised February 12, 2010; accepted February 15, 2010)

Abstract. The effect of market storage methods in Nigeria on the antioxidant properties of *Telfairia occidentalis* was assessed over a period of 96 hours with respect to the vitamin C, total phenol and phytate contents, as typified by their reducing power and free scavenging ability. *T. occidentalis* had a phytate content of 28.83 mg/100 g and there was no significant ($P>0.05$) difference in the phytate content in the first 24 h of storage but significantly ($P>0.05$) reduced at the end of the storage period of 96 h (26.74 mg/100 g) with 7.24% loss. Vitamin C content reduced significantly ($P>0.05$) as the storage period increased with a very high percentage loss (81.58%) at the end of the storage period. The vegetable had 2.78 mg GAE/100 g total phenol and was slightly reduced but not significant ($P>0.05$) during the first 24 h of storage. *T. occidentalis* had scavenging ability $> 90\%$, which significantly ($P>0.05$) decreased as the storage period increased (57.47% loss at 100% conc. and 56.28 % loss at 50% conc.).

Keywords: *Telfairia occidentalis*, vitamin C, total phenol, phytate, storage reducing power, scavenging ability

Introduction

Free radicals are highly reactive chemical substances such as peroxide, hydroxyl radical, singlet oxygen etc. that travel around in the body and cause damage to the body cells (Alia *et al.*, 2003). Antioxidants are powerful free radical scavengers in the body. Antioxidants are believed to play a very important role in the body defence system against reactive oxygen species (ROS), which are the harmful by-products generated during normal cell aerobic respiration (Gutteridge and Halliwell, 2000). Antioxidant nutrients (found in foods) soak up all the excess energy that these free radicals have, turning them into harmless particles or waste products that can be removed (Obboh, 2005). Increasing intake of dietary antioxidants may help to maintain an adequate antioxidant status, therefore, the normal physiological function of a living system (Kaur and Kapoor, 2001; Record *et al.*, 2001). Regular consumption of fruits and vegetables has always been associated with health benefits. Fruits and vegetables contain a wide variety of biologically active, non-nutritive phytochemicals which impart health benefits beyond basic nutrition (Gupta and Prakash, 2009; Oomah and Mazza, 2000). Researchers have estimated that every serving increase in fruit and vegetable consumption reduces the risk of cancer by 15%, cardiovascular disease by 30% and mortality by any cause by 20% (Gupta and Prakash, 2009). This is often attributed to different antioxidant components in fruits and vegetables

such as ascorbic acid, vitamin E, carotenoids, lycopenes, polyphenols and other phytochemicals (Prior and Cao, 2000). Vegetables play significant role in human nutrition, specially as a source of vitamins (A, B, C, E), minerals and dietary fibre (Aletor and Adegun, 1995).

Leafy vegetables are important items of diet in many Nigerian homes (Mepba *et al.*, 2007). They are valuable sources of nutrients specially in rural areas where they contribute substantially to protein, mineral, vitamins, fiber and other nutrients which are usually in short supply in daily diets (Mosha and Gaga, 1999). They also add flavour, variety, taste, colour and aesthetic appeal to what would otherwise be a monotonous diet (Mepba *et al.*, 2007). Vegetables are in abundance shortly after the rainy season but become scarce during the dry season during which cultivated types are used. Some eventually find their way to urban markets (Mepba *et al.*, 2007). In Nigeria, during the season of abundance of vegetables, the market women do not always sell all their vegetables on the day of harvest; it has to be preserved for 24 h or more in order for them to break even financially. The modern preservation method of refrigeration and controlled/modified atmosphere are not available to these market women in Nigeria, so they have to design their own methods of preserving their produce. Much work has been done on the phytochemical content of vegetables but there is paucity of information on the effect of storage on the phytochemical content of vegetables. The aim of this study is, therefore, to determine the effect of market

*Author for correspondence; E-mail: foluadetuyi@yahoo.co.uk

vegetable storage method in Nigeria on the antioxidant-phyto-constituents of *Telfairia occidentalis*.

Materials and Methods

Freshly harvested *Telfairia occidentalis* (Ugwu) was obtained from a farm in Rufus Giwa Polytechnic, Owo. The vegetable was subjected to market condition and stored using market storage method. They were displayed inside a plastic basin; at 6 pm, they were sprinkled with water, placed inside polypropylene bag and left outside at room temperature of 27 ± 1 °C. This process was carried out for 96 h; sampling and antioxidant determination were carried out after 24 h and 96 h of storage.

Sample preparation. The edible portion of the vegetable (50 g) was separated, washed, drained completely, chopped, sundried and analyzed for phytate, ascorbic acid, total phenols, and antioxidant activities. The extracts were prepared in duplicate and all analysis was carried out in triplicate.

Sample analysis. The method of Maga (1982) was used for phytate determination. To the sample (2.0 g), 100 mL of 2% concentrated hydrochloric acid was added. The sample was soaked for 3 h, and then filtered through Whatman # 43 filter paper. 50 mL of the filtrate was placed in 250 mL beaker and 107 mL of distilled water was added to give proper acidity. 10 mL of 0.3% ammonium thiocyanate solution was added as an indicator and the solution was titrated with standard iron (III) chloride solution which contained 0.00195 g iron/mL. The equivalence point was slightly brownish-yellow which persisted for 5 min. Phytate content was expressed as the percentage (%) phytate in the sample. Vitamin C content was determined by AOAC (1990) method. 5 g of the sample was extracted with 100 mL H₂O and 25 mL of 20% glacial acetic acid was added to 10 mL of the sample extract and titrated against standardized 2,6 dichloroindophenol (0.05 g / 100 mL) solution. Total phenol was determined by mixing 0.2 mL phenolic extract (0.2 g of *T. occidentalis* extracted with 20 mL 70% acetone) with 0.8 mL Folin-Ciocalteu reagent and 2 mL of 7.5% sodium carbonate. The mixture was diluted to 7 mL with distilled water and the absorbance was measured after 2 h at 765 nm; the result was calculated as gallic acid equivalent. (Iqbal *et al.*, 2005). The reducing property was determined by assessing the ability of the sample extract to reduce FeCl₃ solution as described by Pulido *et al.* (2000). Briefly, appropriate dilutions (0-1.0 mL) were mixed with 2.5 mL of 200 mM sodium phosphate buffer (pH 6.6) and 2.5 mL of 1% potassium ferricyanide. The mixtures were incubated at 50 °C for 20 min. Thereafter, 2.5 mL of 10% trichloroacetic acid was added and subsequently centrifuged at 650 rpm for 10 min. Then 5 mL of the resulting supernatant was mixed with

equal volume of water and 1 mL of 0.1% ferric chloride. The absorbance was taken at 700 nm against a reagent blank. Increased absorbance of the reaction mixture indicated increased reducing power. Free radical scavenging activity using 1, 1-diphenyl-2-picryl hydrazyl (DPPH) as described by Singh *et al.* (2002) Different concentrations of the methanolic extract were taken in different test tubes and the volume was made to 1 mL with methanol. 4 mL of 0.1 mM methanolic solution of DPPH was added. The tubes were shaken vigorously and allowed to stand for 20 min at room temperature. A control was prepared as above without the sample and methanol was used for base line correction. Changes in absorbance of samples were measured at 517 nm. Free radical scavenging activity was expressed as percentage inhibition and was calculated using the following formula:

$$\text{Free radical scavenging activity (\%)} = (\text{control OD} - \text{sample OD}) / \text{control OD} \times 100$$

Statistical analysis. The results were statistically verified on the basis of analysis of variance, using SAS (2002). Mean separation was carried out where there was significant differences using Duncan multiple range test procedure as described in the SAS soft ware. Significance was accepted at $P > 0.05$.

Results and Discussion

Consumers usually purchase a fresh produce driven by their visual appearance, while other components of quality such as texture and aroma make the consumers to re-purchase the same produce the next time (Kader, 2001). Inadequate storage conditions may negatively affect the produce quality. A produce badly stored may have a good visual appearance but altered taste or aroma. The optimal temperature and relative humidity during storage may help to reduce the degenerative processes that occur in vegetables during the postharvest stages (Kader, 2001). This work was carried out to estimate the antioxidant properties of the vegetable, *Telfairia occidentalis* kept for 96 h under market storage conditions.

Phytate has been shown to have anticancer and antioxidant activity. It forms an iron chelate that suppresses lipid peroxidation by blocking iron-driven hydroxyl radical generation (Oboh, 2006). Phytate content of the vegetable is presented in Table 1; it shows that *T. occidentalis* had a phytate content of 28.83 mg/100 g. This value was lower when compared to the values reported for the same vegetable *T. occidentalis* as 48.8 mg/100 g for leaves harvested 12 weeks after planting and 84.4 mg/100 g for leaves harvested 50 weeks after planting (Akwaowo *et al.*, 2000). This variation may be due to the environmental factors. Phytate content is also low as com-

pared to other vegetables (Udosen and Ukpanah, 1993). There was no significant ($P>0.05$) difference in the phytate content of the vegetable in the first 24 h of storage but content significantly ($P>0.05$) reduced at the end of the storage period of 96 h (26.74 mg/100 g) with 7.24% loss. This reduction of phytate in storage is in agreement with the findings of Hernandez-Unzon and Ortega-Delgado (1989) of a decrease of 4% in phytic acid of stored common bean seeds (*Phaseolus vulgaris* L) under hermetic conditions. The reduction in phytate could be attributed to the action of phytase which hydrolytically cleaves and frees the bound phosphorus from the phytic acid molecule, liberating calcium and magnesium cations at the same time.

Vitamin C is required for the prevention of scurvy and maintenance of healthy skin, gums and blood vessels and acting as an antioxidant, it reduces the risk of arteriosclerosis, cardiovascular diseases and some forms of cancer (Lee and Kader, 2000). Vitamin C content of stored *T. occidentalis* as shown in Table 1 (58.1 mg/100 g), was considerably higher than the values reported for some commonly consumed sundried tropical green leafy vegetables in Nigeria (Oboh and Akindahunsi, 2004), but low in comparison to the value of 101.36 mg/100 g of *Trigonella foenum graecum* (Gupta and Prakash, 2009). Vitamin C content of the vegetable was significantly ($P>0.05$) reduced as the storage period increased with a percentage loss of 81.58% at the end of the storage period. The decrease in Vitamin C content during storage agrees with the observation of Nwufu (1994) of decrease in chlorophyll and ascorbic acid contents of leafy vegetables during storage. The loss in ascorbic acid has also been reported in the study of four different vegetables, with okra having the least and spinach the highest loss during storage (Giannakourou and Taoukis, 2003). Tulio *et al.* (2002), analyzing the effects of storage temperature on the postharvest quality of jute leaves reported that the ascorbic acid content declined at all storage temperatures with the increase of storage period. Oladele and Aborisade (2009) also reported decrease in vitamin C content of Indian spinach (*Basella rubra* L) during storage. However, it has been noted

Table 1. Effect of storage time on the antioxidant phytochemicals of *Telfairia occidentalis* (Ugwu)

Storage period (hours)	Vitamin C (mg/100 g)	Total phenol (mg GAE/100 g)	Phytate (mg/100 g)
0	58.1±0.3 ^a	2.78±0.2 ^a	28.83±0.1 ^a
24	32.9±0.1 ^b	2.56±0.2 ^a	28.80±0.1 ^a
96	10.7±0.1 ^c	2.08±0.1 ^b	26.74±0.1 ^b
Loss (%)	81.58	25.17	7.24

Values represent mean of triplicate analysis; values with the same letter in a column are not significantly different ($P> 0.05$).

that when reporting vitamin C levels, many workers did not take into consideration dehydroascorbic acid (DHA). In many horticultural crops, DHA represents less than 10% of total vitamin C but DHA tends to increase during storage (Wills *et al.*, 1984). Vitamin C is the most sensitive to destruction when the commodity is subjected to adverse handling and storage conditions. Losses are enhanced by extended storage, higher temperature, low relative humidity, physical damage and chilling injury (Lee and Kader, 2000). The loss in vitamin C may be the result of the activity of the enzyme ascorbate oxidase, proposed to be the major enzyme responsible for enzymatic degradation of ascorbic acid.

The antioxidant activity of phenolic compounds is mainly due to redox properties, which allow them to act as reducing agents, hydrogen donors, singlet oxygen quenchers, heavy metal chelators and hydroxyl radical quenchers (Kaur and Kapoor 2002). Value of total phenolics (Table 1), in the vegetable (2.78 mg GAE/100 g) agrees with the value reported for the same vegetable but lower to the value reported for *Amaranthus cruentus* and *Ocimum gratissimum* (Oboh and Akindahunsi, 2004). There was slight reduction in the total phenol content of the vegetable but not statistically significant ($P>0.05$) in the first 24 h of storage; however, it reduced significantly ($P>0.05$) at the end of the storage period of 96 h with 25.17% loss. Ose *et al.* (1997) also reported that the total phenol contents of water convolvulus, *Calendula arvensis*, leaves decreased during storage at low temperature; this may be attributed to the fact that phenols are susceptible to oxidation by the enzyme phenolase which converts them to quinones. These compounds are often extremely reactive and therefore short lived (Kays, 1991).

The antioxidant effect exponentially increases as a function of the development of the reducing power, indicating that the antioxidant properties are concomitant with the development of reducing power (Oyaizu, 1986). Reductones are believed not only to react directly with peroxides but also prevent peroxide formation by reacting with certain precursors (Gupta and Prakash, 2009). The results revealed (Fig. 1) a significant ($P>0.05$) reduction in the reducing power of *Telfairia occidentalis* as the storage period increased, with 41.67% reduction at the end of the storage period of 96 h, agreeing with the decrease in the total phenol content, which could be attributed to the decrease in the proton donors necessary to react with the precursors as a result of the storage.

1,1-Diphenyl-2-picrylhydrazyl (DPPH) radical is a stable, free radical and accepts an electron or hydrogen radical to become a stable diamagnetic molecule. The methodology involves reaction of specific compounds or extracts with DPPH in methanol solution. In the presence of hydrogen donors, DPPH

is reduced and a free radical is formed from the scavenger. The reaction of DPPH is monitored by the decrease in the absorbance of its radical at 517 nm, but upon reduction by an antioxidant, the absorption disappears (Gupta and Prakash, 2009). The effect of storage on the free radical scavenging ability of *T. occidentalis* (Fig. 2) shows that *T. occidentalis* had scavenging ability > 90% and that there was a significant ($P>0.05$) decrease in the free radical scavenging ability of *T. occidentalis* as the storage period increased (57.47% loss at 100% concentration and 56.28 % loss at 50% concentration). This reduction in the scavenging ability may be attributed to the decrease observed in the vitamin C and total phenol contents and reducing power as discussed earlier.

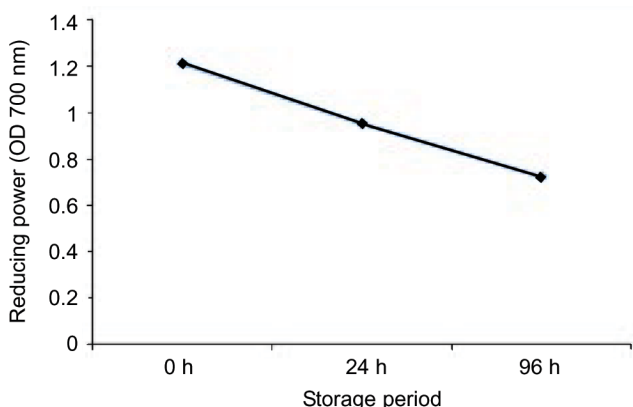


Fig. 1. Effect of storage time on reducing power of *Telfairia occidentalis* (Ugwu).

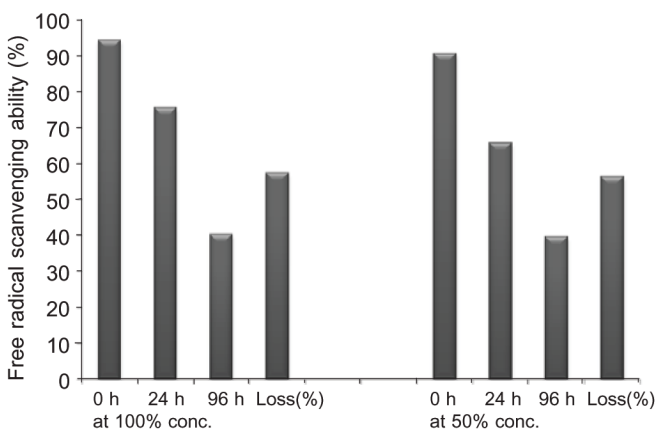


Fig. 2. Effect of storage period on the free radical scavenging ability of *Telfairia occidentalis* (Ugwu).

Conclusion

The results showed that the antioxidant contents of *T. occidentalis* reduced during storage though during the first 24 h of storage, there was no significant ($P>0.05$) difference

in the total phenol and the phytate contents. Consequently, the antioxidant activities were also reduced. Considering this available storage method, vegetables should be sold within 24 h of harvesting in Nigeria.

Acknowledgement

The authors thank specially Dr. G. Oboh of the Federal University of Technology, Akure, for providing the facilities of his personal laboratory, materials and chemicals during the course of this work and also for his critical comments.

References

- Akwaowo, E.U., Ndon, B.A., Etuk, E.U. 2000. Minerals and antinutrients in fluted pumpkin (*Telfairia occidentalis* Hook f.). *Food Chemistry*, **70**: 235-2400.
- Aletor, V.A., Adeogun, O.A. 1995. Nutrient and antinutrient components of some tropical leafy vegetables. *Food Chemistry*, **53**: 375-379.
- Alia, M., Horlajo, C., Bravo, L., Goya, L. 2003. Effect of grape antioxidant dietary fiber on the total antioxidant capacity and the activity of liver antioxidant enzymes in rats. *Nutrition Research*, **23**: 1251-1267.
- A.O.A.C. 1990. *Official Methods of Analysis of Association of Official Analytical Chemists, Food Composition, Additives Natural Contaminant*, R.C. Adrich (ed.), vol. **2**, 15th edition, Association of Official Analytical Chemist Inc., USA.
- Giannakourou, M.C., Taoukis, P.S. 2003. Kinetic modeling of vitamin C loss in frozen green vegetables under variable storage conditions. *Food Chemistry*, **83**: 33-41.
- Gupta, S., Prakash, J. 2009. Studies on Indian green leafy vegetables for their antioxidant activity. *Plant Foods for Human Nutrition*, **64**: 39-45.
- Gutteridge, J.M.C., Halliwell, B. 2000. Free radicals and antioxidants in the year 2000 - A historical look to the future. *Annals of New York Academy of Sciences*, **899**: 136-147.
- Hernandez-Unzon, H.Y., Ortega-Delgado, M.L. 1989. Phytic acid in stored common bean seeds. *Plant Foods for Human Nutrition*, **39**: 209-221.
- Iqbal, S., Bhangar, M.I., Anwar, F. 2005. Antioxidant properties and components of some commercially available varieties of rice bran in Pakistan. *Food Chemistry*, **93**: 265-272
- Kader, A.A. 2001. Quality assurance of harvested horticultural perishables. *Acta Horticulturae*, **553**: 51-56.
- Kaur, C., Kapoor, H.C. 2001. Antioxidants in fruits and vegetables - the millennium's health. *International Journal of Food Science and Technology*, **36**: 703-725.
- Kaur, C., Kapoor, H.C. 2002. Anti-oxidant activity and total phenolic content of some Asian vegetables. *International Journal of Food Science and Technology*, **37**: 153-161.

- Kays, S.J. 1991. *Post Harvest Physiology of Perishable Plant Products*, S.J. Kay (ed.), 532 pp., Von Nostrand Reinhold, New Yorks, USA.
- Lee, S.K., Kader, A.A. 2000. Pre harvest and post-harvest factors influencing vitamin C content of horticultural crops. *Postharvest Biology and Technology*, **20**: 207-220.
- Maga, J.A. 1982. Phytate: Its chemistry, occurrence, food interaction, nutritional significance and methods of analysis. *Journal of Agriculture and Food Chemistry*, **30**: 1-9.
- Mepba, H.D., Eboh, L., Banigo, D.E.B. 2007. Effects of processing treatments on the nutritive composition and consumer acceptance of some Nigerian edible leafy vegetables. *African Journal of Food, Agriculture, Nutrition and Development*, **7**: 1-18.
- Mosha, T.C., Gaga, H.E. 1999. Nutritive value and effect of blanching on trypsin and chymotrypsin inhibitor activities of selected leafy vegetables. *Plant Foods for Human Nutrition*, **54**: 271-283.
- Nwufo, M.I. 1994. Effect of water stress on the post harvest quality of two leafy vegetables *Telfairia occidentalis* and *Pterocarpus soyauxii* during storage. *Journal of the Science of Food and Agriculture*, **64**: 265-269.
- Oboh, G. 2006. Antioxidant properties of some commonly consumed and underutilized tropical legumes. *European Food Research and Technology*, **224**: 61-65.
- Oboh, G. 2005. Effect of blanching on the antioxidant property of some tropical green leafy vegetables. *Lebensm. Wiss.u. Technol Food Science and Technology*, **38**: 513-517.
- Oboh, G., Akindahunsi, A.A. 2004. Changes in ascorbic acid, total phenol and antioxidant activity of some sun-dried leafy vegetable in Nigeria. *Nutrition and Health*, **18**: 29-36.
- Oladele, O.O., Aborisade, A.T. 2009. Influence of different drying methods and storage on the quality of Indian spinach (*Basella rubra* L.). *American Journal of Food Technology*, **4**: 66-70.
- Oomah, B.D., Mazza, G. 2000. Functional foods. In: *The Wiley Encyclopedia of Science and Technology*, F. J. Francis (ed.), pp. 1176-1182, 2nd edition, Wiley, New York, USA.
- Ose, K., Chachin, K.U., Jung-Myung, L., Gross, K.C., Watada, A.E., Lee, S.K. 1997. Relationship between the occurrence of chilling injury and the environmental gas concentration during storage of water convolvulus (*Ipomoea aquatica* F.). *Acta Horticulturae*, **483**: 303-310.
- Oyaizu, M. 1986. Studies on product of browning reaction prepared from glucose amine. *Japanese Journal of Nutrition*, **44**: 307-315.
- Prior, R.L., Cao, G. 2000. Antioxidant phytochemicals in fruits and vegetables - diet and health implications. *Horticultural Science*, **35**: 588-592.
- Pulido, R., Bravo, L., Saura-Calixto, F. 2000. Antioxidant activity of dietary polyphenols as determined by a modified ferric reducing/antioxidant power assay. *Journal of Agriculture and Food Chemistry*, **48**: 3396-3402.
- Record, I.R., Dreosti, I. E., McInerney, J.K. 2001. Changes in plasma antioxidant status following consumption of diets high or low in fruit and vegetables or following dietary supplementation with an antioxidant mixture. *British Journal of Nutrition*, **85**: 459-464.
- SAS, 2002. *Statistical Analysis System Proprietary Software*, Release 8.1, SAS Institute Inc., Cary, North Carolina, USA.
- Singh, R.P., Murthy, C.K.N., Jayaprakasha, G.K. 2002. Studies on the antioxidant activity of pomegranate (*Punica granatum*) peel and seed extracts using *in vitro* models. *Journal of Agricultural Food Chemistry*, **50**: 81-86.
- Tulio Artemio, Z., Kimiko, O.S.E., Chachin, K., Yoshinori, U. 2002. Effect of storage temperatures on the post harvest quality of jute leaves *Corchorus olitorius* L. *Postharvest Biology and Technology*, **26**: 329- 338.
- Udosen, E.O., Ukpanah, U.M. 1993. The toxicants and phosphorus content of some Nigerian vegetables. *Plant Foods for Human Nutrition* **44**: 285-289.
- Wills, R.B.H., Wimalasiri, P., Greenfield, H. 1984. Dehydroascorbic acid levels in fresh fruits and vegetables in relations to total vitamin C activity. *Journal of Agricultural and Food Chemistry*, **32**: 836-838.

Colour Removal from Textile Dyeing Wastewater Using Different Adsorbents

Muhammad Tahir Butt*, Naz Imtiaz, Sameer Ahmed, Farooq Arif and Shahid Rehman Khan

PCSIR Laboratories Complex, Shahrah-e-Jalaluddin Roomi, Lahore - 54600, Pakistan

(received May 28, 2009; revised December 1, 2009; accepted January 6, 2010)

Abstract. The ability of different adsorbents/coagulants, such as liquid and solid polymers, ferric chloride, calcium carbonate and coal ash, was investigated for uptake of (reactive dyes, Red - 120, Yellow - 14 and Blue - 4 from textile dyeing waste. Coal ash was used for the colour removal from the textile dyeing wastewater of reactive dyes. Different adsorbents removed the colour from the effluent in different degrees; in some cases the colour was removed 100%. White polymer was ineffective. Calcium carbonate gave excellent results. Liquid polymers were better effective than the solid ones. Coal ash yielded good results without any further treatment.

Keywords: industrial wastes, dyes, colour removal, adsorbents

Introduction

Textile industry requires large amounts of water and generates large quantities of wastewater from various steps of dyeing processes. Textile wastewater is characterized by high content of dyestuff, salts, high COD deriving from additives, suspended solid (SS) and fluctuating pH depending on the process (Balcoiglu and Arslan, 2001; Yeh and Thomas, 1995; Yeh *et al.*, 1993). Large amounts of dye chemicals in textile industry effluents create severe water pollution. Dyes impart persistent colour with organic load to the receiving water streams leading to disruption of the total ecological balance impairing the visibility in the recipients. This may significantly affect photosynthetic activity in aquatic environment due to reduced light penetration and may also be toxic to aquatic lives due to metals, chlorides etc., associated with the dyes or the dyeing process. It is, therefore, important to reduce the dye concentration in the wastewater before discharging it into the water bodies. However, it is difficult to remove dyes from effluents since dyes are stable to light, heat and oxidizing agents and are non biodegradable (Hai *et al.*, 2003).

Protection of the environment has become a challenge for the chemical industries worldwide and in particular, the water pollution caused by synthetic dyes and chemicals. All over the world, environmental regulations are becoming stricter and are forcing the shift of technology towards less polluting or practically non-polluting areas of technological development (Destailats *et al.*, 2000).

Several physicochemical decolourization techniques have been reported for effluent treatment e.g., adsorption, chemical

transformation, incineration, photocatalysis, ozonation or membrane separation, however, few, have been accepted by the textile industries largely due to high cost, low efficiency and inapplicability of the processes to a wide variety of dyes.

The conventional process used to treat textile wastewater is chemical precipitation with alum or ferrous sulphate. Drawbacks of this process are the generation of a large volume of sludge leading to the contamination with the chemical substances of the treated wastewater and associated disposal problems etc. For a more practical application, different processes were developed to treat textile industry wastewater. Filtration process, biological process, adsorption process, electrochemical process (Xiong and Karlson, 2001; Barlas and Akgun, 2000; Sójka-L *et al.*, 1998; Banat *et al.*, 1996) and ozone process etc., have been investigated for many years in numerous research centres due to their high reactivity but have low selectivity.

In most situations, use of a combination of different methods of treatment is necessary for removal of all the contaminants present in the wastewater (Sójka-L *et al.*, 1998). Therefore, adsorption became one of the most effective methods of decolourization of textile wastewater (Vendevivere *et al.*, 1998; Naumczyk *et al.*, 1996; Venceeslau *et al.*, 1994). Activated carbon is, by and large, the most commonly used adsorbent although other materials such as activated clay, wood and different types of cellulose-based materials have also been recently investigated for chemical adsorption (Los and Perkowski, 2003; Ciardelli *et al.*, 2001). One important point to be considered when choosing an adsorbent is the possibility of easy regeneration, easy availability of material and the running cost of the treatment.

*Author for correspondence; E-mail: mtahirbutt23@hotmail.com

Pakistan is one of the major textiles producing countries in cotton products. There are several thousand big dye houses that are operating day and night. The enormous amount of discharge in the form of industrial effluents with un-reacted dyes and electrolytes can be visualized. The industrial effluents are a constant threat for our ecology and environment. There is a pressing need to look into this problem.

The aim of this work is to determine the efficiency of the removal of reactive dyes, namely red, blue and green mono and dichlorotriazine from textile dyeing wastewater, using different materials as adsorbents. Focus was on coal ash in particular, which is locally available and has lower commercial value than other materials already in practice.

Materials and Methods

Dyes used in the study were the most common dyes used in the textile industry, red, blue and green belonging to the reactive class, from the group of mono and dichlorotriazine namely Indian Reactive Red-120, Reactive Yellow-14 and Reactive Blue-4.

The materials used for colour removal were ferrous chloride, calcium hydroxide, white solid polymer (Imp orient 20 PWG), liquid polymer (Imp orient A-100), Imp orient WWT-50, coal ash-1 (without any treatment), coal ash-2 (first regeneration) and coal ash-3 (second regeneration), coal ash-4 (third regeneration). Reactor of 300 mL was used for adsorption purpose.

The effluent samples were collected and their pH was measured at site. Absorbance of samples was taken in the laboratory before treatment at 480 nm using spectrophotometer, Model Bush and Lomb, USA. After treating the wastewater samples with adsorbents, the absorbance was again measured at the same wavelength of 480 nm; the wavelength was selected so as to obtain the maximum absorbance for each dyestuff used. pH of solutions varied between 1-8.

Effects of contact time on the removal of colour were studied by adding 5.00 g of adsorbent to 100 mL of double distilled water containing 50 ppm of dyestuff at constant temperature. Laboratory scale batch reactors (200 mL) were stirred at a controlled speed. After regular intervals of time, the slurry solution was filtrated and concentration of the dye was determined (Kang *et al.*, 2000; Shimoda *et al.*, 1997).

Results and Discussion

The factors that affect the adsorption of reactive dyes namely, Indian Reactive Red-120, Reactive Yellow-14 and Reactive Blue-4 in aqueous solution were studied using different liquid and solid materials. Colour concentration and absorbance graph of the dyes is given in Fig. 1. The samples were collec-

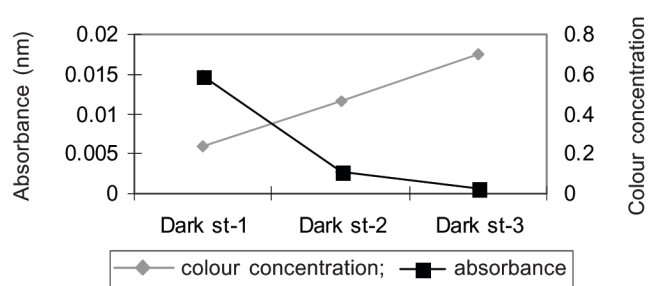
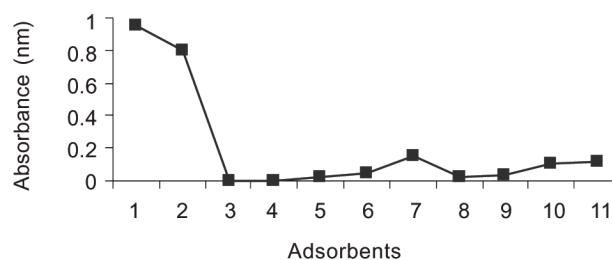


Fig. 1. Absorbance of known colour standards.

ted in 30 L plastic containers and their pH was measured at the site. Then each sample was divided into small portions which in turn were treated with different materials/coagulants.

The results of effluent treated with different materials are presented in the graphic form (Fig. 2). In this study the coal ash was used four times, once in the original form and three times after regeneration. Solid and liquid polymers were imported items and showed good results. However, these are organic materials which may create soil problem after disposal and also increase the pressure on foreign exchange. Different concentrations of the liquid polymer showed good results but poorer than the solid polymer. Coal ash, used to treat the wastewater, showed the results comparable with the solid polymer giving the absorbance 0.02 at the 480 nm. Coal ash is available free of cost and can be regenerated many times.



1: Treatment; 2: untreated effluent; 3: ferrous chloride; 4: calcium hydroxide; 5: imp orient 20 PWG; 6: imp orient A-100; 7: imp orient WWT-50; 8: coal ash 1(untreated); 9: coal ash 2(1st regenerated); 10: coal ash 3(2nd regenerated); 11: coal ash 4(3rd regenerated).

Fig. 2. Colour removal with different materials.

Natural material used in this study showed promising adsorption capacities without any chemical treatment. The high internal mass transfer resistance impairs its satisfactory application as adsorbent for continuous removal of direct and reactive dyestuff from the textile dyeing waste-water (Kang *et al.*, 2000; Shimoda *et al.*, 1997). In the treatment of wastewater, total colour removal occurs due to the breakage of

bonds between the dye molecules by treatment; in the case where dye is not completely removed from wastewater by treatment, excess amount of dye is removed by absorbing the treatment material. The results of treated wastewater samples with different materials are presented in Fig. 2. The residual colour concentration with variation in pH is given in Fig. 3. Absorbance and colour concentration of known colour standards are given in Fig. 1. Known and unknown samples with wavelength are given in Fig. 4. Fig. 5 shows the absorbance and percentage of colour removal.

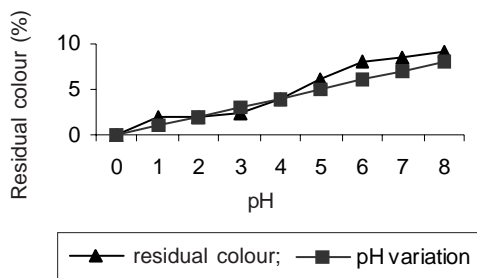


Fig. 3. Residual colour with variations in pH.

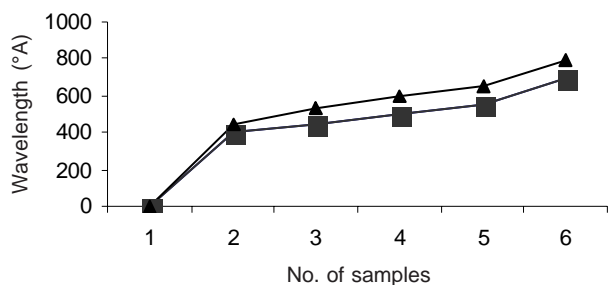


Fig. 4. Colour removal by known and unknown samples (%).

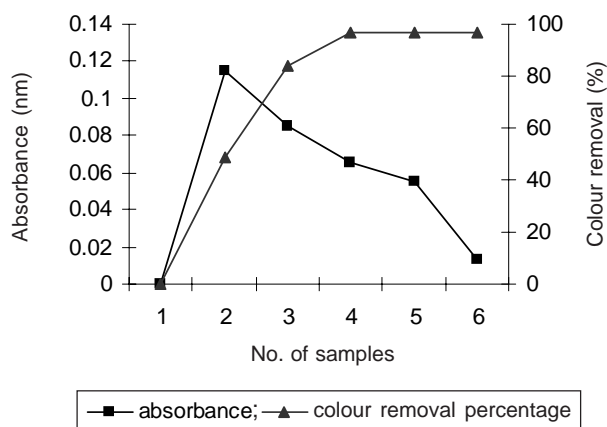


Fig. 5. Colour removal (%) by samples.

The dyes used in this work represent the most commonly used dyes in the textile industry and belong to the reactive class. The red, blue, green dyes from the group of mono and dichlorotriazine were used.

Wastewater sample was decolourized when treated with ferrous chloride, but the latter imparted its own slight yellow colour to the decolourized wastewater which is objectionable. In the second batch, the effluent sample was treated with the calcium carbonate which also absorbed the dye from the wastewater. Solid calcium carbonate showed very excellent results regarding the colour removal but it increased the total dissolved solids in the treated sample making it turbid. In the same way 6 different materials were used for the treatment. White polymer did not show any effect on the colour of the wastewater. Liquid polymer showed excellent result comparable with the ferrous chloride and calcium carbonate. These polymers are organic based and their long term use in bulk may create problems; the large quantity of such treated wastewater on disposal will affect the land quality and fertility. Finally, coal ash was used for the treatment. Coal ash also yielded good results. It is a cheaper material and can be used several times after its regeneration. There was 10% loss during its regeneration. Hence the coal ash is recommended for the treatment of textile dyeing wastewater.

Conclusion

Coal ash used in this study showed promising adsorption capacities without chemical treatment. The high internal mass transfer resistance impairs its satisfactory application as adsorbent due to the continuous removal of reactive dye-stuffs from the textile dyeing wastewater.

References

Balcioglu, I.A., Arslan, I. 2001. Partial oxidation of reactive dyestuff and synthetic textile dye bath process by the O₃ and O₃/H₂O₂ processes. *Water Science and Technology*, **43**: 221-228.

Banat, I.M., Nigam, P., Singh, D., Marchant, R. 1996. Microbial decolourization of textile dye-containing effluents- a review. *Bioresource Technology*, **58**: 217-27.

Barlas, H., Akgun, T. 2000. Colour removal from the textile wastewaters by adsorption techniques. *Fresenius Environmental Bulletin*, **9**: 597-602.

Ciardelli, G., Capannelli, G., Bottino, A. 2001. Ozone treatment of textile wastewaters for reuse. *Water Science and Technology*, **44**: 61-67.

Destailats, H., Colussi, A.J., Joseph, J.M., Hoffmann, M.R. 2000. Synergistic effects on sonolysis combined with ozonolysis for the oxidation of ozobenzene and methyl

- orange. *Journal of Physical Chemistry A*, **104**: 8930-8935.
- Hai, F.I., Fukushi, K., Yamamoto, K. 2003. Treatment of textile wastewater: Membrane bioreactor with special dye-degrading microorganism. In: *Proceedings of the Asian Water Quality*, 2Q3F16, Bangkok, Thailand.
- Kang, S.F., Liao, C.H., Po, S.T. 2000. Decolourization of textile wastewater by photo-fenton oxidation technology. *Chemosphere*, **41**: 1287-1294.
- Los, L., Perkowski, J. 2003. Decolourization of real textile wastewater with advanced oxidation processes. *Fibers and Textile in Eastern Europe*, **11**: 81-85.
- Naumczyk, L., Szpyrkowicz, L., Zilio-Grandi, F. 1996. Electrochemical treatment of textile wastewater. *Water Science and Technology*, **34**: 17-24.
- Shimoda, S., Prengle, W.H., Symons, Jr. M., Symons, J.M. 1997. H₂O₂/Vis UV photo-oxidation process for treatment of waterborne hazardous substances-Reaction mechanism, rate model and data for tubular flow and flow stirred tank reactors. *Water Management*, **17**: 507-515.
- Sójka-L, J., Koprowski, T., Machnowski, W., Knudsen, H.H. 1998. Membrane filtration of textile dyehouse wastewater for technological water reuse. *Desalination*, **119**: 1-9.
- Venceslau, P.C., Tom, S., Simon, J.J. 1994. Characterization of textile wastewater. *Environmental Technology*, **15**: 917-929.
- Vendevivere, P.C., Bianchi, R., Verstraete, W.A. 1998. Treatment and reuse of wastewater from the textile-wet-processing industry. *Journal of Chemical Technology*, **72**: 289-302.
- Xiong, Y., Karlson, H.T. 2001. Approach to a two-step process of dye wastewater containing Acid Red B. *Journal of Environmental Science and Health Part A*, **38**: 321-331.
- Yeh, R.Y., Thomas, A., 1995. Colour difference measurement and colour removal from dye wastewaters using different adsorbents. *Journal of Chemical Technology and Biotechnology*, **63**: 55-59.
- Yeh Ruth, Y.L., Liu, R., Chiu, H.M., Hung, Y.T. 1993. Comparative study of adsorption capacity of various adsorbents for treating dye wastewaters. *International Journal of Environmental Science and Technology*, **44**: 259-284.

Studies on Antifungal Activity and Elemental Composition of the Medicinal Plant *Trianthema pentendra* Linn.

Abdul Jabbar Pirzada*, Wazir Shaikh and Syed Abdul Ghaffar

Institute of Plant Sciences, University of Sindh, Jamshoro, Pakistan

(received October 7, 2009; revised February 13, 2010; accepted February 20, 2010)

Abstract. Antifungal activity of crude solvent and aqueous extracts of the medicinal plant, *Trianthema pentendra* Linn., against the dermatophytic fungi, *Aspergillus niger*, *Aspergillus flavus*, *Paecilomyces varioti*, *Microsporum gypseum* and *Trichophyton rubrum* revealed that ethanol and aqueous extracts were the most effective antifungal agents as compared to methanol, chloroform and ethyl acetate extracts. Some basic elements, Al, Ca, Cu, Fe, Mg, Mn, P, S and Zn were also determined in the medicinal plant, *T. pentendra*, using atomic absorption spectrophotometry and U.V spectrophotometry. *T. pentendra* contained considerable amount of elements which have therapeutic effects in skin diseases.

Keywords: *Trianthema pentendra*, antifungal activity, essential elements

Introduction

Plants are the best source of active secondary metabolites which are beneficial to mankind. Many plant origin drugs have been reported with biological properties like analgesic, anti-inflammatory, antioxidant, hypoglycemic and antifungal agents (Sindhu, 2009). Skin diseases, diarrhoea, diabetes, malaria, respiratory infection, fungal and bacterial infections are the common health problems in developing countries and numerous medicinal plants are used traditionally which are remedial against these diseases (Pinn, 2000).

Trianthema pentendra Linn., commonly known as waho, is a traditional medicinal plant which is utilized in many parts of Pakistan for the treatment of various fungal skin diseases like tinea capitis, tinea pedis, tinea manuum and tinea corporis etc. The root of plant is irritant and cathartic. Leaves of the plant are used as astringent and abortifacient and as remedy in abdominal diseases and bladder pain, for snake bite etc. (Baquar, 1989; Shahani and Memon, 1988; Kirtikar and Basu, 1935).

Elements play essential role in the maintenance of the skin health. Aluminum acetate solution, copper sulphate and zinc lotions are used as skin disinfectant, cleansing agents, antiseptic and soothing and cooling agents. Calcium, magnesium and manganese are used in the formation of the collagen and connective tissue. Phosphorus and sulphur are used for the treatment of scabies and leprosy. (Sahito *et al.*, 2003; Soderberge and Halimans, 1982; Underwood, 1981). Skin diseases are usually caused by fungi and are one of the main problems of Sindh province. The present

paper describes the antifungal potential of different solvent extracts of *T. pentendra* and is also its elemental study.

Materials and Methods

Plant material. The leaves and shoots of *T. pentendra* were collected from different areas of Kohistan regions, District Dadu and reference sample was identified by referring to Flora of Pakistan (Nasir and Ali, 1990). The collected plant materials were washed with distilled water and placed in shade at room temperature for two weeks. One kg of dried plant material was dipped in five litre ethanol in a bottle for 20 days for cold percolation. The extract was filtered and concentrated under reduced pressure below 40 °C using rotary evaporator. The residue was completely dried and from it five different extracts *viz.*, ethanol, ethylacetate, chloroform, methanol and aqueous extracts were prepared using separating funnel. The extracts were left at room temperature, so that the solvents were completely evaporated and organic compounds remained in dry form. The extracts so obtained were mixed with the sterilize water (1 g, 5 ml) and each extract sample was applied for antifungal activity.

Collection of dermatophytes. The dermatophytic fungi namely: *Aspergillus niger*, *Aspergillus flavus*, *Paecilomyces varioti*, *Microsporum gypseum*, *Trichophyton rubrum* were scraped from the skin of different body parts at out patient departments of Liaquat University Hospital, Jamshoro and Hyderabad.

Treatment of different solvent extracts. The human skin pathogens were treated with different extracts and results were taken after 72 h at 30 °C. The percentage of mycelial

*Author for correspondence; E-mail: aj_pirzada@hotmail.com

inhibition was calculated as follows (Ali Shtayeh and Abu Ghdeib, 1999, Usmanghani and Shameel, 1986).

$$\text{Mycelial inhibition (\%)} = [(dc-d1)/dc] \times 100$$

where:

dc = colony diameter in control

d1 = colony diameter in treatment

Methodology for element determination. A suitable dissolution method for biological sample to yield homogenous solution is the crucial first step in elemental determination with atomic absorption spectrophotometric and UV techniques. The decomposition of organic matter must be completed to avoid interference by organic residue. Samples were digested with nitric acid: hydrogen peroxide (30%), for determination of mineral elements. Appropriate working standard solution of aluminum (Al), calcium (Ca), copper (Cu), iron (Fe), magnesium (Mg), manganese (Mn), phosphorus (P), sulphur (S) and zinc (Zn) were prepared from stock standard solution (1000 ppm), in 2 N nitric acid. Calibration curves were drawn for each element using atomic absorption spectrophotometer (Hitachi, model 180-50) and UV-spectrophotometer. The calibration curves obtained for concentration *vs.*, absorbance data were statistically analyzed using fitting of straight line by least square method. A blank reading was also taken and necessary correction was made during the calculation of percentage concentration of various elements. The efficiency of extraction method was checked by standard addition method. The sample was spiked with known standards and digested with nitric acid and hydrogen peroxide mixture. The matrix of the standard and the sample solution was the same. The percentage recovery test for different

elements by the digestion method adopted was 98.5-99% in range.

Results and Discussion

All the crude extracts had significant antifungal activities against most of the fungi, but the activity of inhibition varied for the fungi with respect to the type of plant extract (Table 1).

Ethanol extract. The highest inhibition was observed against *T. rubrum*, *A. niger* and *A. flavus* being 100%, 95% and 95.2%, respectively, while moderate inhibition activity against *P. varioti* (72.73%) and minimum inhibition activity against *M. gypseum* (56.67%) was recorded.

Ethyl acetate extract. The highest inhibition was observed against *P. varioti* and *M. gypseum*, 54.55% and 50%, respectively while moderate inhibition of *A. niger* (45%) and minimum inhibition of *A. flavus* and *T. rubrum* (42.86% and 40%, respectively) was recorded.

Chloroform extract. The highest inhibition was observed against *P. varioti* 72.73% while moderate inhibition against *A. niger*, *T. rubrum* and *A. flavus* being 62.5%, 60% and 57.15%, respectively, and minimum inhibition activity against *M. gypseum* (50%) was noticed.

Methanol extract. The highest inhibition was observed against *P. varioti* 63.64%, while moderate inhibition against *T. rubrum*, *M. gypseum* and *A. niger* (60%, 50% and 50%, respectively) and minimum inhibition against *A. flavus* (42.86%) was determined.

Aqueous extract. The inhibition observed against *T. rubrum* and *A. niger* was 92% and 87.5%, respectively, while

Table 1. Antifungal activity of solvent extracts of *T. pentandra* Linn.

	Colony diameter (mm)*				
	<i>Aspergillus niger</i>	<i>Aspergillus flavus</i>	<i>Paecilomyces varioti</i>	<i>Microsporium gypseum</i>	<i>Trichophyton rubrum</i>
Control	40	35	55	30	25
Ethanol extract	02	05	15	13	00
Inhibition (%)	95	85.72	72.73	56.67	100
Methanol extract	20	20	20	15	10
Inhibition (%)	50	42.86	63.64	50	60
Chloroform extract	15	16	15	15	10
Inhibition (%)	62.5	57.15	72.73	50	60
Ethyl acetate extract	22	20	25	15	15
Inhibition (%)	45	42.86	54.55	50	40
Aqueous extract	05	14	15	15	02
Inhibition (%)	87.50	60	72.73	50	92

* = colony diameter readings taken at 30 °C after 72 h.

moderate inhibition activity against *P. varioti* and *A. flavus* (72.73% and 60%, respectively) and minimum inhibition against *M. gypseum* (50%) was measured.

Elements. Considerable amounts of various elements were found in the medicinal plant *T. pentendra* such as aluminum, calcium, copper, iron, magnesium, manganese, phosphorus, sulphur and zinc (Table 2). These elements are biologically very important in the treatment of different skin diseases.

Table 2. Quantity of different elements in *T. pentendra* Linn.

Elements	Amount (mg/kg)
Aluminum	6.93-7.95
Calcium	6491.09-7603.85
Copper	12.18-12.89
Iron	156.31-174.43
Magnesium	5722.16-6015.41
Manganese	67.70-81.00
Phosphorous	87.94-104.96
Sulphur	213.66-233.85
Zinc	53.64-66.91

In the study, it was observed that all the crude extracts showed significant antifungal activity against most of the fungi, but ethanol and aqueous extract had comparatively maximum inhibition activity being 50% and 100%, respectively. In comparison, methanol, ethyl acetate and chloroform extracts had inhibition activity in the range of 42-72% against test dermatophytes. Although many scientists (Pirzada *et al.*, 2007; Bajwa *et al.*, 2006; Anjum and Khan, 2003; Natarjan *et al.*, 2003; Ficker *et al.*, 2003; Adedotum and Okoli, 2002; Thebo and Abro, 2000; Sakharkar and Patil, 1999; Skaikh *et al.*, 1990; Usmanghani and Shameel, 1986), had screened the antifungal activity of medicinal plants against dermatophytes, but in this study, first attempt was made to investigate the antifungal activity of medicinal plant *T. pentendra* against dermatophytic fungi *viz.*, *Aspergillus flavus*, *A. niger*, *M. gypseum*, *P. varioti*, *T. rubrum* which cause different skin diseases like tinea capitis, tinea pedis, tinea manuum and tinea corporis.

Furthermore, some basic elements *viz.*, aluminum, calcium, copper, iron, magnesium, manganese, phosphorous, sulphur and zinc were found in variable range in the medicinal plant *T. pentendra*. But the concentration levels of the elements sulphur and zinc were found to be sufficient in the range of (213.66-233.85) and (53.64-66.91) mg/kg, respectively. All

these elements play essential role in the treatment of skin diseases (Saily *et al.*, 1994; Janjua, 1990).

References

- Adedotum, A.A., Okoli, S.O. 2002. Antifungal activity of crude extracts of *Alfia barteri* Oliver (Apocynaceae) and *Chasmanthera dependens* Hochst (Menispermaceae). *Hamdard Medicus*, **45**: 52-56.
- Ali-Shtayeh, M.S., Abu Ghdeib, S.I. 1999. Antifungal activity of plants extracts against dermatophytes. *Mycoses*, **42**: 665-672.
- Anjum, N., Khan, Z. 2003. Antimicrobial activity of the crude extract of *Cuscuta reflexa* Roxb. *Pakistan Journal of Botany*, **35**: 999-1007.
- Bajwa, R., Anjum, T., Shafique, S. 2006. Evaluation of anti fungal activity of *Cicer arietinum* L. *Pakistan Journal of Botany*, **38**: 175-184.
- Baqaar, S.R. 1989. *Medicinal and Poisonous Plants of Pakistan*, 506 pp., Printas, Karachi, Pakistan.
- Ficker, C.E., Arnason, J.T., Vindas, P.S. 2003. Inhibition of human pathogenic fungi by ethnobotanically selected plant extracts. *Mycoses*, **46**: 29-37.
- Janjua, K.M. 1990. Trace elements in *Allium cepa* (Onion) and their therapeutic importance. *Hamdard Medicus*, **33**: 87-90.
- Kirtikar, K.R., Basu, B.D. 1935. *Indian Medicinal Plants*, 1-IV, Lalit Mohan Basu, pp. 426-428, Allahabad, India.
- Nasir, E., Ali, S.I. 1990-1992. *Flora of Pakistan*, Department of Botany, University of Karachi, Karachi, Pakistan.
- Natarjan, V., Venugopal, P.V., Memon, T. 2003. Effect of *Azadirachta indica* (neem) on the growth pattern of dermatophytes. *Indian Journal of Medical Microbiology*, **21**: 98-101.
- Pinn, G. 2000. Herbal medicine, an overview. *Australian Family Physician*, **29**: 1059-1062.
- Pirzada, A.J., Shaikh, W., Kazi, T.G. 2007. Isolation of essential elements and inhibition activity of medicinal plant *Rhazya stricta* Dcne. against dermatophytic fungi. *Pakistan Journal of Agriculture, Agricultural Engineering and Veterinary Sciences*, **23**: 34-38.
- Sahito, S.R., Memon, M.A., Kazi, T.G., Kazi, G.H. 2003. Evaluation of mineral contents in medicinal plant *Azadirachta indica* (neem). *Journal of Chemical Society of Pakistan*, **25**: 139-143.
- Saily, A., Sahu, R., Gupta, B., Sondhi, S.M. 1994. Analysis of mineral elements of medicinal plants used for the treatment of asthma, syphilis, diarrhea, skin diseases and rheumatism, *Hamdard Medicus*, **37**: 18-22.
- Sakharkar, P.R., Patil, A.T. 1999. Antifungal activity of *Cassia*

- alata*. *Hamdard Medicus*, **41**: 20-22.
- Shaikh, W., Shameel, M., Hayee-Memon, A., Usmanghani, K., Bano, S., Ahmed, V.U. 1990. Isolation and characterization of chemical constituents of *Stoechospermum marginatum* (Dictyotales, Phaeophyta) and their antimicrobial activity. *Pakistan Journal of Pharmaceutical Sciences*, **3**: 1-9.
- Shahani, N.M., Memon, M.I. 1988. Survey and Domestication of Wild Medicinal Plants of Sindh, Pakistan. Research Report, Pakistan Agricultural Research Council (PARC).
- Sindhu, G. 2009. Antibacterial and antifungal studies of *Abutilon indicum* leaf extract. *Pharmacology*, **2**: 567-571.
- Soderberg, T., Halimans, G. 1982. Treatment of leprosy with adhesive Zinc tapes. *Leprosy Review*, **53**: 271.
- Thebo, N.K., Abro, H. 2000. Antifungal activity of *Azadirachta indica* against human pathogenic fungi. *Sindh University of Research Journal (Science Series)*, **32**: 35-42.
- Underwood, E. 1981. Trace metal in human and animal health. *Journal of Human Nutrition*, **53**: 37.
- Usmanghani, K., Shameel, M. 1986. Studies on the antimicrobial activity of certain seaweeds from Karachi coast. In: *Prospects for Biosaline Research, Proceedings of US-Pak Biosaline Research Workshop*, R. Ahmad and A. San Pietro (eds.), pp. 519-526, Department of Botany, University of Karachi, Karachi, Pakistan.

Culture of *Ceriodaphnia cornuta*, Using Chicken Manure as Fertilizer: Conversion of Waste Product into Highly Nutritive Animal Protein

Kareem Altaff* and Mehraj Ud Din War

Unit of Reproductive Biology and Live Feed Culture, Department of Zoology,
The New College (Autonomous), Chennai-600 014, Tamilnadu, India

(received August 6, 2009; revised January 26, 2010; accepted February 10, 2010)

Abstract. For finding a cheap and suitable feed for culture of *Ceriodaphnia cornuta* studies were carried out for 21 days using chicken manure as fertilizer whereupon *C. cornuta* population ranged between 50 ± 2 and $10,232 \pm 202$ Ind./L. (individuals/L). The culture peaked on the 17th day producing the maximum density of $10,232 \pm 202$ Ind./L. Thus chicken manure can be used as a fertilizer for mass culture of cladocerans, specially *C. cornuta*.

Keywords: culture, chicken manure, *Ceriodaphnia cornuta*, live feed

Introduction

The need for large quantities of live feed organisms in aquaculture and the increasing need for valorizing organic wastes, such as animal manure and agro-industrial residue, have been the major initiatives for research on the culture of live feed organisms (DePauw *et al.*, 1980). Chicken manure is a waste produced in poultry farms in large quantities and is cheap. According to Banerjee *et al.* (1979) it is a complete fertilizer with both organic and inorganic fertilizer characteristics. Ray and David (1969) opined that chicken manure-fertilized medium produced a large population of cladocerans quicker than cattle manure and the plankton biomass increased with the increase of its dosage. The bacteria (gram positive and gram negative) and protozoans (*Paramaecium* sp.) produced in the fertilized medium form the suitable feed for mass production of this species. Different culture techniques are being developed to increase yield of cladocerans by employing different waste organic products as feed sources (Tay *et al.*, 1991; Punia, 1988; Shim, 1988). Although *Artemia* nauplii (Versichele *et al.*, 1986) and rotifers (Pourrito, 1986) are common live feed organisms which are mass cultured for hatchery use, there is growing interest for the production of Cladocera (Adeyemo *et al.*, 1994). But availability of live feed is still a bottle neck in commercial seed production (Rao and Tripathi, 1993). A variety of artificial pelletized feed are available to rear the voracious larval stages of cultivable species which are not preferred as compared to live feed (Sumitra, 1987).

As the cladocerans are considered to be suitable live feed for fish larvae, they were mass cultured successfully by many

investigators using different cheap organic waste products, (Golder *et al.*, 2007; Shrivastava *et al.*, 2006; Sivakumar, 2005; Suresh Kumar, 2000). Due to the smaller size and locomotive behaviour, *C. cornuta* has become the most preferable species of the fish larvae (Suresh Kumar, 2000).

The aim of this paper is to demonstrate the feasibility of maintaining culture for mass production of *Ceriodaphnia* solely on chicken manure and to provide practical guidelines to run such cultures.

Materials and Methods

Chicken manure was collected from a local broiler chicken shop and was dried for 2 days to remove the moisture and then in plastic jars for further use. Chicken manure was micronized by grinding and the required quantity was dissolved in distilled water to get suspension of 400, 700 and 1000 ppm and was used to fertilize culture medium. Chicken manure suspension of 700 ppm concentration supported higher density of *C. cornuta* than other concentrations during preliminary trials carried out in 1 L beaker and was used to fertilize the medium for mass culture in 50 L tanks. Zooplankton sample was collected from Chetpet Freshwater Pond, Chennai India and was brought to the laboratory with the least disturbance. The adult *C. cornuta* were separated using binocular dissection microscope based on the key characters outlined by Suresh Kumar and Sivakumar (2004).

The experimental aquarium tanks of 50 L capacity were filled with 40 L of filtered water and were fertilized with chicken manure at the rate of 700 ppm. The tanks were arranged in triplicate and after 4 days, *C. cornuta* were inoculated in each experimental tank at the rate of 50 Ind./L (individual per litre) containing both adults and neonates. The culture experiment

*Author for correspondence; E-mail: kaltaff@rediffmail.com

was conducted for 21 days. Water change was carried out after every 3 day interval by removing 50% of the water. Food was administered as a function of population density every 3rd day using the formula of DePauw *et al.* (1981):

$$Y = [(\log 10^N/10) - 0.2] \times V \times d.$$

where:

Y = quantity of chicken manure

N = population density (Ind./L)

V = volume of culture (L)

d = number of days for which the food is to be given

The culture water used in all experiments was tap water, previously aerated for 24 h to dechlorinate the water (Ivleva, 1973). To avoid anaerobic conditions in the medium, the sediment (unconsumed food, faeces and pseudofaeces) was siphoned from the bottom three times a week. Excessive fouling was also removed from the walls of the tanks. Population density was estimated by counting samples, taken at random with 1 L beaker, after mixing the culture volume. Subsamples of 100 mL and then 10 mL were drawn from these samples. Samples were immobilized using alcohol and counting was carried out using Sedgwick Rafter cell under a binocular dissection microscope. Results were expressed as number of individuals per litre (Ind./L).

Results and Discussion

In the current study, the highest population of *C. cornuta* was observed in the tanks fertilized with 700 ppm concentration of chicken manure which suggested that 700 ppm might be the optimum level. Nutrients beyond the optimum level reduced population and this may be due to the rapid degradation of high nutrient content in the medium, resulting in increased ammonia and growth of pathogenic microbes (Adeyemo *et al.*, 1994). Tucker *et al.* (1979) and Doyle and Boyd (1984) reported that water quality deteriorated in the systems receiving high organic input or commercial feed. Similarly, concentration of nutrients below the optimum level also resulted in reduced population of *C. cornuta* which may be due to insufficient microbial and protozoan populations. Reduced population in low concentration may also be due to the lack of sufficient organic compounds that are required for the growth and survival of the live feed organisms.

During the culture period, the *C. cornuta* population ranged between 50 ± 2 and $10,232 \pm 202$ Ind./L. The culture peaked on the 17th day producing a maximum density of $10,232 \pm 202$ Ind./L (Fig. 1). Compared to the previous reports, higher population of *C. cornuta* was recorded in the present study at 700 ppm. Suresh Kumar (2000) and Sivakumar (2005)

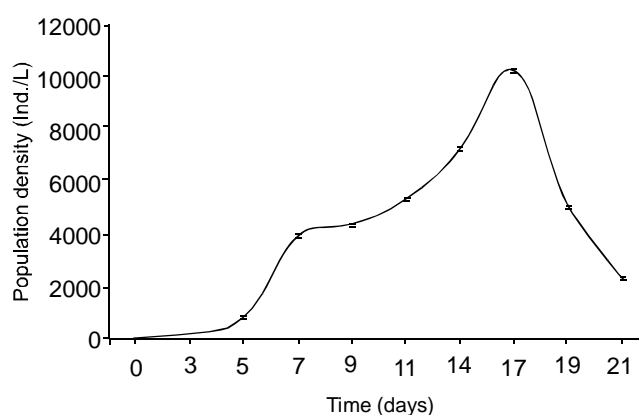


Fig. 1. Population density of *C. cornuta* (Ind./L) on different days during the culture (mean \pm SE).

reported 5817 Ind./L and 6247 Ind./L in chicken manure and mixed algae mixture, respectively. Using a mixture of organic manure (cattle manure, poultry droppings and mustard oil cake), Shrivastava *et al.* (2006) cultured *C. cornuta* at a maximum density of 1930 Ind./L. Ray and David (1969) opined that chicken manure-fertilized medium produced a large population of cladocerans quicker than cattle manure; the plankton biomass increased with the increase of dosage. An absolute prerequisite to maintain cultures is to renew part of the culture water at regular intervals, to ensure a permanent good water quality. Our experiments prove that chicken manure is a suitable feed for *Ceriodaphnia*. It has many advantages in comparison to other live feeds (e.g., microalgae): it is available in large quantities, it can be purchased easily at low price; it can be used directly after drying, it can be stored for longer periods, it is easy to dose and it has none of the problems involved in maintenance of algal stocks and cultures (Sivakumar, 2005). It has been reported that a wide range of live and inert feeds can be successfully used in culturing live feed organisms (Sorgeloos and Persoone, 1975). A cheap feed, available worldwide, will be more helpful and will reduce the cost of expenditure on live feed culture, thereby reducing the cost of seed production in hatcheries. *Ceriodaphnia* can be grown to a high density on chicken manure. However, a necessary prerequisite is the exact dosing. The quantity of feed used in our experiment was based on the estimation of population density (DePauw *et al.*, 1981).

Overfeeding causes high mortality due to unfavorable conditions for culture. Frequent addition of small quantities appears to be the best regime. The maximum interval between the two consecutive feedings should not exceed 2-3 days. The more frequent the administration of appropriate small doses, the lower the risk of overfeeding (DePauw *et al.*, 1981). This prac-

tice also decreases the amount of culture medium which must be renewed at regular intervals. Under constant culture conditions, a feeding programme can be worked out as a function of the expected population development. By enriching the medium with chicken manure the culture revives in a few days (Muthupriya and Altaff, 2009). Thus the present study reveals that dehydrated chicken manure-fertilized medium at 700 ppm appears to be a suitable medium for successful culture of *C. cornuta* to high density.

Acknowledgement

The authors are thankful to ICAR-NAIP for providing funds to carry out this research work under the project F. No.1 (5)/2007-NAIP, dt. 22 Aug. 2008.

References

- Adeyemo, A.A., Oladosu, G.A., Ayinla, A.O. 1994. Growth and survival of fry of African catfish species, *Clarias gariepinus* Burchell, *Heterobranchus bidorsalis* Geoffrey and *Heteroclarias* reared on *Moina dubia* in comparison with other first feed sources. *Aquaculture*, **119**: 41-45.
- Banerjee, R.K., Ray, P., Singit, G.S., Dutta, B.R. 1979. Poultry droppings - its manurial potentiality in aquaculture. *Journal of Inland Fishery Society of India*, **2**: 94-108.
- DePauw, N., De Leenheer, L. Jr., Laureys, P., Morales, J., Reartes, J. 1980. Cul-pisciculture d'algues et d' invertébrés sur déchets agricoles. In: *La Pisciculture Enetang*, R. Billard (ed.), pp. 189-214, INRA Publications, Paris, France.
- DePauw, N., Laureys, P., Morales, J. 1981. Mass cultivation of *Daphnia magna* Straus on rice bran. *Aquaculture*, **25**: 141-152.
- Doyle, K.M., Boyd, C.E. 1984. The timing of inorganic fertilization of sunfish ponds. *Aquaculture*, **37**: 169-177.
- Golder, D., Rana, S., Paria, S.D., Jana, B.B. 2007. Human urine is an excellent liquid waste for the culture of fish food organism *Moina micrura*. *Ecological Engineering*, **4**: 326-332.
- Ivleva, I.V. 1973. *Mass Cultivation of Invertebrates: Biology and Methods*, Translated from Russian, 148 pp., Israel Program for Scientific Translations, Jerusalem, Isarel.
- Muthupriya, P., Altaff, K. 2009. Mass culture of *Ceriodaphnia cornuta* in chicken manure fertilized medium. *Journal of Experimental Zoology India*, **12**: 157-158.
- Pourrito, R. 1986. Les rotifères: biologie. In: *Aquaculture*, G. Barnabe (ed.), vol. **1**, pp. 201-222, Lavoisier, Paris, France.
- Punia, P. 1988. Culture of *Moina micrura* on various organic waste products. *Journal of Indian Fisheries Association*, **18**: 129-134.
- Rao, K.J., Tripathy, S.D. 1993. A manual of giant freshwater prawn hatchery. *CIFA Manual Series*, **2**: 50 pp.
- Ray, P., David, A. 1969. Poultry manure as potential plankton producer. *Labdev Journal of Science and Technology*, **7**: 229-231.
- Shim, K.F. 1988. Mass production of *Moina* in Singapore using pig manure. *World Aquaculture*, **19**: 59-60.
- Shrivastava, A., Rathore, R.M., Chakrabarthi, R. 2006. Effects of four different doses of organic manures in the production of *Ceriodaphnia cornuta*. *Bioresource Technology*, **97**: 1036-1040.
- Sivakumar, K. 2005. Freshwater Fish and Prawn Larval Rearing Using Indigenous live-feed. *Ph. D Thesis*, pp. 1-147, University of Madras, India.
- Sorgeloos, P., Persoone, G. 1975. Technological improvements for the cultivation of invertebrates as food for fishes and crustaceans. II. Hatching and culturing of the brine shrimp, *Artemia salina* L. *Aquaculture*, **6**: 303-317.
- Sumitra, V. 1987. Cultivation of live food organisms status and scope in India. In: *Advances in Aquatic Biology and Fisheries*, Natarajan, H. Suryanarayanan and P.K.A. Azis, (eds.), Prof. N. Balakrishnan Nair, Felicitation Volume, pp. 239-249, Kerala, India.
- Suresh Kumar, R., Sivakumar, K. 2004. Key to common cladocerans. In: *A Manual of Zooplankton*, Compiled for the National Workshop on Zooplankton, Chennai, K. Altaff (ed.), pp. 58-67, Unit of Reproductive Biology and Live Feed Culture, Department of Zoology, The New College, Chennai, India.
- Suresh Kumar, R. 2000. Studies of Freshwater Cladocerans use as Livefood in Aquaculture. *Ph.D Thesis*, pp. 1-147, University of Madras, India.
- Tay, S.H., Rajbanshi, V.K., Ho, W.H., Chew, J., Yap, E.A. 1991. Culture of cladoceran *Moina micrura* Kurz using agroindustrial wastes. In: *Proceedings of The Fourth Asian Fish Nutrition Workshop*, S.S. De Silva (ed.), pp.135-141, Manila, Phillipines.
- Tucker, L., Boyd, C.E., McCoy, E.W. 1979. Effects of feeding rate on water quality, production of channel Catfish and economic returns. *Transactions of The American Fisheries Society*, **108**: 389-396.
- Versichele, D., Leger, P., Lavens, P., Sorgeloos, P. 1986. Utilization d' *Artemia*. In: *Aquaculture Collective Techniques Documents*, G. Barnabe (ed.), pp. 239-258, Lavoisier, Paris, France.

Contribution of Micronutrient Fertilization in Wheat Production and its Economic Repercussions

Ehsan-ul-Haq Chaudhary^{a*}, Muhammad Akram Chaudhary^a, Vincent Timmer^a,
Rizwan Khalid^a and Majid Raheem^b

^aSoil Fertility Survey and Soil Testing Institute, Rawalpindi, Pakistan

^bSoil Fertility Survey and Soil Testing Institute, Gujranwala, Pakistan

(received March 30, 2009; revised February 15, 2010; accepted February 16, 2010)

Abstract. Wheat response to the application of Zn, Fe and B in rice-wheat cropping pattern at ten locations in the fields in the Punjab, Pakistan was studied. The highest mean wheat grain yield (4707 kg/ha) was recorded with application of Zn:B @ 5:1 kg/ha, followed by 4678 kg/ha with Zn:Fe @ 5:10 kg/ha. The three micronutrients increased the grain yield from 1.8 to 11.8% over control, highest being recorded with the application of Zn:B @ 5:1 kg/ha. Combined application of all the three micronutrients reduced the grain yield by 1% compared to the highest yield attained by the combine application of Zn and B. However, the application of Zn @ 5 kg/ha proved to be the most economical micronutrient application with VCR of 4.80. None of the three nutrients increased the wheat grain yield in Gujrat, whereas Zn significantly increased the grain yield over control in Mandi Bahauddin. Straw to grain ratio of wheat was significantly decreased by the application of micronutrients over control mainly due to increase in grain weight.

Keywords: micronutrients, wheat, fertilizer, zinc, iron, boron

Introduction

Wheat (*Triticum aestivum*) is an important rabi (winter) crop of Pakistan and is the most extensively cultivated crop in both the irrigated and the rainfed areas of the country. In Pakistan, during the year 2006-07, wheat was grown on an area of 8.58 million hectares with a total production of 23.30 million tones and average yield of 2716 kg/ha (GOP, 2008). To maintain the yield on a sustainable basis, proper amount of nutrients have to be added to each crop. Continuous cropping and contrasting edaphic requirement of crops have shown evidence of soil nutrient depletion and imbalances, low nutrient use efficiency, decline in organic matter and stagnant yield (Gupta *et al.*, 2003). To get optimum yield, a balance dose of macronutrients as well as micronutrients are required. The soils of Pakistan, across much of the 22 m/ha cultivated area, have been formed from calcareous alluvium and loess, and are low in most of the essential plant nutrients. Loss of organic matter, whether by erosion or high temperature, in agro ecosystem adds to impoverishment of soil resources of several nutrient elements (Hadda and Arora, 2006).

Deficiency of various micronutrients is related to soil type, crop and to various cultivars. Introduction of new high yielding hybrids or cultivars, demanding a higher level of soil fertility, has further accentuated the incidence of micronutrient deficiencies.

*Author for correspondence; E-mail: rizwank08@gmail.com

The widespread deficiencies of Fe and Zn on the world scale are estimated to be 30-50% of the cultivated area (Cakmak, 2002). Soil and plant analyses show that >50% of the cultivated soils of the country are unable to provide sufficient Zn and B to meet the need of many crops (Khattak, 1995). The information obtained from 329 soil samples collected from various depths during the period of seven months revealed widespread deficiency of Zn and B followed by Fe (Zia *et al.*, 2004). The widespread Zn and B deficiencies and micronutrient disorders have been reported for different field crops in all the four provinces of the country. More than 60% of soil in Punjab, 21% in NWFP, 6-94% in Sindh and 90% in Baluchistan, are reported to be Zn deficient; Fe and B deficiency has been reported by Aziz *et al.* (2004) in citrus, deciduous fruits, groundnut and many other crops, who also found that make-up dose of nutrients improved the crop quality and increased resistance in plants against biotic and abiotic stresses. Chaudhry *et al.* (2001) reported that 5 kg/ha Zn appeared to be the optimum dose for wheat crop. Rashid (2006) reported that wheat responded to B. Pervaiz *et al.* (2003) found that straw grain ratio (SGR) decreased with the subsequent increase in Zn application. The present study was, therefore, under taken to identify the wheat response to micronutrients and their economic contribution towards wheat production.

Materials and Methods

Ten experiments were conducted in fields of two districts, *viz.* Mandi Bahauddin and Gujrat, in the Punjab province of

Pakistan under irrigated condition for three years during 2004-5 to 2006-07. The samples were collected from experimental sites at the depth of 0-15 and 15-30 cm before sowing the wheat crop. Soil samples were analyzed for texture, EC_e, pH, soil organic matter, extractable phosphorus (P) and potash (K) by the methods described by Ryan *et al.* (2001) and Page *et al.* (1982). The micronutrients (Zn and Fe) were analysed using atomic absorption spectrophotometer (Ryan *et al.*, 2001) while boron (B) was analyzed by 0.05 M HCl extraction method (Rashid *et al.*, 1994) using spectrophotometer.

A basal dose of NPK @ 80:114:120 kg/ha were applied to all plots in the form of urea, triple super phosphate (TSP) and sulphate of potash (SOP), respectively. Full amount of PK and half of N were applied at sowing while remaining half amount of N was applied at the first irrigation. All the micronutrients Zn:Fe:B @ 5:10:1 kg/ha were applied at the sowing alone and in different combinations as zinc sulphate (ZnSO₄.7H₂O), Iron sulphate (FeSO₄.7H₂O) and boric acid (HBO₃), respectively. Three wheat varieties *viz.*, Inqulab-91, AS 2000 and NIAB were grown in randomized complete block design (RCBD). Net plot size was 252.9 m² for all the treatments. The agronomic efficiency for micronutrients (Zn, Fe and B) was computed according to Craswell (1987), as follows:

Agronomic efficiency (AE) = grain yield (fertilized plot) - grain yield (control plot)/micronutrient fertilizer rate.

Yield and fertilizer rates were in kg/ha.

The economic analysis of crop response to micronutrients was calculated through gross profit and value cost ratio (VCR) as described by Ahmed and Rashid (2003). The price of wheat grain was Rs. 23.75/kg and that of the fertilizers, Zn, Fe and B, was Rs. 340, 249 and 910/kg, respectively. The statistical analysis of the data was carried out by applying Analysis of Variance technique (Steel and Torrie, 1980) using MSTAT package.

Results and Discussion

Original soil characteristics. The physicochemical properties of soil of the fields, prior to sowing of crop, are described in Table 1. Mean soil pH value was 7.42 in the range of 6.7-7.7 with the variation of 0.27. The electrical conductivity (EC) was 0.28 in the range of 0.1-0.4 dS/m with the variation of 0.23 at all the experimental sites in the category of normal soils *i.e.* free from salinity and sodicity. The organic matter in all the experimental sites ranged from 0.40-0.80% with the average values of 0.60%, whereas bicarbonate extractable soil phosphorus ranged from 3-6 mg/kg with the mean value of 4.37 mg/kg indicating that soil organic matter and

bicarbonate extractable phosphorus were low. Boron in the soil ranged from 0.10-0.86 mg/kg with the mean value of 0.31 mg/kg and Zn ranged from 0.54-2.69 with the average value of 1.58 mg/kg. It indicates that the soils are low to medium range making B and Zn fertilization probable. Similarly, iron ranged from 0.96-2.67 mg/kg with the mean value of 1.97 mg/kg indicating low range of Fe.

Table 1. Physicochemical properties of experimental sites

Soil properties	Units	Mean	Range	Standard deviation
pH	-	7.42	6.7-7.7	0.27
EC	dS/m	0.28	0.1-0.40	0.23
Organic matter	%	0.60	0.40-0.80	0.12
Available phosphorous (P)	mg/kg	4.37	3.0-6.0	0.71
Available potassium (K)	mg/kg	116	110-130	12.16
Zinc (Zn)	mg/kg	1.58	0.54-2.69	1.53
Iron (Fe)	mg/kg	1.97	0.96-2.67	1.43
Boron (B)	mg/kg	0.31	0.10-0.86	0.73

Wheat response to micronutrients. Wheat responded significantly ($P < 0.05$) to individual micronutrient application across all the experimental sites. The pooled data revealed that increase in grain yield with the application of individual nutrient compared to control was 1.78% for B, 4.35% for Fe and 8.12% for Zn (Table 2). This increase in wheat grain yield with application of micronutrients was due to the improvement in grain weight. It is evident from Table 5 that straw to grain ratio decreased with the application of micronutrients as compared to control. The data also indicated that wheat was consistently responsive to Zn followed by Fe and B application. The combined application of three micronutrients reduced the grain yield by 1% compared to the highest yield of 4707 kg/ha attained with combined application of Zn (5 kg/ha) and B (1 kg/ha). It might be due to the antagonistic effect of Zn and Fe or of Fe with P (Imtiaz *et al.*, 2003; Alam and Shereen, 2002). It is a well established fact that different nutrients may interact with each other by affecting the availability of each other from soil and their status in the plants through the process of growth and absorption. Interaction of nutrients in crop plants occurs when the supply of one nutrient affects the absorption and utilization of the other nutrient (Fageria *et al.*, 1997). This type of interaction is most common when one nutrient is in excess concentration in the growth medium. Similarly, Imtiaz *et al.* (2003) found that as the Zn concentration in the substrate increased, the concentration of Fe in the plants decreased. In another study, Alam and Shereen (2002) indicated that chlorophyll content generally increased at low level of Zn and P, while at higher Zn and P level, it decreased as compared to the control.

Table 2. Impact of micronutrients on wheat yield and economic performance

Nutrients (kg/ha)			Yield (kg/ha)	Increase in yield (%)	Net return (Rs.)	VCR	GNR
Zn	Fe	B					
0	0	0	4211 ^d	-	-	-	-
0	0	1	4286 ^{cd}	1.78	879	1.97	75
0	10	0	4394 ^{bc}	4.35	1856	1.75	18.3
5	0	0	4553 ^{ab}	8.12	6423	4.79	68.4
0	10	1	4663 ^a	10.73	7343	3.16	41.10
5	0	1	4707 ^a	11.78	9178	4.53	82.70
5	10	0	4678 ^a	11.09	6901	2.65	31.13
5	10	1	4636 ^a	10.09	5004	1.98	26.56

VCR = value: cost ratio; GNR = grain: nutrient ratio; means followed by different letters are significantly different at 5% level of probability.

Varietal response to micronutrients. The response of three wheat genotypes *viz.* Inqlab-91, AS-2000, NIAB to micronutrients (B, Fe and Zn) fertilization were studied through ten field experiments located in two irrigated districts *viz.* Mandi Bahauddin and Gujrat (Table 3). These wheat varieties responded significantly to micronutrients when applied singly as well as in various combinations. Data also indicated that yield potential of NIAB variety was greater than the other two varieties. Yield variations in various varieties with the application of micronutrients might be due to the difference in their yield potential (Kausar and Hamid, 1998) or micronutrient accumulative behaviour. Application of Zn alone to all the three varieties produced higher yield as compared to the yield obtained by the application of Fe and B alone. It revealed that application of Zn alone produced about 3 and 6% more yield compared to the yield obtained with the application of Fe and B alone, respectively. It also indicated that all the wheat varieties were more responsive to Zn followed by Fe and B. The integrated use of these micronutrients revealed that combined application of Zn and B gave the highest yield compared to all other combinations. Combined application of all the three nutrients impaired the yield by about 1.5% in all

the varieties compared to the highest yield obtained by Zn and B. The results are in line with those of Chaudhary *et al.* (2007) who reported that response of Inqlab 91 to Fe and B was higher than Chakwal 97, and in case of Zn, Chakwal 97 performed better than Inqlab 91 by increasing the wheat grain yield under water stressed condition. Graham *et al.* (1987) reported that Zn reduced the toxic effects of excessive B in crop plants.

Site specific response to micronutrients. The results of ten experiments, conducted on wheat in irrigated area of two districts *viz.* Mandi Bahauddin and Gujrat during 2004-05 to 2006-07, revealed a site specific response to B, Fe and Zn, when applied either singly or in combination (Table 4). The wheat grain yield of control in Gujrat district was about 7% higher than the control yield in Mandi Bahauddin. It might be due to the variation in original soil status of nutrients (Table 1). Individual application of all the three micronutrients did not significantly increase the wheat grain yield compared to control yield in Gujrat district; whereas, response to all the micronutrients applied individually was statistically significant in Mandi Bahauddin. It means that Mandi Bahauddin area is more responsive to micronutrients than Gujrat district.

Table 3. Response of wheat varieties to micronutrients and economic performance

Nutrients (kg/ha)			Inqlab 91				AS 2000				Niab			
Zn	Fe	B	Yield (kg/ha)	Net return	VCR	GNR	Yield (kg/ha)	Net return	VCR	GNR	Yield (kg/ha)	Net return	VCR	GNR
0	0	0	4139 ^c	-	-	-	2967 ^c	-	-	-	5385 ^c	-	-	-
0	0	1	4213 ^c	0	0.05	74	3022 ^{bc}	404	1.44	55	5481 ^{bc}	1378	2.52	96
0	10	0	4320 ^{bc}	99	1.04	18.1	3096 ^{abc}	574	1.23	12.9	5624 ^{abc}	3186	2.28	23.9
5	0	0	4472 ^{ab}	4499	3.65	66.60	3215 ^{abc}	4190	3.47	49.6	5830 ^{ab}	8869	6.23	89.0
0	10	1	4584 ^{ab}	5467	2.61	40.45	3299 ^{ab}	4499	2.32	30.18	5964 ^a	10359	4.05	52.64
5	0	1	4627 ^a	7278	3.80	81.33	3316 ^a	5667	3.19	58.16	6038 ^a	12907	5.96	108.83
5	10	0	4598 ^{ab}	5001	2.19	30.6	3296 ^a	3624	1.87	21.93	5998 ^a	10369	3.48	40.87
5	10	1	4557 ^{ab}	3128	1.61	26.13	3266 ^{ab}	2001	1.40	18.69	5943 ^{ab}	8163	2.62	35.06

VCR = value: cost ratio; GNR = grain: nutrient ratio; means followed by different letters are significantly different at 5% level of probability.

Table 4. Districtwise wheat response to micronutrients and economics

Nutrients (kg/ha)			Gujrat				Mandi Bahauddin			
Zn	Fe	B	Yield (kg/ha)	Net return	VCR	GNR	Yield (kg/ha)	Net return	VCR	GNR
0	0	0	4342 ^c	-	-	-	4071 ^e	-	-	-
0	0	1	4419 ^c	927	2.02	77	4144 ^{cd}	832	1.92	73
0	10	0	4531 ^{bc}	1999	1.80	18.9	4248 ^{bcd}	1714	1.69	17.2
5	0	0	4695 ^{abc}	6684	4.93	70.6	4402 ^{abcd}	6161	4.62	66.2
0	10	1	4808 ^{ab}	7676	3.26	42.36	4509 ^{abc}	7011	3.07	39.82
5	0	1	4853 ^a	9534	4.66	85.17	4552 ^a	8822	4.39	80.16
5	10	0	4824 ^{ab}	7258	2.73	32.13	4523 ^{abc}	6545	2.56	30.13
5	10	1	4780 ^{ab}	5313	2.04	27.38	4483 ^{abc}	4695	1.92	25.75

VCR = value: cost ratio; GNR = grain: nutrient ratio; means followed by different letters are significantly different at 5% level of probability.

The highest increase of 10% in grain yield of wheat over control was observed with the application of Zn alone followed by 4% with Fe alone in both the districts.

The capacity of soil to supply plant-available nutrients can vary greatly among fields and seasons leading to insufficient plant use across large areas (Dobermann *et al.*, 2004; Dobermann and White, 1999). Combined application of Zn and B gave the highest yield in both the districts. Combined application of the entire three micronutrients decreased wheat grain yield by 1.5% compared to the highest yield in both the districts. It might be due to antagonistic effect of Fe with Zn or Zn with P (Imtiaz *et al.*, 2003; Alam and Shereen, 2002). High level of several minerals (Ca, P, N, Mn, Cu and Zn) in soil contributes to Fe chlorosis presumably because they are involved in interaction with Fe nutrition, although Fe deficiency *per se* may inhibit absorption of some other elements (Madero *et al.*, 1993).

Agronomic performance of micronutrients for wheat. The agronomic efficiency of micronutrients varied considerably when applied singly or in combination (Table 2). The overall data revealed that agronomic efficiency of B (75) was at the highest followed by Zn (68.4) when applied singly. It might be due to low requirement of wheat for B as compared to that for Zn and Fe. The GNR increased with the combined application of Zn and B by about 10% and 21% compared to individual application of B and Zn, respectively. It may be explained by the fact that application of higher rate of Zn *viz.* 5 kg/ha reduced GNR compared to low dose of B (1 kg/ha). The GNR was reduced by the combined application of three micronutrients. While comparing different varieties, B efficiency was higher in NIAB followed by Inqlab 91 and AS 2000. The site specific agronomic performance was almost the same in both the districts.

Economic importance of micronutrients for wheat. The net return is the value of increased yield as a result of applied

fertilizer after providing the cost of fertilizer whereas the value cost ratio (VCR) is the rate of return from the money spent on fertilizer. The value 2 of VCR means a 100% return from the money spent on fertilizer. Variable tested with VCR value below 2 is not recommended for farmers because in this case net profit decreases (Ahmed and Rashid, 2003). The net return and VCR values were affected by micronutrients when applied singly as well as in combination (Table 2). The pooled data revealed that among the individual application of micronutrients, Zn application gave the highest net return of Rs. 2841 with the VCR value of 4.79. The application of Fe and B may not be recommended to farmers as the VCR by Fe and B application was lower than 2. The integrated use of micronutrients revealed that application of any two micronutrients gave the net return ranging from Rs. 3045 to Rs. 4058 with VCR value above 2. Combined application of three micronutrients may reduce the net profit which may be due to the reduction of efficiency of micronutrients. In case of various genotypes, application of each nutrient performed better whether applied singly or in combination as the VCR in most of the treatments was above 2 (Table 3). Based on site specific response to micronutrients, application of Zn and B is recommended in Gujrat district; whereas application of Zn is recommended in Mandi Bahauddin district.

Straw to grain ratio. Straw to grain ratio (SGR) of wheat crop was significantly decreased by the application of micronutrients (Table 5 and 6). The maximum decrease in SGR was observed in the treatment where only Zn was applied that was about 24% lower than the control. There was a decrease in SGR in all the varieties with the application of individual micronutrient as compared to combined application of these micronutrients. Application of Fe alone impaired the SGR of Inqlab 91 and NIAB to about 30% and 27% followed by 24% and 19% with Zn application, respectively, whereas, the trend was reciprocal in AS-2000 variety, in which Zn performed better to increase the grain yield. The combined application of

Table 5. Impact of micronutrients on straw: grain ratio of wheat (districtwise)

Nutrients (kg/ha)			Mandi Bahauddin		Gujrat		Over all	
Zn	Fe	B	SGR	Decrease (%)	SGR	Decrease (%)	SGR	Decrease (%)
0	0	0	2.114	-	1.75	-	1.950	-
0	0	1	1.766	16.46	1.63	6.76	1.704	12.61
0	10	0	1.490	29.52	1.37	21.49	1.437	26.30
0	10	1	1.682	20.43	1.58	9.46	1.637	16.05
5	0	0	1.478	30.09	1.47	16.04	1.472	24.51
5	10	0	1.548	26.77	1.52	12.72	1.537	21.17
5	0	1	1.756	16.93	1.62	7.44	1.693	13.18
5	10	1	1.868	11.64	1.71	1.89	1.799	7.74

SGR = straw: grain ratio.

Table 6. Effect of micronutrients on straw: grain ratio of three wheat varieties

Nutrients (kg/ha)			Inqlab91		AS2000		NIAB		Over all	
Zn	Fe	B	SGR	Decrease (%)	SGR	Decrease (%)	SGR	Decrease (%)	SGR	Decrease (%)
0	0	0	2.033	-	2.02	-	1.807	-	1.950	-
0	0	1	1.770	12.94	1.843	8.76	1.677	7.19	1.704	12.61
0	10	0	1.420	30.15	1.780	11.88	1.320	26.95	1.437	26.30
0	10	1	1.704	16.18	1.580	21.78	1.703	5.76	1.637	16.05
5	0	0	1.540	24.25	1.200	40.59	1.467	18.18	1.472	24.51
5	10	0	1.636	19.28	1.270	37.12	1.607	11.06	1.537	21.17
5	0	1	1.784	12.25	1.493	26.09	1.810	0.66	1.693	13.18
5	10	1	1.904	6.35	1.533	24.11	1.943	0.08	1.799	7.74

SGR = straw: grain ratio.

all the three nutrients did not significantly increase the grain weight of Inqlab 91 and NIAB compared to the yield obtained by the application of other micronutrients. The higher response of AS 2000 to Zn might be due to micronutrient accumulative behaviour of this cultivar. Pervaiz *et al.* (2003) found that SGR decreased with the increase in Zn application. Non-significant effect of integrated application of micronutrients over control might be due to antagonistic effect that reduced the grain weight of wheat. Imtiaz *et al.* (2003) reported that Zn application has adverse effect on Fe concentration and Fe uptake by plants. They also reported that Zn has also antagonistic effect on the uptake of Mn and Cu in plants.

Conclusion

This study showed that differences in grain yield between individual micronutrient application and control was significantly higher with Zn followed by Fe and B. Application of Zn alone to the three varieties produced higher yield compared to the yields obtained by Fe and B. None of the three micronutrients augmented the wheat grain yield in Gujrat district whereas Zn performed significantly better in Mandi Bahauddin District. Agronomic efficiency of B was the highest followed by Zn and Fe when applied singly. The economic performance revealed that Zn gave the highest net

return (Rs. 2841) with the VCR value of 4.79. The application of Fe and B may not be recommended to the farmers as the VCR is < 2. SGR of wheat decreased by the application of micronutrients, mainly due to the increase in grain weight.

References

- Ahmed, N., Rashid, M. 2003. *Fertilizer Use in Pakistan*. National Fertilizer Development Center, 138 pp., Planning and Development Division, Islamabad, Pakistan.
- Alam, S.M., Shereen, A. 2002. Effect of different levels of Zinc and phosphorus on growth and chlorophyll concentration of wheat. *Asian Journal of Plant Sciences*, **2**: 364-366.
- Aziz, T., Gill, M.A., Rahmatullah, Sabir, M. 2004. Mineral nutrition of fruit trees. In: *Proceedings of 1st International Symposium on Plant-Nutrition Management for Horticultural Crops Under Water-Stress Conditions*, M. Ibrahim (ed.), pp. 28-33, Agricultural Research Institute, Saria Road, Quetta, Pakistan.
- Cakmak, I. 2002. Plant nutrient research: Priorities to meet human needs for food in sustainable way. *Plant and Soil*, **247**: 3-24.
- Chaudhary, E.H., Timmer, V., Javed, A.S., Saddique, M.T. 2007. Wheat response to micronutrients in rain fed area of Punjab. *Soil and Environment*, **26**: 97-101.

- Chaudhry, R.A., Akram, M., Gill, K.H., Qazi, M.A. 2001. Zinc requirement of wheat crop. *Pakistan Journal of Soil Science*, **20**: 110-111.
- Craswell, E.T. 1987. The efficiency of urea fertilizer under different environment conditions. Paper presented at the International Symposium on Urea Technology and Utilization (FADINAP) Kuala Lumpur, Malaysia. 16-18 March, 1987, pp. 1-11.
- Dobermann, A., White, P.F. 1999. Strategies for nutrient management in irrigated and rainfed low land rice systems. *Nutrient Cycling Agroecosystem*, **53**: 1-18.
- Dobermann, A., Abdulrachman, S., Gines, H.C., Nagarajan, R., Son, T.T. 2004. Agronomic performance of site specific nutrient management in intensive rice cropping system of Asia. In: *Increasing Productivity of Intensive Rice Systems Through Site Specific Nutrient Management*, A. Dobermann, C. Witt and D. Dawe (eds.), pp. 307-336, Science Publishers Inc., International Rice Research Institute (IRRI), Banos, Philippines.
- Fageria, N.K., Baligar, V.C., Jones, C.A. 1997. *Growth and Mineral Nutrition of Field Crops*, 2nd edition, Marcel Dekker Inc., New York, USA.
- GOP, 2008. *Statistical Year Book of Pakistan-2008*, Statistics Division, Federal Bureau of Statistics, Govt. of Pakistan, Islamabad, Pakistan.
- Graham, R.D., Welch, R.M., Grunes, D.L., Cary, E.E., Norvell, W. A. 1987. Effect of Zinc deficiency on the accumulation of boron and other mineral nutrients in barley. *Soil Science American Journal*, **51**: 652-657.
- Gupta, R.K., Noresh, R.K., Hobbs, P.R., Jianguo, Z., Ladha, J.K. 2003. Sustainability of post green revolution agriculture, the rice wheat cropping systems of the Indo-Gangetic plains and China. In: *Improving the Productivity and Sustainability of Rice Wheat Systems Issues and Impact*, J. Ladha and K. J. E. Hill (eds.), pp. 1-25, ASA Special publication No. 65, ASA-CSSA-SSSA, Madison, Wisconsin, USA.
- Hadda, M.S., Arora, S. 2006. Soil and nutrients management practices for sustaining crop yields under maize-wheat cropping sequence in submountain Punjab, India. *Soil and Environment*, **2**: 1-5.
- Imtiaz, M., Alloway, B.J., Shah, K.H., Saddiqui, S.H., Memon, M.Y., Aslam, M., Khan, P. 2003. Zinc nutrition of wheat. II. Interaction of Zinc with other trace elements. *Asian Journal of Plant Sciences*, **2**: 156-160.
- Kausar, M., Hamid, A. 1998. Susceptibility of fourteen wheat varieties to low soil copper. *Pakistan Journal of Soil Science*, **14**: 135-139.
- Khattak, J. 1995. Micronutrients in Pakistan Agriculture, PARC Islamabad and Department of Soil Science. NWFP Agricultural University, Peshawar, Pakistan.
- Madero, P., Pequerul, A., Perez, C., Val, J., Monge, E. 1993. Specificity of iron in some aspects of soybean (*Glycine max L.*). In: *Optimization of Plant Nutrition*, M. A. C. Frago and M. L. Beusichem (eds.), pp. 497-502, Kulwer Academic Publishers, Dordrecht, The Netherlands.
- Page, A.L., Miller, R.H., Keeney, D.R. 1982. *Methods of Soil Analysis, Part 2*, pp. 506-509, 2nd edition, American Society of Agronomy, Madison, Wisconsin, USA.
- Pervaiz, Z., Hussain, K., Kazmi, S.S.H., Akhtar, B. 2003. Zinc requirement of barani wheat. *Asian Journal of Plant Science*, **2**: 841-84.
- Rashid, A. 2006. Boron deficiency in soils and crops of Pakistan: Diagnosis and management, 40 pp., Pakistan Agricultural Research Council, Islamabad, Pakistan.
- Rashid, A., Rafique, E., Bughio, N. 1994. Diagnosing B deficiency in rapeseed and mustard by plant analysis and soil testing. *Communications in Soil Science and Plant Analysis*, **25**: 2883-2897.
- Ryan, J., Estefan, G., Rashid, A. 2001. *Soil and Plant Analysis Laboratory Manual*, pp. 42 and 165, 2nd edition, Jointly published by ICARDA and NARC, Pakistan.
- Steel, R.G.D., Torrie, J.H. 1980. *Principles and Procedures of Statistics*, 2nd edition, pp. 188-189, McGraw Hill Book Company Inc., New York, USA.
- Zia, M.S., Aslam, M., Ahmed, N., Cheema, M., Shah, A., Laghari, H. 2004. Disgnosis of plant nutrient disorders in fruit plants. In: *Proceedings of 1st International Symposium on Plant-Nutrition Management for Horticultural Crops Under Water-Stress Conditions*, M. Ibrahim (ed.), pp. 16-27, Agricultural Research Institute, Sariab Road, Quetta, Pakistan.

Grain Yield Losses in Wheat by Russian Wheat Aphid *Diuraphis noxia* (Mordvilko)

Lal Hussain Akhtar^{a*}, Altaf Hussain Tariq^b, Manzoor Hussain^b, Rana Muhammad Iqbal^b,
Muhammad Arshad^c and Marghub Amer^c

^aRegional Agricultural Research Institute (RARI), Bahawalpur, Pakistan

^bCholistan Institute of Desert Studies, The Islamia University of Bahawalpur, Pakistan

^cSub-campus University of Agriculture Faisalabad at Depalpur (Okara), Pakistan

(received December 18, 2008; revised November 2, 2009; accepted December 2, 2009)

Abstract. Eight wheat cultivars were sown at the Regional Agricultural Research Institute, Bahawalpur, Pakistan, to evaluate their response to Russian wheat aphid (RWA) *Diuraphis noxia* (Mordvilko). Significant variability was observed among cultivars with respect to aphid infestation and yield losses. Cultivar V-2707 was the least infested with the aphid (6.3 aphids/tiller) giving maximum grain yield (4638 kg/ha), with cultivar V-2047 the second best with 6.43 aphids/ tiller infestation and grain yield of 4206 kg/ha. Commercial cultivars (Inqlab-91 and Punjab-96) were heavily infested with 14.4 and 12.6 aphids/tiller, respectively, and yielded 2245 and 2490 kg/ha harvest, respectively. Aphid population increased upto the fourth week of March and then declined. Aphid infestation resulted in 3.96 to 7.36% yield loss. The cultivar V-2707 was later released for general cultivation, under the name of Punjab-1.

Keywords: *Triticum aestivum*, aphid, yield loss, *Diuraphis noxia*

Introduction

Pakistan, with a population of 160.9 million by mid-2008 is the sixth most populous country in the world. The country's population is estimated to double by the year 2045 if population growth continues at 1.8% per annum (Economic Survey of Pakistan, 2008). Wheat is the most widely grown crop in the world. In Pakistan, wheat is a staple crop and is cultivated on some 8.459 million hectares giving production of 22.5 million tons during 2006-2007. It shares 13.7% of the value of Pakistan agricultural produce and 3.0% to GDP (Economic Survey of Pakistan, 2008).

Wheat crop suffers from a number of biotic and abiotic stresses from sowing to harvesting, including heat, drought, diseases and insect damage. One of the most recent and important pests of small grains is the Russian wheat aphid (RWA) *Diuraphis noxia* (Mordvilko). It spends its entire life cycle on the grains and grasses and is a serious pest of wheat. Russian wheat aphid prefers to live in leaf whorls and emerging tightly rolled leaves feeding on them. Infestation on leaves, stems, awns and heads result in necrosis and blackening of these plant parts, affecting grain yield. Aphid attack results in curling of leaves, delayed head emergence causing improper maturity of grains. Therefore, the early detection of pest infestation is important for its timely and proper control. Each 1% infestation level results in 0.5% yield

loss at harvest (Karren and Reeve, 1989). Aphid attack starts from emergence and continues upto maturity (Shea *et al.*, 2000; Karren and Reeve, 1989).

The aphid incidence level differs in different cultivars of wheat (Wratten and Redhead, 1976). Advanced lines of wheat differ significantly with respect to population of aphids and grain yield. The aphid population attains peak level in mid March (Chen *et al.*, 1994; Aheer *et al.*, 1993). Aphid population varies on test cultivars of wheat during February-April 2001 and peak level of aphids was noted during the third week of March (Parvez and Ali, 1999). Aheer *et al.* (2006) reported mean densities of wheat aphids to be 2.29, 2.07, 2.41, 2.23 and 2.22/tiller on wheat cultivars, Inqlab-91, Pasban-90, Pak-81, Uqab-2000 and Iqbal-2000, respectively, and found that infestation of aphids mainly concentrated on leaves, on heads (spikes) and stem of wheat plant. The present studies were aimed at determining the effect of aphid populations on different wheat cultivars under field conditions.

Materials and Methods

The field experiment, to evaluate the response of different wheat cultivars to Russian wheat aphid (RWA), was conducted at Regional Agricultural Research Institute, Bahawalpur, Pakistan. Bahawalpur is located at an altitude of 112 meters, latitude 29° 23' 60 N and longitude of 71° 40' 60 E. Eight wheat cultivars, including two checks (Inqlab-91, Punjab-96, V-2047, V-2236, V-2239, V-2251, V-2707 and V-7222), were sown in two

*Author for correspondence; E-mail: lhakhtar@yahoo.com

sets (sprayed and unsprayed). In the sprayed set, Furathiocarb was sprayed at 625 ml/ha during February (1st and 3rd weeks) and March (1st and 3rd weeks) in order to control aphid population. The experiment was laid out in a randomized complete block design with three replications of each set. Plot size was 5 m × 1.2 m in both the sets. N and P₂O₅ fertilizers were applied at the rate of 160 and 110 kg/ha, respectively. The experiment was sown on November 30, 2001. Four irrigations were applied to the crop at crown root, tillering, milky and grain filling stages. Weeds were controlled chemically with Bromoxynil. Aphid infestation was recorded at weekly intervals from the first week of February to the 3rd week of April, 2000. Fifteen tillers were selected randomly from each plot. Each tiller was clipped with a pair of scissors, brought to the laboratory and the aphids were separated from the stem and spikes with the help of a camel hairbrush, placed on a white paper and counted. At maturity, the yield data were recorded and percent loss was determined by using the following formula:

$$\text{Yield loss (\%)} = \frac{\text{Yield in sprayed set} - \text{Yield in unsprayed set}}{\text{Yield in unsprayed set}} \times 100$$

The yield and aphid data were subjected to analysis of variance by using computer package MSTATC and means were compared by calculating LSD (Steel and Torrie, 1980).

Results and Discussion

Aphid infestation. The highest aphid population was found on Inqlab-91 (14.4 aphids/tiller) followed by Punjab-96 (12.6 aphids/ tiller). The lowest mean aphid population (6.3 aphids/ tiller) was found on cultivar V-2707 (Table 1). Cultivars differed significantly with respect to aphid population ($P < 0.01$). Aphids were first observed at the beginning of February (Aheer *et al.*, 2006; Shea *et al.*, 2000). The maximum infestation (8.92 to 18.36 aphids/ tiller) was recorded during the month of March (Table 2). Minimum infestation (3.20 to 10.24 aphids/tiller) was observed during April. Aphid infestation gradually increased up to the 4th week of March and then decreased down to the 3rd week of April. The population peak from middle to the 4th week of March is consistent with the reported observations (Aheer *et al.*, 2006; Ahmad and Nasir, 2001; Rios and Conde, 1986). Decline in aphid population during April may be attributed to high minimum (21.5 °C) and maximum (37.2 °C) temperatures (Table 2). According to Aheer *et al.* (2007) and Kieckhefer and Elliotte (1989), the gross and net reproductive rates of both morphs were greater at low temperature regimes and decreased with an increase in the temperature. Thus aphid population decreased when maximum and minimum temperatures were 28.3-30.6 °C and

Table 1. Average Russian wheat aphid populations on different wheat cultivars during various months during the year 2000

Varieties	Russian wheat aphid population per tiller			
	February	March	April	Average
V-2047	6.23	8.92	4.14	6.43
V-2236	7.58	9.58	6.54	7.90
V-2239	6.02	12.75	4.12	7.63
V-2251	5.44	10.74	3.65	6.61
V-2707	4.98	10.72	3.20	6.30
V-7222	5.94	11.29	4.07	7.10
Inqlab-91	14.76	18.20	10.24	14.4
Punjab-96	12.89	18.38	6.53	12.6
Average	7.98	12.57	5.31	

Table 2. Maximum and minimum temperature recorded at Bahawalpur, during the year 2000

Months	Temperature (°C)	
	Maximum	Minimum
January	20.1	6.5
February	21.1	6.7
March	27.4	11.1
April	37.2	21.5

9.57-10.0 °C, respectively. Present results are in line with these findings.

Aphids were found on each tiller, head, leaf and stem. During the present study, aphid infestation was observed to result in the rolling of the flag leaf and trapping of the emerging heads and awns. This phenomenon may have caused reduction in pollination resulting in improper maturity and low grain yield in the tested cultivars (Aheer *et al.*, 2006; Shea *et al.*, 2000; Parvez and Ali, 1999).

Grain yield. The data of grain yield subjected to analysis of variance revealed significant differences between sprayed and unsprayed sets ($P < 0.01$). Significant differences were also observed among cultivars with respect to grain yield ($P < 0.01$). Cultivar V-2707 produced the highest yield (4638 kg/ha) followed by V-2047 (4206 kg/ha). Cultivar V-2707 had the lowest aphid population among all other cultivars. The cultivar with the lowest yield was Inqlab-91 (2245 kg/ha). Perusal of the data (Table 3) reveals that genotypes having maximum attack of aphids had the lowest yield and *vice versa*, suggesting direct relationship between mean aphid population and reduction in yield. The average loss in grain yield due to a single aphid/ tiller was 0.51% to 0.66%. Kieckhefer and Kantack (1980) reported substantial yield losses as the

Table 3. Yield, aphid infestation and loss in yield in various wheat genotypes

Genotypes	Yield (kg/ha)		Loss in grain yield over unsprayed set (%)	Aphid population/tiller (average of 12 weeks)	Average loss/aphid
	Sprayed	Unsprayed			
V-2047	4206	4026	4.47	6.43	0.70
V-2236	2965	2838	4.47	7.90	0.57
V-2239	3217	3077	4.55	7.63	0.60
V-2251	3927	3758	4.50	6.61	0.68
V-2707	4638	4454	4.13	6.30	0.66
V-7222	3664	3508	4.47	7.10	0.63
Inqlab-91	2245	2080	7.93	14.4	0.55
Punjab-96	2490	2333	6.73	12.6	0.53
LSD (5%)	256	312	-	2.67	1.87

direct effect of aphid feeding (Blackman and Eastop, 1984). The present results also get support from the findings of Kuroli and Nemeth (1987) who found 50 and 70% loss in grain weight in winter and spring wheat, respectively. Kieckhefer and Gellner (1992) also reported 35-40% losses at 15 aphids/plant (2.3-2.7% per aphid). Aheer *et al.* (1993) observed that 7.2 aphids/tiller caused a 16.4 % loss in grain yield (2.3% per aphid). Koryukovski (1984) reported 30-80% losses with 100-200 aphids/stem (0.3-0.4% aphid). Aphid infestation at the level of 1% causes 0.50% yield loss at harvest (Karren, 1989).

Conclusion

The wheat genotype V-2707 was found to be the least infested with RWA, producing the highest grain yield (4638 kg/ha) with 6.30 aphids/tiller. The wheat variety Inqlab-91 with 14.4 aphids/tiller had the highest infestation with a yield of 2245 kg/ha. The aphid infestation gradually increased upto the 4th week of March and then decreased upto the 3rd week of April and was affected by an increase in maximum and minimum temperatures. Genotypes responded differently to aphid infestation. There was a loss in grain yield in various genotypes ranging from 3.96 to 7.36% with increasing infestation of aphid. The genotype V-2707 was later on released for general cultivation based on its better performance in the name of Punjnad-I. It is concluded that aphid infestation causes significant loss to grain yield in wheat. The check varieties had higher infestation rate and greater loss in grain yield as compared with the new strains. The loss in grain yield, specially in the checks, demands plant protection measures but wheat being a staple food, the use of insecticides on wheat is not advisable. Therefore, the studies on RWA occurrence in the area and identification of resistant cultivars should be encouraged. Area sown to wheat cultivars with low levels of resistance should be decreased.

References

- Aheer, G. M., Munir, M., Ali, A. 2007. Impact of weather factors on population of wheat aphids at Mandi Baha-ud-Din District. *Journal of Agricultural Research (Pakistan)*, **45**: 61-68.
- Aheer, G. M., Munir, M., Ali, A. 2006. Screening of wheat cultivars against aphids in ecological conditions of District Mandi Baha-ud-Din. *Journal of Agricultural Research (Pakistan)*, **44**: 55-59.
- Aheer, G. M., Rashid, A., Afzal, M., Ali, A. 1993. Varietal resistance/susceptibility of wheat of aphids *Sitobion avenae* F. and *Rhopalosiphum rufiabdominalis* Sesaski. *Journal of Agricultural Research (Pakistan)*, **31**: 307-311.
- Ahmad, F., Nasir, S. 2001. Varietal resistance of wheat germplasm against wheat aphid (*Sitobion avenae* F.). *Pakistan Entomologist*, **23**: 5-7.
- Blackman, R.L., Eastop, V.F. 1984. *Aphids on The World's Crops: An Identification Guide*, pp. 210-214, John Wiley & Sons, New York, USA.
- Chen, J.L., Guo, Y.Y., Ni, H.X., Ding, H.J., Cao, Y.Z., Xia, Y.L. 1994. Studies on the dynamics of the field populations of the rose grain aphid. *Acta Phytomycolica Sinica*, **21**: 7-13.
- Economic Survey of Pakistan, 2008. *Population, Labour Force and Employment*, 195 pp., Economic Survey of Pakistan, Government of Pakistan.
- Karren, J.B., Reeve, T.A. 1989. *Russian Wheat Aphid in Utah*. Cooperative Extension Service, Extension Entomology, Fact Sheet No.67, Utah State University, Logan, Utah, USA.
- Kieckhefer, R.W., Kantack, B.H. 1980. Losses in yield in spring wheat in South Dakota. *Journal of Economic Entomology*, **69**: 421-422.
- Kieckhefer, R.W., Gellner, J.L. 1992. Yield losses in winter wheat caused by low density cereal aphid population. *Agronomy Journal*, **84**: 180-183.

- Kieckhefer, R.W., Elliotte, N.C. 1989. Effect of fluctuating temperatures on development of immature Russian wheat aphid (Homoptera, Aphididae) and demographic statistics. *Journal of Economic Entomology*, **82**: 119-122.
- Kostyukovski, M.G. 1984. Aphid and productivity of wheat. *Wheat, Barley and Triticale Abstracts*, **3**: 2014.
- Kuroli, G., Nemeth, I. 1987. Aphid species occurring on winter wheat, their damage and results of control experiments. *Nevenyedelem*, **23**: 385-394.
- Parvez, A., Ali, Z. 1999. Field screening of wheat germplasm against wheat aphids for the source of resistance. *Pakistan Entomologist*, **21**: 85-87.
- Rios De Saluso, M.L.A., Conde, A.A. 1986. Evaluation of the damage caused to wheat by the grain aphid, *Sitobion avenae*. *Serie Tecnica, Estacion Experimental Agropecuaria, Prana, Argentine*, **53**: 15.
- Shea, G., Botha, J., Hardie, D. 2000. *Russian Wheat Aphid: An exotic threat to Western Australia Agriculture*, Western Australia. Fact Sheet No. 22/2000.
- Steel, R.G.D., Torrie, J.H. 1980. *Principles and Procedures of Statistics: A Biometrical Approach*, pp. 187-188, 2nd edition, McGraw Hill Book Company, New York, USA.
- Wratten, S.D., Redhead, P.C. 1976. Effects of cereal aphids on growth of wheat. *Annals of Applied Biology*, **84**: 44-473.

Staining Effect of Yellow Dye Extracted from Wood of *Berberis vulgaris* L. on Angiospermic Stem Tissues

Faizanullah^a, Asghari Bano^{a*} and Yunus Dogan^b

^aDepartment of Plant Sciences, Quaid-i-Azam University, Islamabad, Pakistan

^bFaculty of Education, Department of Biology, Dokuz Eylul University, Buca / Izmir, Turkey

(received March 31, 2009; revised February 11, 2010; accepted February 13, 2010)

Abstract. Yellow dye was chemically extracted from wood of *Berberis vulgaris* L. using water and ethanol and its effectiveness as staining agent for angiosperm stem tissues was studied. The dye stained the lignified tissues of both monocotyledonous as well as dicotyledonous stem cross sections. However, the dye extracted in ethanol (10% w/v) was found more effective to stain the lignified tissues of plants.

Keywords: yellow dye, *Berberis vulgaris* L., angiospermic stem tissues

Berberis vulgaris L., belonging to family Berberidaceae, is a shrub commonly growing in the southern Europe, northwest Africa and western Asia. It bears great medicinal importance. It was formerly used as a source of yellow dye and contains an antibacterial compound berberine (Kong *et al.*, 2004). Berberine can be used as staining agent when dissolved in lactic acid (Lux *et al.*, 2005).

Staining anatomical sections of plant tissues provides an adequate method for rapid and inexpensive microscopic observation of their internal structure. For section staining both natural and synthetic dyes are used (Drury and Wallington, 1976). The commonly used natural dye is haematoxylin, obtained from wood of Mexican tree, *Haematoxylon campechianum* (Baker and Silvertown, 1985). Although synthetic dyes are very effective but their utilization is limited due to their harmful effects on human and animals. Some synthetic dyes have been in disuse due to their recognized adverse effects (Bhuyan and Saikia, 2004). Owing to the global demand for the use of environmental friendly and biodegradable materials, the use of natural dyes has once again gained interest (Garg *et al.*, 1991). The aim of the present investigation was to explore the effectiveness of yellow dye extracted from the wood of *B. vulgaris* L. for staining stem tissues of angiospermic plants.

Air dried wood of *B. vulgaris* L. was extracted with petroleum ether and after evaporating the petroleum ether, solutions were made using crystals in water and ethanol and used for staining. Free hand stem sections of *Pennisetum typhoides* (Burm.f.) Stapf. and C.E.Habb. syn: *P. glaucum* (L) R.Br. and *Chenopodium murale*, were prepared in ethanol, water, acetic acid and formalin, and stained with *Berberis* wood extracts

(water and ethanol) (Ruzin, 1999). Then they were observed under light microscope (Olympus BX51) and the intensity of staining was determined (Lux *et al.*, 2005).

The solutions of dye made in water and ethanol were found to stain the lignified tissues of both *P. typhoides* and *C. murale* stem cross sections (Table 1 and 2). However, ethanolic extract was more effective than aqueous extract. The colour of the dye extracted with water was light yellow while that extracted with ethanol was dark yellow. The ethanolic extract of dye imparted dark yellow colour to vascular tissues of the stem cross sections. The dye extract 10% (w/v) in ethanol was found to be more effective in staining vascular bundles of monocotyledonous as well as dicotyledonous stem cross sections; however, the staining effects were more pronounced on the latter. The results further revealed that the dye extract in ethanol could be used successfully to stain lignified plant tissue. Similar results were obtained by Avwioro *et al.* (2005) for dye extracted from wood of *Pterocarpus osun* and Faizanullah (2004) for dye extracted from leaves of Henna

Table 1. Staining effect of *Berberis vulgaris* L. wood dye on stem tissues of *Pennisetum typhoides*

Berberis wood extract	Tissue stained	Intensity of staining
I. In ethanol		
1%	Vascular	+
5%	Vascular	++
10	Vascular	+++
II. In water		
1%	Vascular	Traces
5%	Vascular	Traces
10	Vascular	Traces

*Author for correspondence; E-mail: asgharibano@yahoo.com

Table 2. Staining effect of *Berberis vulgaris* L. wood dye on stem tissues of *Chenopodium murale*

Berberis wood extract	Tissue stained	Intensity of staining
I. In ethanol		
1%	Vascular	+
5%	Vascular	++
10	Vascular	++++
II. In water		
1%	Vascular	Traces
5%	Vascular	Traces
10	Vascular	Traces

(*Lawsonia alba* Lam.) which can be used as an effective histological stain even in absence of mordants. The search for suitable mordants would further improve the feasibility of the extracted dye in ethanol for usage in plant micro techniques. The basic stains generally stain the nucleus while cytoplasm is stained by acidic stains (Baker and Silverton, 1985). In view of this, it can be expected that the dye extracted from wood of *Berberis* is acidic in nature. More experiments are needed to identify the exact nature of the yellow dye extracted in ethanol from *Berberis* wood by utilizing advanced chromatographic techniques as majority of the natural dyes contain several impurities and other dye fractions (Banerjee and Mukherjee, 1981), the identification of active ingredients of dye will open a new avenue of research in the field of dyeing. Although the dye extracted in ethanol was not tested against microorganisms, it could be tested as histological stain for bacteria and fungi. Moreover, search for different solvents for dye extraction and their implication as staining agents is also needed. Lux *et al.* (2005) reported that solving berberine in lactic acid was highly effective in staining the root tissues in plants.

References

- Avwioro, O., Aloamaka, G., Ojiana, P.C., Oduolat, N.U., Ekpo, E.O. 2005. Extracts of *Pterocarpus osun* as a histological stain for collagen fibers. *African Journal of Biotechnology*, **4**: 460-462.
- Baker, F.J., Silverton, R.E. 1985. The theory of staining. In: *Introduction to Medical Laboratory Technology*, pp. 385-391, 6th edition, Butterworths, London, UK.
- Banerjee, A., Mukherjee, A.K. 1981. Chemical aspects of santalin as a histological stain. *Stain Technology*, **56**: 83-86.
- Bhuyan, R., Saikia, C.N. 2004. Isolation of colour components from native dye bearing plants in Northeastern India. *American Journal of Pathology*, **164**: 873-877.
- Drury, R.A.B., Wallington, E.A. 1976. *Carleton's Histological Techniques*, 4th edition, Oxford University Press, London, UK.
- Faizanullah. 2004. Staining effect of the dyes extracted from leaves of Henna (*Lawsonia alba* Lam.) on angiospermic stem tissues. *M.Sc. Thesis*, pp. 1-45, Government Post Graduate College Bannu, NWFP, Pakistan.
- Garg, A., Shenda, S., Gupta, K.C. 1991. Effect of mordants on colour of natural dye extracted from tissue flowers (*Butea mongosperma*). *Colourage*, **38**: 50-53.
- Kong, W., Wei, J., Abidi, P., Lin, M., Inaba, S., Li, C., Wang, Y., Wang, Z., Si, S., Pan, H., Wang, S., Wu, J., Wang, Y., Li, Z., Liu, J., Jiang, J.D. 2004. Berberine is a novel cholesterol-lowering drug working through a unique mechanism distinct from statins. *Nature Medicine*, **10**: 1344-1351.
- Lux, A., Morita, S., Abe, J., Ito, K. 2005. An improved method for clearing and staining free-hand sections and whole-mount samples. *Annals of Botany*, **96**: 989-996.
- Ruzin, S.E. 1999. *Plant-Microtechnique and Microscopy*, 334 pp., Oxford University Press, New York, USA.

Effect of Low Cost Iron Oxide with Si Additive on Structural Properties of Ni-Zn Ferrite

Uzma Ghazanfar

Department of Physics, University of Wah, Wah Cantt, Pakistan

(received November 13, 2009; revised January 12, 2010; accepted January 15, 2010)

Abstract. Mixed Ni-Zn ferrites ($x = 0.66, 0.77, 0.88, 0.99$) were prepared by double sintering ceramic method using locally available low cost Fe_2O_3 with 0.5% (by wt) of Si additive. The chemical phase analysis, carried out by X-ray powder diffraction method, confirms the major phase of Ni-Zn ferrite. Study of the effect of composition on structural properties of ferrite system revealed a decreasing trend of lattice parameters with increasing Ni content. X-ray density and mass density increase with increasing Ni content, which in turn decreases the porosity due to successive presence of Si in Fe_2O_3 . This decrease in porosity along with chemical homogeneities, distribution of phases and grain formation were also observed in scanning electron micrographs.

Keywords: Ni-Zn ferrites; Si additive; iron oxide; ceramics

Introduction

Ferrites, being ceramic materials formed by sintering, have mechanical properties similar to those of pottery. In particular the properties depend on the sintered density. It was reported by Costa *et al.* (2003) and Snelling (1988), that during sintering, oxides react to form crystallites or grains which, nucleating at discrete centres, grow outwards until the boundaries meet those of neighbouring crystallites. During this process, the density rises; if this process were to yield perfect crystals meeting at perfect boundaries, the density would rise to the theoretical maximum, i.e., the X-ray density.

In practice, imperfections occur and the sintered mass has microscopic voids, both within the grains and at the grain boundaries. The resulting density is referred to as the sintered density. In normal production, the sintered density for Ni-Zn ferrite, suggested by Snelling (1988), is 4600 kg/m^3 (pressed), and porosity is 13.5%. It is a well-known fact that the properties of ferrite materials are strongly influenced by the materials composition and microstructure. But according to He *et al.* (2003), Da silva and Mohallem (2001), Heck (1974) and Von Aulock (1965), properties can also be changed by the sintering conditions employed and the impurity levels present in or added to these materials. The density and porosity can be improved further by using different techniques, like special sintering conditions and selecting suitable composition with addition of small amount (a few mols %) of metal oxide to ferrites. Researchers like, He *et al.* (2008), Goldman (1990), Heck (1974) and Von Aulock (1965), indicated that optimum properties of Ni-Zn ferrites were obtained

when sintered at 1200-1250 °C. The sintering temperature 1200- 1250 °C proved to be the most appropriate condition to obtain Ni-Zn ferrites and gave satisfactory values of density and other parameters comparable with the theoretical values reported for ferromagnetic Ni-Zn ferrites. In addition to this, He *et al.* (2008), Wu *et al.* (2006; 2004) and Goldman (1990), investigated the effect of Si, which improved the properties of ferrite products.

The present work was aimed at sintering Ni-Zn ferrite using low cost iron oxide, having 0.5 wt % of Si additive, and studying its effect on improvement of the properties of ferrite samples and overcoming the cost of finally achieved ferrite products. The presence of Si improves density, but the amount must be low enough to prevent growth of large grains, which is confirmed through scanning electron micrographs.

Materials and Methods

Ferrite samples with compositions $\text{Ni}_x\text{Zn}_{1-x}\text{Fe}_2\text{O}_4$, ($x = 0.66, 0.77, 0.88$ and 0.99) were prepared in polycrystalline form through high temperature solid-state reaction method. The compositions, $\text{Ni}_x\text{Zn}_{1-x}\text{Fe}_2\text{O}_4$, were prepared from powder mixture of NiO, ZnO, of purity better than 99% along with locally available low cost Fe_2O_3 with 0.5 wt% of Si as an additive. The powder mixture were pressed into pellets of 16 mm diameter under a uni-axial pressure of 2.5 tons. Initially the samples were sintered in a muffle furnace at 1000 °C for prolonged period and finally heated for 6 h at 1200 °C for making a homogenous product. The samples were quenched in air and X-ray diffraction (XRD) patterns were taken by Rigaku XRD D/MAXIIA diffractometer using $\text{CuK}\alpha$ radiations with

scanning speed of 1° (2θ/min) to identify the phases formed and to confirm the completion of the chemical reaction. In the present work, the surface of the pellets were cleaned with SiC grinding paper in order to remove any contamination and used to study structural properties.

Results and Discussion

All the four compositions of Ni_xZn_{1-x}Fe₂O₄ ferrite, sintered at 1200 °C, were analyzed by XRD. The XRD pattern of these samples confirmed the completion of major phase of ferrite structure, (Ni-Zn ferrite) with few peaks of zinc silicate (Zn₂SiO₄) as an additive, as shown in Fig. 1. The lattice constant values were compared with values reported in JCPDS cards by Bayliss *et al.* (1986). These values of the lattice constant as a function of Ni-concentration are plotted in Fig.2a. It was observed in the graph that the lattice constant decreases linearly with the nickel content, x, in Ni-Zn ferrite system because the Ni²⁺ ions have a marked preference for octahedral sites due to their favourable fit of charge distribution of these ions in the crystal field of the octahedral site. On the other hand Zn²⁺ ions have preference for tetrahedral site because of their readiness to form covalent bonds involving sp³ hybrid orbital. So the linear decrease of lattice constant with Ni content can be attributed to the smaller ionic radius of Ni²⁺(0.74 Å) as compared to the ionic radius of Zn²⁺(0.84 Å) (Hossain *et al.*, 2007; El-Sayed, 2002).

The X-ray densities were calculated using the following relation used by Islam *et al.* (1999), in his work;

$$dx = 8M/Na^3 \dots\dots\dots(i)$$

where 8 represents the number of molecules in a unit cell of spinal lattice, M is the molecular weight of the sample; a, is the lattice constant and N is the Avogadro’s number.

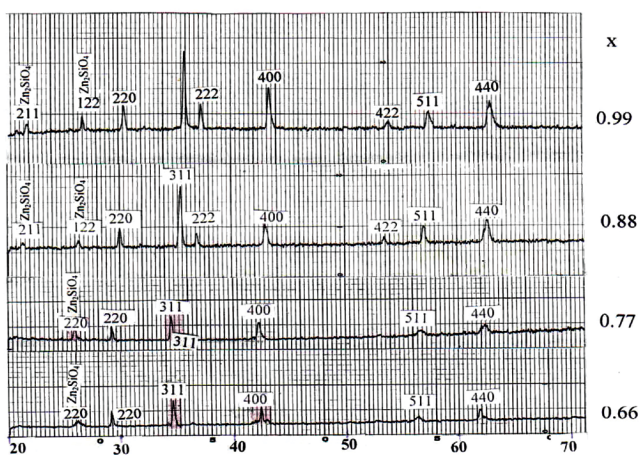


Fig. 1. XRD patterns of Ni-Zn ferrites (Ni_x Zn_{1-x} Fe₂ O₄) with x= 0.66, 0.77, 0.88, 0.99.

The X-ray density depends on the lattice constant and molecular weight of the sample and the mass density calculated from the geometry and mass of the samples. Both the densities dx and ds (plotted in Fig. 2b, as a function of Ni concentration) were found to increase with increase in the Ni content, x. Increase in mass density can be attributed to the difference in specific gravity of the ferrite components, since NiO (6.72 g/cm³) is heavier than ZnO (5.60 g/cm³), as mentioned by Lide (1995). The increase in X-ray density is because of the decrease in lattice constant with the increase of Ni content, x, as predicted from the above equation (i). For each concentration, mass density and X-ray density were calculated to obtain the porosity, P by the following equation used by Hossain *et al.* (2007):

$$P = (1-ds/dx) \dots\dots\dots(ii)$$

Porosity vs., Ni-concentration has been plotted in Fig. 2c, which shows that porosity decreases with increasing Ni con-

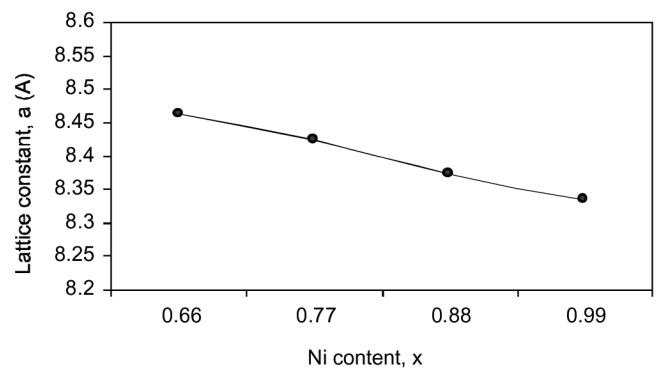


Fig. 2(a). Plot showing lattice parameters vs. Ni concentration for Ni-Zn ferrite system.

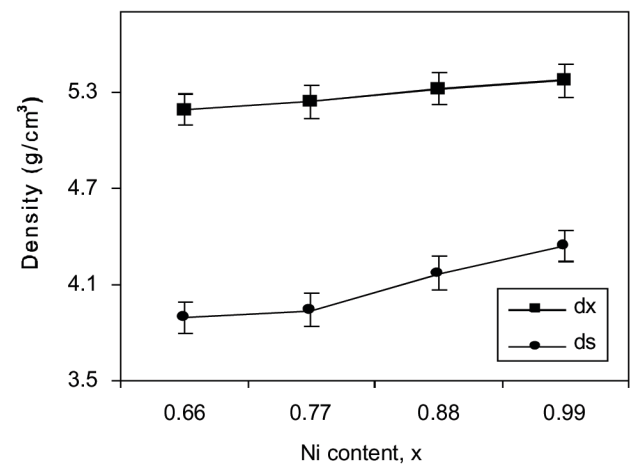


Fig. 2(b). Plot showing X-ray and bulk densities vs. Ni concentration for Ni-Zn ferrite system.

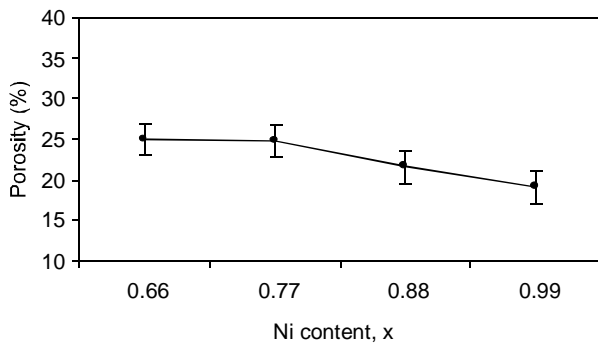


Fig. 2(c). Porosity plotted against Ni concentration for Ni-Zn ferrite system.

tent, x , from 0.66 to 0.99. It can be observed that the value of X-ray density is increasing because the lattice constant is decreasing with the increase of Ni content. Hence the ratio ds/dx decreases which leads to the decrease in porosity. The other reason is that porosity depends on different factors, like sintering temperature, quality of the oxide used and somehow on melting points of the oxide used. Sintering at higher temperature generally brings about reduced porosity and an improvement in the homogeneity.

Hu *et al.* (2005), suggest that at a higher sintering temperature, the number of pores is reduced, as a result of which individual grains come closer to each other and the effective area of grain to grain content increases. This, in turn results in greater densification or less porosity, as Ni content, x , was increased having melting point of NiO (1955 °C) less than ZnO (1975 °C) used. The XRD data were supported by observations from scanning electron micrographs. The microstructure analysis of these samples was carried out using the high resolution scanning electron microscope operated at 25 kV in the secondary electron image mode. It is useful to study the microstructure and to identify the phases formed during sintering. It is also useful to interpret the amount of porosity and find out the size of grains and their positions in the crystal. The morphology of grain structure of $Ni_xZn_{1-x}Fe_2O_4$, as seen from the scanning electron microscopy in Fig.3, shows maximum of cellular type particles with major phase of NiZn ferrite and minor phase of Zn_2SiO_4 (zinc silicate) due to its less energy of formation (Gibb's energy) as mentioned by Smithells (1967). It also shows an average grain size of 3-7 μm . It is to be noted that small grains due to Si are preferred in ferrites as it shows better microstructure and chemical homogeneity. It is also interpreted from the micrograph of this series of Ni-Zn Fe_2O_4 (Fig. 3), that second phase (zinc silicate) dominates more for $x = 0.88$ and $x = 0.99$, which is also clear through XRD patterns.

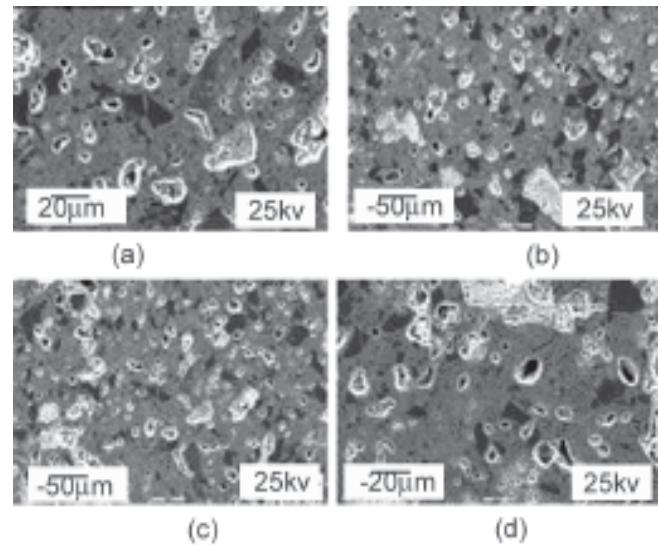


Fig. 3. SEM micrographs of Ni-Zn ferrite system for $x =$ (a) 0.66, (b) 0.77, (c) 0.88, (d) 0.99.

Conclusion

The aim of the present study was to produce homogenous ferrite having small average grain size. Use of low cost Fe_2O_3 with 0.5 wt% Si as an additive in the system was considered in order to improve the properties of the samples and control the process economics. The presence of Si was found to suppress the ceramic grain growth, which further confirms that the formation of major phase of Ni-Zn ferrite structure with lattice content decreases linearly to the nickel content, x , due to the difference in ionic radius. There is increasing trend of dx and ds with the increase in Ni concentration, x , but porosity decreases with increase in Ni concentration, x .

Scanning microscopy was used to observe the distribution of phases, chemical homogeneities and porosity along with grains formation. It was observed that all the samples of ferrite were sound, homogeneous and free from any sort of macro porosity and in agreement with XRD results.

References

- Bayliss, P., Erd, D.C., More, M.E., Sabina, A.P., Smith, D.K. 1986. *Mineral Powder Diffraction File*, Data book, JCPDS International Centre for Data Swathmore, USA.
- Costa, A.C.F.M., Tortella, E., Morelli, M.R., Kininami, R.H.G.A. 2003. Synthesis, microstructure and magnetic properties of Ni-Zn ferrite. *Journal of Magnetism and Magnetic Materials*, **256**: 174-182.
- Da silva, J.B., Mohallem, N.D.S. 2001. Preparation of composites of nickel ferrites dispersed in silica matrix. *Journal of Magnetism and Magnetic Materials*, **226-230**:

- 1393-1396.
- El-Sayed, A.M. 2002. Influence of Zn content on some properties of Ni-Zn ferrites. *Ceramics International*, **28**: 363-367.
- Goldman, A.1990. *Modern Ferrite Technology*, Van Nostrand Reinhold, New York, USA.
- He, X., Zhang, Z., Ling, Z. 2008. Sintering behavior and electromagnetic properties of Fe-deficient Ni-Zn Ferrites. *Ceramics International*, **34**: 1409-1412.
- He, X., Zhang, Q., Ling, Z. 2003. Kinetics and magnetic properties of sol-gel derived Ni-Zn ferrite-SiO₂ composite. *Materials Letters*, **57**: 3031-3036.
- Heck, Carl. 1974. *Magnetic Materials and Their Applications*, Butterworths, London, UK.
- Hossain, A.K.M.A., Mahmud,S.T., Seki, M., Kawai, T., Tabata, H. 2007. Structural, electrical transport and magnetic properties of Ni_{1-x}Zn_xFe₂O₄. *Journal of Magnetism and Magnetic Materials*, **312**: 210-219.
- Hu, J., Yan, M., Luo, W. 2005. Preparation of high-permeability Ni-Zn ferrites at low sintering temperatures. *Physica B: Condensed Matter*, **368**: 251-266.
- Islam, M.U., Ahmed, I., Abbas,T., Chaudhry, M.A. 1999. Effect of Cu substitution for Ni on the properties of NiFe₂O₄ system. In: *Proceedings of the 6th International Symposium on Advanced Materials*, pp.155-158, Topi, Pakistan.
- Lide, David R.1996. *Handbook of Chemistry and Physics*, CRC Press, New York, USA.
- Smithells, C.J. (ed.) 1967. *Metals Reference Book*, 4th edition, Butterworths, London, UK.
- Snelling, E.C. 1988. *Soft Ferrites: Properties and Applications*, 2nd edition, Butterworths, Heinemann, London, UK.
- Von Aulock, W.H. 1965. *Handbook of Microwave Ferrite Materials*, Academic Press Inc., London, UK.
- Wu, K.H., Ting, T.H., Li, M.C., Ho, W.D. 2006. Sol-gel auto-combustion synthesis of SiO₂-doped NiZn Ferrite by using various fuels. *Journal of Magnetism and Magnetic Materials*, **298**: 25-32.
- Wu, K.H., Chang, Y.C., Wang, G.P. 2004. Preparation of Ni Zn ferrite/SiO₂ nano-composite powders by sol-gel auto-combustion method. *Journal of Magnetism and Magnetic Materials*, **269**: 150-155.

A Review of Σ Hypernuclear Physics

Masroor Hussain Shah Bukhari^{ab}

^aDepartment of Physics, University of Houston, Houston, Texas 77204, USA

^bResearch Laboratory of Physical Sciences, Dow University, Karachi-74200, Pakistan

(received December 9, 2009; revised February 9, 2010; accepted February 18, 2010)

Abstract. A concise overview of fundamental Σ hypernuclei physics and the mechanisms of hypernucleus formation and interactions are presented. Σ - Λ interaction and strong force-mediated hyperon-nucleon interaction are introduced to give an epigrammatic background and current perspective of the subject. A model phenomenological elementary Sigma-Nucleus (Σ -N) potential has been constructed and reported here as an instance of Σ N interaction. The potential incorporates both spin and isospin dependence and may be useful in calculating Hamiltonians, cross sections and decay widths in Σ hypernuclear reactions.

Keywords: Σ N potential; Σ - Λ conversion; woods-saxon potential; lane potential

PACS numbers: 21.80.+a, 24.50.+g; 25.80.Nv

Introduction

A hypernucleus is an unstable nucleus formed *in situ* with a constituent hyperon, a baryon comprising at least one strange quark, such as a Λ , Σ or Ξ hyperon, in a nucleus, such as Helium. Since the discovery of the first hypernucleus event in 1952 at Warsaw University with the detection of a Λ -hyperon by Danysz and Pniewski, (1953a;1953b; Danysz *et al.*, 1963a; 1963b; Mladjenovic, 1992), the area of hypernuclear physics has seen a steady growth (Fig. 1). A number of further findings were made in the following years, recording more instances of hypernuclear detection, which are summarized in a detailed survey (Danysz, 1956). Nishijima (1954) predicted the Σ and Ξ particles for the first time and not only gave valuable insight into these hyperons but defined strangeness as an empirical quantum number connected to hypercharge. On the basis of this he did a complete classification of strange particles. This became one of the inspiring milestones for Schwinger (1956) to formulate his *dynamic theory of κ mesons*, as cited in his paper on this topic.

Since the Danysz and Pniewski (1953a;1953b) discovery, hypernuclei have been abundantly produced and studied at various physics laboratories in the world, most notably at the CERN in 1960's and 1970's epoch, Brookhaven (BNL) AGS during 1970's to 1990's, KEK, 1980's to 1990's, and at the BNL, KEK and US Jefferson labs (JLab) in the contemporary years, using both kaon and pion beams.

In addition to the terrestrial efforts at various laboratories, physicists turned to astronomy in order to see the presence of hyperons and strange baryonic matter in celestial bodies. It

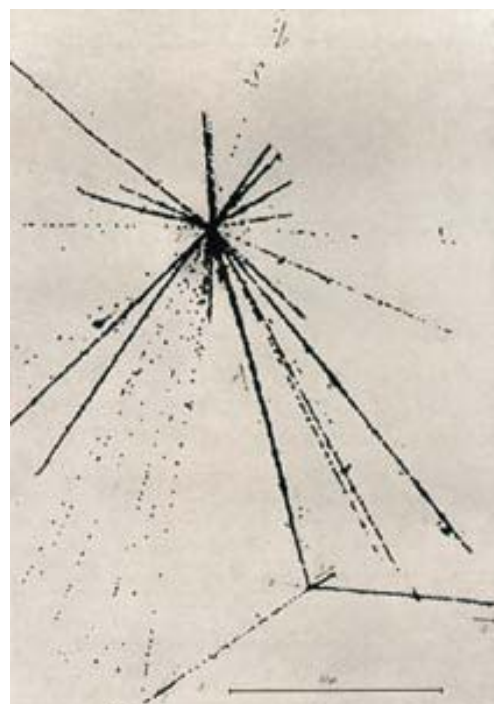


Fig. 1. The first observation of a hypernucleus. A cosmic ray coming in from the top right collides with a nucleus in the emulsion to create the star of tracks. One of the fragments from the collision disintegrates lower down the image to produce three new tracks. The faintest of these, traveling towards the lower left, is probably due to a pion. The total energy released in the disintegration is consistent with the decay of a lambda particle in the original nuclear fragment. (Courtesy and Copyrights CERN Courier, CERN, Geneva).

^bPresent address; E-mail: mbukhari@gmail.com

has been suggested that a prospective site suitable for finding large amounts of strange matter is in the interior of neutron stars, where not only the stellar radii and masses, but even their thermal and structural evolution, are influenced by the presence of contained strange matter, such as strange quarks, hyperons, or kaon-condensates (Glendenning, 1997; Prakash *et al.*, 1997). It is believed that neutron star cores bearing strange quarks or kaon-condensates have substantially lower stellar radii and higher masses as compared to those without strange matter. It has also been reported in studies elsewhere (Pons *et al.*, 1999; Prakash *et al.*, 1994; Lattimer *et al.*, 1991) that strange matter affects the long-term thermal evolution of neutron stars and causes production of metastable neutron stars, a factor which has been suggested to affect the probability of the formation of low-mass black holes. Currently, investigations are underway to search for these effects with the help of a number of experiments and observations. These efforts include multi-wavelength photon observations of neutron stars in various experiments like ROSAT, HST, AXAF, and XMM. In addition, laboratory studies on phase-shift analyses of nucleon-hyperon, nucleon-meson and hyperon-hyperon interactions (both for many-body calculations of dense matter and for studies of superfluidity and superconductivity) are being explored.

In recent times, physicists have begun looking for a number of interesting phenomena and effects, such as different mechanisms in hypernuclei production, existence of bound states, and the appearance of narrow widths in the hypernuclear spectra. It has been proposed that an important effect in strange physics, *strangeness enhancement*, may be a signature of the creation of quark-gluon plasma in nucleus-nucleus collisions at high energies (Sibirtsev *et al.*, 1999; Sibirtsev and Cassing, 1998). One of the current aims of research pursuit in the area of hypernuclei is the search for inter-hyperonic conversion, for which a prime candidate is the Σ - Λ conversion. This report is based on an extensive theoretical, computational and experimental study carried out in the search of Σ - Λ conversion (Bukhari, 2006).

Λ and Σ Hypernuclei. The lambda hyperon (Λ) is the lightest of the hyperons, with a mass of 1115.64 MeV/c² and exists in the form of a charge singlet with a spin half, strangeness -1 and isospin zero. Its important parameters and quantum numbers are enumerated in Table 1. Because of its low mass, it is stable as far as the strong interaction is concerned and thus can form a stable hypernuclear system. It has a lifetime of about 2.6×10^{-10} s and can decay in a nucleus *via* either of two decay modes - mesonic or non-mesonic. The mesonic decay mode involves a Λ decay by meson (a pion) and a nucleon duo, whereas the non-mesonic decay involves a decay *via* a pair of nucleons (proton/neutron). A free Λ decays *via* the mesonic mode. On the other hand, if the Λ is embedded within a nucleus and the momentum of the decay proton is lower than the Fermi momentum, Pauli blocking inhibits this decay mode. In such cases, a non-mesonic decay predominates, mediated *via* the weak interaction, causing Λ decay by emission of nucleons.

The non-mesonic decay modes are less studied, but are interesting, as we can use them to obtain a knowledge of strangeness-changing, four-fermion baryon-baryon weak interactions. In these decays, another important applicable factor is an empirical rule, called the “ $\Delta I=1/2$ Rule” (Hungerford and Furic, 1999; Gibson and Hungerford, 1995), whereby the weak decays of hyperons predominantly occur with a change in isospin by one-half. Thus, the hyperon’s interaction with nucleons is greatly dependent on spin as well as isospin. Spin-dependence of ΛN interaction in p shells have been established quite well, based on a ΛN potential model and analysis of hypernuclear data by various sources (Millener *et al.*, 1985).

The sigma (Σ) is the next hyperon after lambda in terms of mass. Unlike a Λ , a Σ hyperon exists as a charge triplet, i.e. in the form of three charge eigenstates - positive, negative and neutral sigma. They have the common quantum numbers of spin half, isospin unity and strangeness of -1. The mass of each of these is different and approximately ~ 76 -80 MeV higher than the lambda.

All the three flavours of sigma have their individual decay modes and interaction channels with the nucleons.

Table 1. Λ and Σ Hyperon characteristics.

Hyperon (structure)	Mass (M, MeV)	Charge (Q)	Spin (J)	Isospin (T and T ₃)	Strangeness (S)	Mean Life (τ , s.)
Λ^0 (uds)	1115.64	0	1/2	0, 0	-1	2.63×10^{-10}
Σ^0 (uds)	1192.5	0	1/2	1, 0	-1	7.0×10^{-20}
Σ^- (dds)	1197.43	-1	1/2	1, +1	-1	1.5×10^{-10}
Σ^+ (uus)	1189.37	+1	1/2	1, -1	-1	0.8×10^{-10}

The Σ^0 has an extremely short lifetime $\langle\tau\rangle \sim 7 \times 10^{-20}$ s. (making it the shortest-lived particle in the triplet). It can also decay electromagnetically by forming a Λ and emitting a single gamma photon ($\sim 100\%$ B.R.) or a Λ with a pair ($<3\%$ B.R.) of gamma photons. Though Σ^0 and Λ^0 share the same quark constituents, their difference of isospin quantum number implies a structural difference and relevant symmetries between the two. An in-depth study of the conversion of Σ into Λ could help resolve this structure.

The Σ^- has the highest mass in the triplet. It has only one significant decay channel (99.84% B.R.) through which it decays (weakly) to a neutron and a pion (π^-) with a mean life of $\sim 1.5 \times 10^{-10}$ s.

In the case of the Σ^+ , this eigenstate has the lowest mass in triplet. There are two decay channels available to it, both weak and mesonic, one with a proton and a neutral pion (51.57%) and one with a neutron and a positive pion (48.3%), and has a mean life of 0.8×10^{-10} s.

Interactions of a Σ with a nucleon are known as ΣN interactions. Owing to a stronger spin and isospin dependence, this interaction is not only richer and more complicated than a ΛN interaction, it has farther-reaching implications. For instance, it can play a significant role in the Σ -nucleus dynamics and production of narrow Σ states.

While residing in a nucleus, a Σ has a number of interaction channels available, by the virtue of which it can undergo a strong interaction with any of the nucleons, leading to its conversion into a lambda (Λ^0) and an accompanying particle. These conversion pathways include five distinct channels, favoured by conservation laws and kinematics;

1. $\Sigma^- p^+ \rightarrow \Lambda^0 n^0$
2. $\Sigma^- p^+ \rightarrow \Sigma^0 n^0$
3. $\Sigma^0 n^0 \rightarrow \Lambda^0 n^0$
4. $\Sigma^0 p^+ \rightarrow \Sigma^+ n^0$
5. $\Sigma^+ n^0 \rightarrow \Sigma^0 p^+$

In the case of Σ interaction with the nucleus, through the channel $\Sigma N - \Lambda N$, a large width is exhibited, recorded on the order of ~ 25 MeV (Batty *et al.*, 1978). Though some studies (Bertini *et al.*, 1980) suggested the existence of bound nuclear states, they were later on disproved by more accurate measurements. Thus to date, all the searches for narrow or bound states for this hyperon have been negative, except one case, the ${}^4_2\text{He}$, which has a reported bound state (Nagae *et al.*, 1998). The reasons cited for the unavailability of any bound states in Σ have mainly been due to the shallow Σ -N potential and the process of $\Sigma - \Lambda$ conversion. Thus the conversion is an important process in hypernuclear physics.

Hypernucleus formation. In studies of hypernuclei, efforts have mainly been focused on the investigations of hypernuclei decay modes and hypernuclei spectroscopy. Both of these rely, in most cases, on one common theme - the knowledge of hypernuclear formation and decay. Hypernuclei are unstable, short-lived systems and the hyperons embedded within them, whether bound or quasi-free, have very short lifetimes and decay *in situ* within the nucleus. Hence, the only way to study these interactions is by indirectly measuring their decay products. Both production and decay have a number of possible mechanisms, ranging from simple modes to intricate ones.

There are a number of different production mechanisms by which hypernuclei are produced. These mainly include strangeness exchange and associated production (photo-production, electroproduction and double-strangeness-exchange) reactions. In order to form hypernuclei, in general, charged kaon beams are used to produce a strange quark inside a nucleus. A beam of incoming particles with a strange quark in them has to be incident with a momentum in an appropriate range, in order to satisfy the criteria of 'momentum matching' and 'sticking probability' (Bandō *et al.*, 1990). The sticking probability is related to the momentum transfer which allows the produced hyperon to remain in the nucleus after the interaction (The lower the momentum of the hyperon, the higher is this probability.) This momentum optimizes the sticking probability, and in general is higher than the Fermi momentum and lower than the threshold momentum required to disintegrate the nucleus into its constituent nucleons. This maximizes the probability of a projectile's interaction with the nucleus to form a hyperon. When an incident projectile with this momentum interacts with one of the nucleons in the s or p shells, it can form a hyperon in the shells available to it, undergoing a strangeness exchange reaction.

A general hypernuclear production reaction is written as:

$$a + A = {}_A Y + b$$

where a is the incident projectile which interacts with nucleus A and creates a hypernucleus ${}_A Y$, comprising of a hyperon and a nucleon system. A by-product meson b is emitted from the process as one of output products of reaction. The ${}_A Y$ hypernucleus forms the recoil system left over from the nucleus.

For instance, in the production of a hypernucleus by means of a stopped-kaon reaction, an incident projectile, such as a kaon, takes a position into the atom's Bohr orbitals on its interaction with the atom. By traversing and cascading down through these orbitals, when its radius becomes small, and it is in the proximity of the nucleus, it interacts with the nucleons and

forms a hyperon, within the nucleus. It is in sharp contrast to the production of hyperons in Quasi-Free (QF) form where they are produced in a scattering state with high values of momenta (enabling them to escape capture by a nucleus) and do not lead to the formation of hypernuclei.

Stopped projectile reactions are often employed for hypernucleus production. These offer benefits as efficient production of hyperons, complete absorption of incident projectiles at the nuclear surface, large formation probability of hypernuclei and the population of non-substitutional states (such as the ground and low-lying states). These can also lead to the formation of “*Stretched States*”, which are stretched-spin states with large momentum transfer values. An example is the production of Λ hypernuclei in the ${}^4\text{He}(k^-_{\text{stopped}}, \pi^0)X$ reaction, where non-substitutional stretched-spin states are excited preferentially by substantial transfer of momenta.

Contemporary hypernuclear production is facilitated by a number of mechanisms. These include processes as in-flight reactions and stopped incident particle reactions, which can lead to either recoilless production or recoil production of hypernuclei. In all these, recoilless production using the in-flight reaction (K^-, π^+) is a special case of in-flight reactions and is important and relevant in this context.

In a kaon-induced strangeness exchange reaction, the strange quark in the kaon substitutes for an up or down quark in the nucleon and directly converts the nucleon into hyperon – it is possible to have very little amount of momentum transferred from the projectile to the nucleus and the collision remains recoilless. The momentum of the incoming particle (in *lab* frame) is borne almost entirely by an out-going projectile (in this case, a pion), which is emitted in the same direction as the kaon (in *lab* frame) and this whole process can result in a recoilless *in-flight* reaction. The reaction involves no change in quantum numbers (n, l or m). Owing to the constancy of linear momentum as a result of the involved kinematics, it does not induce any angular momentum change and the overall state of the system remains the same. These are thus referred to as “*substitutional states*”, as the incoming projectile with its specially-tuned momentum matching causes a preferential excitation of only the substitutional states, causing $\Delta L = 0$. These kinds of reactions are *exothermic*, i.e. they yield a positive Q-value, liberating the energy from the reaction while producing a hypernucleus. The ${}^3\text{He}(k^-, \pi^\pm)\Sigma\text{NN}$ reactions are an example of this case, using a projectile momentum range of 400 to 800 MeV/c and cross section on the order of $10^3 \mu\text{b/sr}$.

In most of the other cases, a recoil mechanism takes place in hypernucleus production, and a substantial amount of momentum is transferred to the hypernuclear system.

This study was based on and discussed reactions of the first type, i.e. recoilless production of Λ and Σ hypernuclei in s-shell by means of an in-flight reaction, ${}^3\text{He}(\kappa^-, \pi^+)\Sigma\text{-NN}$ involving excitation of non-stretched, substitutional states. A study by Barakat and Hungerford (1992) contributes valuable insight into understanding this reaction.

Σ -N interaction and potentials. An essential step in the understanding of hyperon-nucleon interaction is the understanding of nuclear and nucleon-nucleon potential. This knowledge is relatively well-understood after decades of theoretical and experimental investigation. In contrast, the hyperon-nucleon potential and consequent interaction has yet to achieve the same footing, as it is difficult to obtain hyperon beams to study Y-N scattering. Besides, the extremely short hyperon lifetimes and their inter-conversion processes can also pose problems in studying these interactions. Nevertheless, this interaction offers a rich spectrum of knowledge and countless new vistas to explore.

When it comes to expressing the potential of any spin-vector particle or system, spin is an important degree of freedom, not just limited to hypernuclei but in ordinary nuclei as well. It is a well-established fact that the nuclear potential is spin-dependent, due to the two-body tensor force which induces a strong one-body spin-orbit potential experienced by the nucleus. A similar tensor force must prevail for a hypernucleus, where spin and orbital angular momentum should couple to a collective spin-dependent nuclear potential. It has been reported by Dover *et al.* (1989) that the coupling strength of Σ -N spin-orbit interaction is about one-half of its N-N counterpart, whereas the ratios of the strengths of the averaged NN, Λ -N and Σ -N potentials were proposed to exist in proportion:

$$\begin{aligned} NN / \Sigma N &\sim 3/1, \\ NN / \Lambda N &\sim 3/2 \end{aligned}$$

In the Λ N and Σ N interactions, there are two more degrees of freedom – strangeness, by the virtue of the strange quark embedded into a hyperon, and isospin, because of the isospin-coupling and the strong isospin-dominant symmetries involved with the hyperonic structure. These, as well as the unstable nature of the hyperons, make it more difficult, and at the same time interesting, to define quantitatively or illustrate qualitatively a hyperon-nucleon interaction.

In particular, spin and isospin play an intertwined role in the interaction of a hyperon with a nucleon and consequently on the potential formed by their combination. The strong spin–isospin dependence in Σ N interaction is evidently

because of the exchange of both isoscalar (ω , η) and isovector (π , ρ) mesons, which presents a wide spectrum of coupling states.

One dimension of this problem is understanding the isospin structure, as the nuclear potential itself depends significantly on the isospin. A further dimension enters in this problem from the fact that the hyperons are distinguishable from nucleons in terms of their quantum numbers, specifically in terms of the strangeness. Thus, Pauli blocking does not apply and the hyperons inhabit their own individual nuclear shells, following the same shell model scheme as the nucleons.

The ΛN interaction (Dalitz *et al.*, 1972) is relatively well known as compared to ΣN interaction, as a Λ within a nucleus forms bound states with the nucleons and enables studies to probe this potential. However, the ΣN interaction is not understood very well and requires a lot of experimental data to quantify its core potential. Hence the ΣN potential is a crucial piece of information.

Σ -N potentials. One existing model which describes a Σ -N potential is the *Nijmegen Model*, comprising two variations, models I and II (Maessen *et al.*, 1989; Nagels *et al.*, 1978). It proposes an elementary potential for the interaction of a Σ with a nucleon, in form of a *one-boson-exchange (OBE)* model. In quantum hadrodynamics, these models are also termed as *one-pion-exchange (OPE)* or *one-meson-exchange (OME)* models and are very useful in understanding the interaction at the level of exchange particles. The Nijmegen model is largely based on $SU(3)_f$ symmetry and uses the existing nucleon-nucleon data in order to determine its parameters. The spin splittings predicted in the model for Λ hypernuclei were later measured in an experiment at Brookhaven (Dover *et al.*, 1989). Nevertheless, investigations are still underway to validate the model's applicability to the ΣN potential. It has been suggested (Alberico and Garbarino, 2002) that the Σ -N interaction exhibits a long range *One-Pion-Exchange (OPE)* component, with the central part weaker than the Λ -N part. Thus, investigations of this interaction within the framework of One-Boson-Exchange (OBE) models, is a viable approach.

Harada *et al.* (Harada and Akishi, 1996; Koike and Harada, 1996; Harada, 1992; Harada *et al.*, 1990), using the Nijmegen model, proposed an effective Σ -nucleus potential derived from this model and based on many-body calculations. In a *Mean Field Model* (Walecka, 1995; Jaminon and Mahaux, 1989), they assumed that the hyperon is embedded in a collective mean field of nucleons where it retains its individual structure and undergoes interactions with nucleons in the form of Nijmegen potentials. This model is considered a reasonable

formulation of an effective potential to explain the interaction of a hyperon in the effective potential created by the surrounding nuclear medium. It uses a Lane potential (Lane, 1962) and incorporates an isospin mixing term $\tau_N \cdot t_\Sigma$ to describe isospin mixing of Σ and N.

In connection with actual observations of Σ -N potentials, there have been a few studies which attempted to quantify these potentials on the basis of experimental data. Some quantitative estimates of the sigma-nucleus potential were established from the analysis of Σ^- -atom X-ray data by Batty (1979), who reported estimates of the sigma-nucleus potential at the center of the nucleus to be $-(25-30)$ MeV for the real part and $-(10-15)$ MeV for the imaginary part, with a form proportional to the nuclear density.

In addition to isospin and spin degrees of freedom, there is one more important factor in the quest for finding this potential, i.e., the continuum – which is represented by quasi-free states which do not have a discrete sets of states and lie in the continuum. The continuum plays an important role in both hypernuclear production and the potential. Studies by Tang *et al.* (1988) and Chrien *et al.* (1987) have highlighted the effects of the continuum in $^{16}\text{O}(k, \pi^+)X$, $^{12}\text{C}(k, \pi^+)X$ and $^6\text{Li}(k, \pi^+)$ reactions. As the Σ potential is shallower than that of a Λ , fewer states can be expected in the bound regions of the spectrum, in turn manifesting a more profound role of the continuum.

In view of the paucity of available experimental data and intricacies involved in the understanding of the underlying processes, the subject of the Σ -N potential remains intriguing and controversial. However, one thing remains paramount- as suggested by Bandō *et al.* (1990) as well, “*The strong isospin-spin dependence of the Σ -N interaction should generally play an important and characteristic role in the Σ -nucleus dynamics*”. An exhaustive review, which discusses the Σ -nucleus potential, spin-isospin role and consequent interactions in $A=3,4$ systems (Barakat and Hungerford, 1992), presents various important aspects of this problem in further detail.

Here, to illustrate a general form of a Y-N potential, an attempt has been made to construct a simple elementary Σ -N potential which is in its class similar to an optical potential and incorporates both spin and isospin dependence.

Constructing an elementary Σ -N optical potential. The interaction of a Σ inside a nucleus can be modeled as an incident particle interacting with a complex optical potential formed by the nucleons in a nucleus. If this optical model is devised on the lines of a Woods-Saxon type potential in the shell model paradigm (Jensen, 1963; Mayer and Jensen, 1955; Mayer, 1950; 1949; 1948), one can construct a form:

$$U(r) = -[V(r) + iW(r)] + V_{s.o.} \quad (1)$$

where $V(r)$ is the real part of the potential and $W(r)$ the imaginary part, and $V_{s.o.}$ is the spin-orbit coupling term. The imaginary part here corresponds to absorption, which manifests its effects in the form of inelastic scattering, as well as in the form of Σ -N isospin mixing and Σ - Λ conversion channel. Both of these parts have a scaling behavior in energy, i.e. they depend on the energies involved.

In an approach similar to one taken by Eder *et al.* (1977), in which a potential for the neutron-nucleus interaction was constructed, one can formulate a Σ -N phenomenological potential within the framework of the shell model, and express it as:

$$U(r) = -V_0 f(x) - i \left(W f(x) - 4W_s \frac{d}{dx} f(x) \right) + 2\zeta m^2 V_{s.o.} \left(\frac{\vec{\sigma} \cdot \vec{L}}{\hbar} \right) \frac{1}{r} \frac{d}{dx} f(x),$$

$$f(x) = \frac{1}{e^x + 1}, x = \frac{r-R}{a}, R = r_0 A^{1/3} \quad (2)$$

Here, r is the nucleonic separation, R the nuclear radius, a the diffusivity, and σ and L the spin and orbital momentum vectors, whereas W , W_s and ζ are shell parameters calculated from the energy tables (Perey and Perey, 1974).

The potential is incomplete yet, because of a lack of isospin dependence. Here, one can incorporate a suitable potential with embedded isospin dependence, such as the one introduced by Lane (1962) to describe inter-nucleonic potentials. If the depths of the nucleon potentials are known, this potential can be determined conveniently and can be used to construct a suitable nuclear potential.

If a Lane term (Harada and Akishi, 1996; Koike and Harada, 1996; Lane, 1962) is assumed in the real part of this potential and isospin dependence is introduced, we obtain a complete potential which describes the Σ -N interaction. This kind of Σ -N potential is also suggested by Harada *et al.* (1990) in the Harada model. It has a form:

$$U_{C\Sigma}(R) = U^0(R) + U^\tau(R)(T_C \cdot t_\Sigma) \quad (3)$$

Here, C and Σ denote the nuclear core and Σ hyperon, respectively. The first term describes the usual central nuclear potential and the second term is the $1/A$ Lane Term, including a dot product of the isospin operators for the two entities. This potential is illustrated in Fig. 2 (Harada and Akishi, 1996; Koike and Harada, 1996), featuring an $A=4$ Σ NNN system for the two Σ -N system isospin states, $T=1/2$ and $T=3/2$. Here, Σ hypernucleus potentials for the $T=1/2$ and $T=3/2$ states in the four-body Σ NNN system, as calculated by Harada (1992) and Harada *et al.* (1990) are shown. In the

$T=1/2$ state, the real part is attractive and has a small contribution from a repulsive part, but has an imaginary part. This imaginary part corresponds to absorption and is attributed to the isospin mixing and Σ - Λ conversion processes. Based on Harada's work, it can be surmised that two processes are going on in the nuclear core nearly simultaneously—first, a Σ is being absorbed into the nucleon(s), and second, this absorption goes on inversely proportional to the potential depth. On the other hand, in the $T=3/2$ state, these trends are unavailable. This seems to agree with the findings (Albercio and Garbarino, 2002) in some models supported by experimental data, which have shown the Σ -N effective potential to be strongly repulsive at short distances.

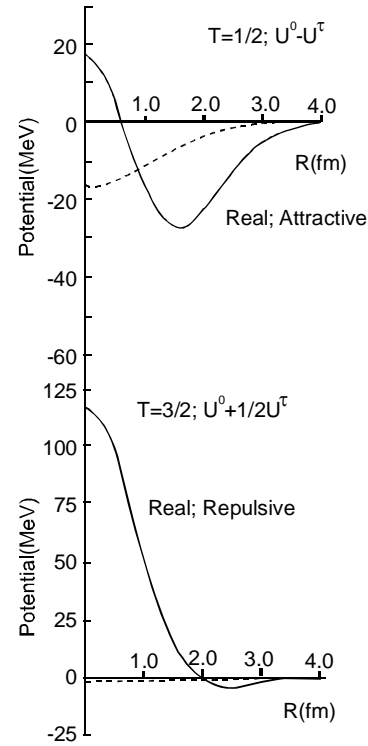


Fig. 2. Σ N potentials as calculated by Harada (Image courtesy of Harada, 1996).

As the Σ is an isospin vector with total isospin of unity, in a ${}^4_\Sigma\text{He}$ hypernucleus, the sigma-nucleon system has two available isotopic spin states; the $T=1/2$ and $T=3/2$. In contrast, a Λ with its scalar isospin, can exist in only one isotopic spin state, $T=1/2$. For instance, the ${}^4\text{He}(\kappa, \pi)\Sigma\text{NNN}$ reaction populates both of these states for ΣNNN , while the ${}^4\text{He}(\kappa, \pi^+)\Sigma\text{NNN}$ reaction populates only the $T=3/2$ state (Afnan and Gibson, 1993). The reaction investigated in this study, the ${}^3\text{He}(\kappa, \pi^+)\Sigma\text{NN}$ reaction, leads to a total $T=1$ state for the Σ - ${}^2\text{H}$ system, as deuteron has a ($J=1$, $T=0$) state, whereas a Σ has the state ($J=1/2$, $T=1$).

The Lane-term-modified potential term for isospin is then substituted in the potential in equation 2, and a suitable form for a phenomenological Σ -N potential can be constructed, as given below in the equation 4. The potential has both spin-dependence and isospin dependence in the form of spin-orbit coupling and isospin coupling, respectively. A Coulomb interaction between the hyperon and the nucleus has been included (which was not included in the equation 2). The Coulomb interaction being a long-range force is difficult to handle in the short-range potentials, but it has been added for completeness.

$$U(r) = -U^0 f(x) + U_{coul}^{\Sigma N} - U^\tau f(x)(\vec{T}_C \cdot \vec{T}_Z) - i[Wf(x) - \xi f'(x)] + 2\zeta m^2 V_{s.o.} \left(\frac{\vec{\sigma} \cdot \vec{L}}{\hbar} \right) \frac{1}{r} f'(x) \quad (4)$$

Here, the symbols ξ and ζ have been arbitrarily chosen to represent the energy-dependent shell parameters, which replace W_s and ζ in the equation (2), and can be determined from the experimental data. The form of the coulomb potential is taken as a uniformly charged sphere of a radius R_c which can be expressed as;

$$U_{coul}^{\Sigma N}(r) = \frac{Ze^2}{r} \Rightarrow r > R_c \quad (5)$$

$$U_{coul}^{\Sigma N}(r) = a + br^2 \Rightarrow r \leq R_c$$

where, a and b are given by:

$$a = \frac{3Ze^2}{2R_c} \quad (6)$$

$$b = -\frac{Ze^2}{2R_c^3}$$

and the values for the constant parameters r_0 , a_0 and R_c can be chosen from the studies described earlier.

The potential expressed in equation 4 is a complete and physical expression for a Σ -N potential, incorporating both the spin and isospin dependence. It can be used to formulate a suitable Hamiltonian or Lagrangian for the Σ N hypernuclear interactions, and possible solutions could be determined in the available degrees of freedom.

Conclusion and Discussion

This report presents a general overview of Σ and Λ physics and presents the development of an elementary Σ N phenomenological potential as a model. The report primarily deals with the formation, decay and interaction of a Σ hyperon with a nuclear medium. A detailed report in this connection has appeared elsewhere (Bukhari, 2006),

including detailed development of the potential, and in particular, a study of the mechanics of the Σ conversion into a Λ hyperon. Another useful study, reported in recent years (Saha *et al.*, 2005) based on some theoretical work and experimental data collected at the KEK proton synchrotron, presents an overview of the Σ N potential and decay widths in a p-shell system.

Acknowledgement

This work was supported by the State of Texas and the University of Houston, Houston, Texas. The author acknowledges valuable discussions with Professor Ed V. Hungerford III at the Department of Physics, University of Houston, Houston, Texas.

References

- Afnan, I.R., Gibson, B.F. 1993. Resonances in Λ d scattering and the Σ hypertriton. *Physical Review C*, **47**: 1000-1012.
- Alberico, W.M., Garbarino, G. 2002. Nucleon-nucleon coincidence spectra in the non-mesonic weak decay of Λ hypernuclei and the Γ_n/Γ_p puzzle. *Physical Reports*, **369**: 1-109.
- Bandō, H., Motoba, T., •ofka, J. 1990. Production, structure and decay of hypernuclei. *International Journal of Modern Physics A*, **5**: 4021-4198.
- Barakat, M., Hungerford, E.V. 1992. Sigma nucleus interactions in the A=3,4 systems. *Nuclear Physics A*, **547**, 157C-164C.
- Batty, C.J. 1979. Nuclear bound states of negatively charged hadrons. *Physics Letters B*, **87**: 324-326.
- Batty, C.J., Biagi, S.F., Blecher, M., Hoath, S.D., Riddle, R.A.J., Roberts, B.L., Davies, J.D., Pyle, G.J., Squier, G.J.A., Asbury, D.M., 1978. Measurement of strong interaction effects in Σ atoms. *Physics Letters B*, **74**: 27.
- Bertini, R., Bing, O., Birien, P., Bruckner, W., Catz, H., Chaumeaux, A., Durand, J.M., Faessler, M.A., Ketel, T.J., Kilian, K., Mayer, B., Niewisch, J., Pietrzyk, B., Povh, B., Ritter, H.G., Uhrmacher, M. 1980. Hypernuclei with sigma particles. *Physics Letters B*, **90**: 375-378.
- Bukhari, M.H.S. 2006. A Search for $\Sigma - \Lambda$ Conversion. *PhD Dissertation*, Department of Physics, University of Houston, Houston, Texas, USA.
- Chrien, R.E., Hungerford, E.V., Kishimoto, T. 1987. Continuum effects and the interpretation of Σ hypernuclei. *Physical Review C*, **35**: 1589.
- Dalitz, R.H., Herndon, R.C., Tang, Y. C. 1972. Phenomenological study of s-shell hypernuclei with Λ N and Λ NN

- potential. *Nuclear Physics B*, **47**: 109-137.
- Danysz, M., Garbowska, K., Pniewski, J., Pniewski, T., Zakrzewski, J., Fletcher, E.R., Lemonne, J., Renard, P., Saction, J., Toner, W.T., Sullivan, D.O., Shah, T.P., Thompson, A., Allen, P., Heeran, Sr.M., Montwill, A., Allen, J.E., Beniston, M.J., Davis, D.H., Garbutt, D.A., Bull, V.A., Kumar, R.C., March, P.V. 1963a. The identification of a double hyperfragment. *Nuclear Physics*, **49**: 121-132.
- Danysz, M., Garbowska, K., Pniewski, J., Pniewski, T., Zakrzewski, J., Fletcher, E.R., Lemonne, J., Renard, P., Saction, J., Toner, W.T., O'sullivan, D., Shah, T.P., Thompson, A., Allen Sr., P., Heeran, M., Montwill, A., Allen, J.E., Beniston, M.J., Davis, D.H., Garbutt, D.A., Bull, V.A., Kumar, R.C., March, P.V. 1963b. Observation of a double hyperfragment. *Physical Review Letters*, **11**: 29-32.
- Danysz, M. 1956. Hyperfragments. *Nuovo Cimento, Supplement*, **4**: 609-614.
- Danysz, M., Pniewski, J. 1953a. Disintegration delayed passage of a heavy emitted in nuclear explosion. *Bulletin de L'Academie Polonaise Des Sciences*, **1**: 42-47.
- Danysz, M., Pniewski, J. 1953b. Delayed disintegration of a heavy nuclear fragment. *Philosophical Magazine*, **44**: 348-350.
- Dover, C.B., Millener, D.J., Gal, A. 1989. On the production and spectroscopy of Σ hypernuclei. *Physics Reports*, **184**: 1-97.
- Eder, G., Leeb, H., Oberhummer, H. 1977. Shell effects in the neutron-nucleus optical potential. *Journal of Physics G: Nuclear Physics*, **3**: L127-L128.
- Gibson, B.F., Hungerford, E.V. 1995. A survey of hypernuclear physics. *Physics Reports*, **257**: 349-388.
- Glendenning, N.K. 1997. *Compact Stars, Nuclear Physics, Particle Physics, and General Relativity*, Springer-Verlag, New York, USA.
- Harada, T., Akaishi, Y. 1996. Σ -Hypernuclear responses in ${}^4\text{He}$ (in-flight K^- , π) spectra. *Progress of Theoretical Physics*, **96**: 145-178.
- Harada, T. 1992. Production and structure of light Σ -hypernuclei. *Nuclear Physics A*, **547**: 165-174.
- Harada, T., Shinmura, S., Akaishi, Y., Tanaka, H. 1990. Structure of the ${}^4\text{He}$ hypernuclear bound state. *Nuclear Physics A*, **507**: 715-730.
- Hungerford, E.V., Furic, M. 1999. Strange nuclear physics: a brief status report. *Fizika B*, **8**: 21-28.
- Jaminon, M., Mahaux, C. 1989. Effective masses in relativistic approaches to the nucleon-nucleus mean field. *Physical Review C*, **40**: 354-367.
- Jensen, J.H.D. 1963. *Glimpses at the history of the nuclear structure theory, Nobel Lecture, December 12, 1963*. Nobel Foundation, Stockholm, Sweden.
- Koike, Y. H., Harada, T. 1996. Structure of the $A=3$ Σ -hypernuclei. *Nuclear Physics A*, **611**: 461-483.
- Lane, A.M. 1962. Isobaric spin dependence of the optical potential and quasi-elastic (p,n) reactions. *Nuclear Physics*, **35**: 676-685.
- Lattimer, J.M., Pethick, C.J., Prakash, M., Haensel, P. 1991. The direct urca process in neutron stars. *Physical Review Letters*, **66**: 2701-2704.
- Maessen, P.M.M., Rijken, Th.A., deSwart, J.J. 1989. Soft-core baryon-baryon one-boson-exchange model II. Hypernucleon potential. *Physical Review C*, **40**: 2226-2245.
- Mayer, M.G., Jensen, H.J.D. 1955. *Elementary Theory of Nuclear Shell Structure*, John Wiley, New York, USA.
- Mayer, M.G. 1950. Nuclear configurations in the spin-orbit coupling model. I. Empirical evidence. *Physical Review*, **78**: 16-21.
- Mayer, M.G. 1949. On closed shells in nuclei. II. *Physical Review* **75**: 1969-1970.
- Mayer, M.G. 1948. On closed shells in nucleus. *Physical Review*, **74**: 235-239.
- Millener, D.J., Gal, A., Dover, C., Dalitz, R.H. 1985. Spin dependence of the ΛN effective interaction. *Physical Review C*, **31**: 499-509.
- Mladjenovic, M. 1992. *The History of Early Nuclear Physics (1896-1931)*, World Scientific, Singapore.
- Nagae, T., Miyachi, T., Fukuda, T., Outa, H., Tamagawa, T., Nakano, J., Hayano, R.S., Tamura, H., Shimizu, Y., Kubota, K., Chrien, R.E., Sutter, R., Rusek, A., Briscoe, W.J., Sawafuta, R., Hungerford, E.V., Emple, A., Naing, W., Neerman, C., Johnston, K., Planinic, M. 1998. Observation of ${}^4\text{He}$ bound state in the ${}^4\text{He}$ (K^- , π^0) reaction at 600 MeV/c. *Physics Review Letters*, **80**: 1605-1609.
- Nagels, M.M., Rijken, T.A., deSwart, J.J. 1978. Low-energy nucleon-nucleon potential from Regge-pole theory. *Physical Review D*, **17**: 768-776.
- Nishijima, K. 1954. Some remarks on the even-odd rule. *Progress of Theoretical Physics*, **12**: 107-108.
- Perey, C.M., Perey, F.G. 1974. Compilation of phenomenological optical model parameters 1969-1972. *Atomic Data and Nuclear Data Tables*, **13**: 293-337.
- Pons, J.A., Reddy, S., Prakash, M., Lattimer, J.M., Miralles, J.A. 1999. Evolution of protoneutron stars. *The Astro-*

- physical Journal*, **513**: 780-804.
- Prakash, M., Bombaci, I., Prakash, M., Ellis, P.J., Lattimer, J.M., Knorren, R. 1997. Composition and structure of protoneutron stars. *Physics Reports*, **280**: 1-77.
- Prakash, M., Bombaci I., Prakash, M., Ellis, P.J., Lattimer J.M., Knorren, R., 1994. Rapid cooling of neutron stars. *Physics Reports*, **242**: 297-312.
- Saha, P.K., Fukuda, T., Imoto, W., Ahn, J.K., Ajimura, S., Aoki, K., Bhang, H.C., Fujioka, H., Hotchi, H., Hwang, J.I., Itabashi, T., Kang, B.H., Kim, H.D., Kim, J.J., Kishimoto, T., Krutenkova, A., Maruta, T., Miura, Y., Miwa, K., Nagae, T., Noumi, H., Outa, H., Ohtaki, T., Sakaguchi, A., Sato, Y., Sekimoto, M., Shimizu, Y., Tamura, H., Tanida, K., Toyoda, A., Ukai, M., Yim, H.J.
2005. Production of the neutron-rich hypernucleus ^{10}Li in the (π^0, K^+) double charge-exchange reaction. *Physical Review Letters*, **94**: 52502 (4 pp).
- Schwinger, J. 1956. Dynamic theory of K mesons. *Physical Review*, **104**: 1164.
- Sibirtsev, A., Tsushima, K., Cassing, W., Thomas, A. W. 1999. The role of the $P_{11}(1710)$ in the ${}^1_0N\text{-}K$ reaction. *Nuclear Physics A*, **646**: 427-443.
- Sibirtsev, A., Cassing, W. 1998. Strangeness production in proton-proton collisions. *Nuclear Theory* (33 pages), nucl-th/9802019.
- Tang, L. *et al.* 1988. *Physical Review C*, **38**: 846.
- Walecka, J.D. 1995. *Theoretical Nuclear and Sub-Nuclear Physics*, 2nd edition, Oxford University Press, UK.